Alma Mater Studiorum – Università di Bologna

DOTTORATO DI RICERCA IN

ONCOLOGIA, EMATOLOGIA E PATOLOGIA

Ciclo XXXI

Settore Concorsuale di afferenza: 06/A2

Settore Scientifico disciplinare: MED/04

MEMBRANE FATTY ACID REMODELING ALONG CYTOTOXIC EVENTS INDUCED BY A NOVEL COPPER-BASED ANTITUMORAL AGENT AND TUMOR PROGRESSION IN MICE MODELS

Presentata da: Maria Louka

Coordinatore Dottorato

Prof. Pier-Luigi Lollini

Supervisore

Prof. Andrea Bolognesi

Esame finale anno 2019

To my family and Bastien,

‘The route marks an address. And a route is much more than a result.’

Jorge Bucay - Let Me Tell You a Story

Acknowledgements

First and foremost, I would like to express my gratitude to Dr. C. Ferreri and Dr. C. Chatgilialoglu for giving me the opportunity to perform this 3-year training within Lipinutragen and take part in the European research network 'ClickGene'. This was a particularly rich experience and their support and encouragement guided me through it.

I would like to thank Prof. A. Bolognesi for offering me a Ph.D candidate position at the University of Bologna and giving me access to his laboratory. The thesis supervision was accompanied by his insightful comments and suggestions. Special thanks to the members of his group Dr. L. Polito and Dr. M. Bortolloti for their invaluable guidance and help in experiments execution.

I am also grateful to Dr. V. Sunda, Dr. A. Sansone and G. Menounou for sharing their knowledge and being always willing to lend a hand. Thanks to all the members of Lipinutragen laboratory and Bio Free Radicals' group at ISOF, CNR that created a nice working environment and supported me, whenever needed.

Furthermore, I appreciate my collaboration with Prof. E. Efthimiadou and Dr. M. Krokidis, who hosted me in their lab during my secondment at the NCSR Demokritos and contributed to my research activities. A special mention to G. Toniolo and N. Fantoni for producing and providing me materials within the frame of collaborative projects.

I gratefully acknowledge the Marie Skłodowska-Curie action for providing my fellowship. This project has indeed received funding from the European Union's Horizon 2020 framework programme for research and innovation under grant agreement No 642023.

Finally, I would also like to address thanks to all my friends who contributed to my every day's happiness and personal balance. Last but not least, I am grateful towards my family and Bastien for their unconditional love and support throughout this 'journey'.

Table of contents

Abstract

Lipid metabolic reprogramming is an established hallmark of cancer development, which among others includes a distinct fatty acid biosynthesis and metabolism due to the enhanced cellular growth and proliferation of cancer cells. Cell membranes are built by phospholipids, which are fatty acid-containing lipid species. Alterations to the fatty acid content may influence the membrane properties, such as fluidity, permeability and membrane lipid-related signaling, thus favoring tumor growth, progression and metastasis. The membrane remodeling is highly affected by the intracellular lipid pool, which in turn depends on both the endogenously produced fatty acids and their dietary intake. Key enzymes that are involved in lipid biosynthesis, show increased activity along tumor development and progression. Some chemotherapeutics have also been reported to influence the characteristics of the plasma membrane, while the final outcome of chemical exposure depends on membrane-related signaling (e.g. lipid rafts involving the death receptor pathway).

The first part of the present thesis aimed at the in vitro evaluation of the effects of the compound [Cu(TPMA)(Phenanthroline)]$(ClO_4)_2$, a novel copper complex, on the cell viability and membrane fatty-acid lipidome. The copper complex was studied in vitro as a free compound or under an encapsulated form within polymeric nanoparticles in the neuroblastoma derived cell line NB100 cell line and breast carcinoma cell line MCF7. Its cytotoxicity was determined and the cell death pathways were analyzed with parallel monitoring of caspase activation. The membrane fatty acid composition was examined in cells treated with the half maximal effective concentration (EC_{50}) of copper complex. Inhibitors of apoptosis and necroptosis and scavengers of oxidative stress were tested to evaluate their protective effect against copper's cytotoxicity and membrane lipidome alterations. The copper complex exerted oxidative stress-mediated cytotoxicity and induced apoptosis and necroptosis in both cell lines. Membrane remodeling took place upon treatment with the copper complex with a specific increase of saturated fatty acids (SFA) and a decrease of monounsaturated fatty acids (MUFA), but not polyunsaturated fatty acids (PUFA). Assessment of the stearoyl-CoA desaturase (SCD1) activity in the presence of copper complex using a cell-free assay showed no enzymatic inhibition of MUFA biosynthesis and therefore no metabolic involvement to the observed membrane remodeling. Cells pre-treatment with apoptosis inhibitor and ROS scavengers prevented

both the cytotoxicity and the changes on fatty acid composition, suggesting a correlation between membrane remodeling and the cytotoxic mechanism caused by the complex. Palmitic acid supplementation influenced the cell response to copper complex exposure by enhancing its cytotoxic effect. Finally, encapsulation of the complex in polymeric nanoparticles protected the cell viability and prevented any changes on membrane fatty acid composition.

The second project undertaken within the frame of this thesis involved the monitoring of fatty acid composition of erythrocyte membrane at different stages of tumor occurrence and at early points of tumor occurrence after administration of iron nanoparticles (Fe-NPs) and bleomycin. The animal model studied consisted in the tumor-bearing SCID mice, xenografted with the human glioblastoma U87MG cell line, while non-xenografted SCID and healthy Swiss mice were used as controls. Late stage tumor-bearing mice were characterized by statistically significant increase of SFA, accompanied by a decrease in total PUFA, unsaturation and peroxidation indices. Fe-NPs caused a notable membrane remodeling in healthy Swiss mice, characterized by lower SFA and PUFA levels and higher MUFA content. Although both relative amounts of ω-6 and ω-3 PUFA families decreased, their ratio (ω-6/ω-3) appeared to be increasing in Fe-NPs treated Swiss mice, compared to the untreated group. Tumor-bearing mice did not show altered fatty acid profile under any treatment. Bleomycin did no exert any significant effect on erythrocyte membrane lipidomic profile of either the tumor-bearing mice or the healthy ones. However, co-treatment of tumor diseased mice with Fe-NPs and bleomycin led to a decrease of the ω-6/ω-3 ratio in erythrocyte membranes. Erythrocyte membrane fatty acid analysis may provide insights on the endogenous fatty acid metabolism through the relative proportion of SFA to MUFA, while the effect of high oxidative stress can be depicted through the PUFA consumption and the consequent membrane remodeling. Since the fatty acids are part of our dietary intakes, their balance can also impact the drug outcomes and tumor progression.

In conclusion, we could demonstrate through these studies that fatty acid-based membrane lipidomics can be a valuable tool for evaluating the nutritional conditions and metabolic status of an organism. Indeed, by enabling the monitoring of selected fatty acid alterations, this method can contribute to the development of multi-targeted antitumoral approaches through customized cell membrane rearrangement.

1. Introduction

1.1 Fatty acid-based membrane lipidomics

1.1.1 Plasma membrane

The cell membrane is crucial for the organization and function of every living cell. It constitutes the physical and semi-permeable barrier separating the intracellular from the extracellular environment, thus circumscribing the cellular content [1]. The plasma membrane is involved in every aspect of cellular fate, from cell division to programmed cell death [2-4]. Besides its structural role, it is involved in the regulation of transmembrane transport of small molecules either through passive or active mechanisms. Cell membrane also participates in various cellular processes such as cell adhesion, recognition and signaling [1, 5].

1.1.1.1 Structure

The plasma membrane is a dynamic, complex structure of lipids and proteins in a fluid state, organized in the well-known mosaic model, according to which most of its molecules are able to move about in the plane of the membrane [6]. The most abundant membrane lipid species are the amphipathic glycerol-based phospholipids, which spontaneously form the lipid bilayer due to the hydrophobic effect [7]. Therefore, the major core of a biological membrane is self-organized, with the hydrophobic tails being eliminated from water and facing each other, while the polar headgroups form an ionic surface interacting with water (see Figure 1.1). Cholesterol is another major lipid component of the plasma membrane, which is embedded in the phospholipid bilayer and contributes to its fluidity [8]. Transmembrane or anchored integral proteins are also found in the membrane assembly and they are connected to phospholipids mainly by noncovalent interactions [9]. Membrane protein-lipid interaction has been recently reported to have a significant effect on the stabilization of membrane protein oligomers and on cell susceptibility to aberrant protein oligomers [10, 11]. Peripheral proteins are bound to the integral ones at specific binding sites [9]. Membrane protein molecules are mediating almost all membrane-related

functions, such as transport of specific molecules, detection and transduction of chemical signals [1, 12]. In addition, the plasma membranes may also contain glycolipids and glycoproteins, whose carbohydrates components play a significant role in cell-cell interaction processes [13, 14].

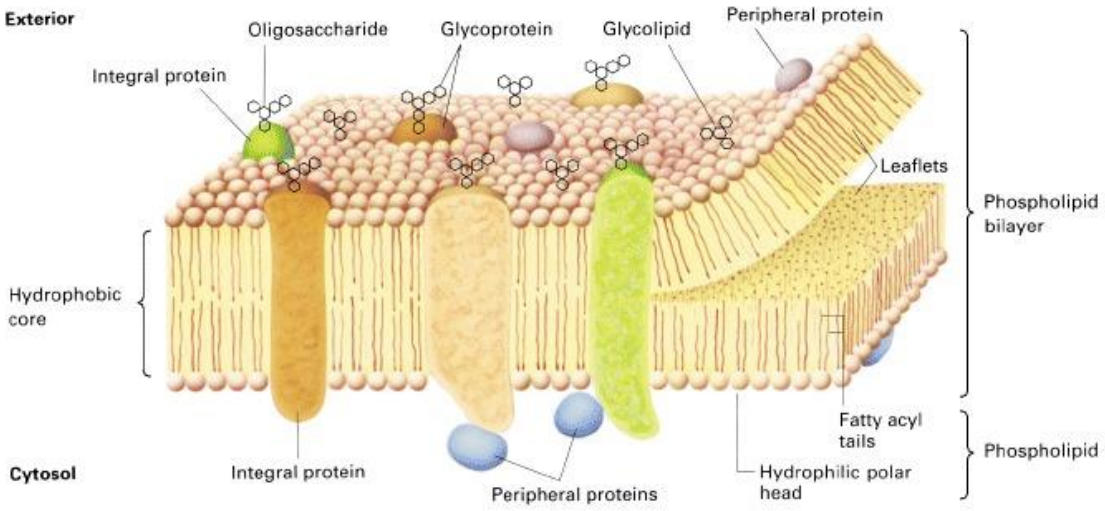

Figure 1.1: Schematic diagram of the structure of a typical biological membrane. The phospholipid bilayer, the main matrix of all cellular membranes, is made of two phospholipid leaflets whose fatty acyl tails form the hydrophobic core of the bilayer; their polar, hydrophilic head groups face the aqueous cytoplasm and extracellular environment. Integral proteins are embedded in the bilayer and peripheral ones are mainly associated with the membrane by specific protein-protein interactions. Oligosaccharides bind to membrane proteins and lipids, forming glycoproteins and glycolipids, respectively (Lodish H *et al*., 2000, *Molecular Cell Biology*, New York: W. H. Freeman, 4th edition).

As mentioned above, the fundamental matrix of the plasma membrane is the lipid bilayer, which is formed by phospholipids. Every phospholipid molecule is made of a hydrophilic head and a hydrophobic tail, as shown in Figure 1.2. The backbone of membrane lipids can be either the glycerol or the sphingosine, thus respectively forming the glycerophospholipids (GPLs) or the sphingophospholipids (SPLs). Within an individual glycerophospholipid, fatty acyl chains are attached to the C1 and C2 carbon atoms, while a phosphate group is attached to the C3 carbon atom of the glycerol molecule. Variable

polar groups are attached to the phosphate, such as choline, ethanolamine, serine, and inositol. Based on the type of polar head the major structural lipids in eukaryotic membranes are the phosphatidylcholine (PC), phosphatidylethanolamine (PE), phosphatidylserine (PS), phosphatidylinositol (PI) and phosphatidic acid (PA) when no polar group is attached to the phosphate. Sphingomyelin (SM) consists of a phosphocholine polar group and it is among the few phospholipids that contain a sphingosine molecule as a backbone, in the amine group of which a fatty acid is attached. The relative distribution of the phospholipids varies within the different cell types and tissues. However, PC is the most abundant (>50%) phospholipid in eukaryotic membranes.

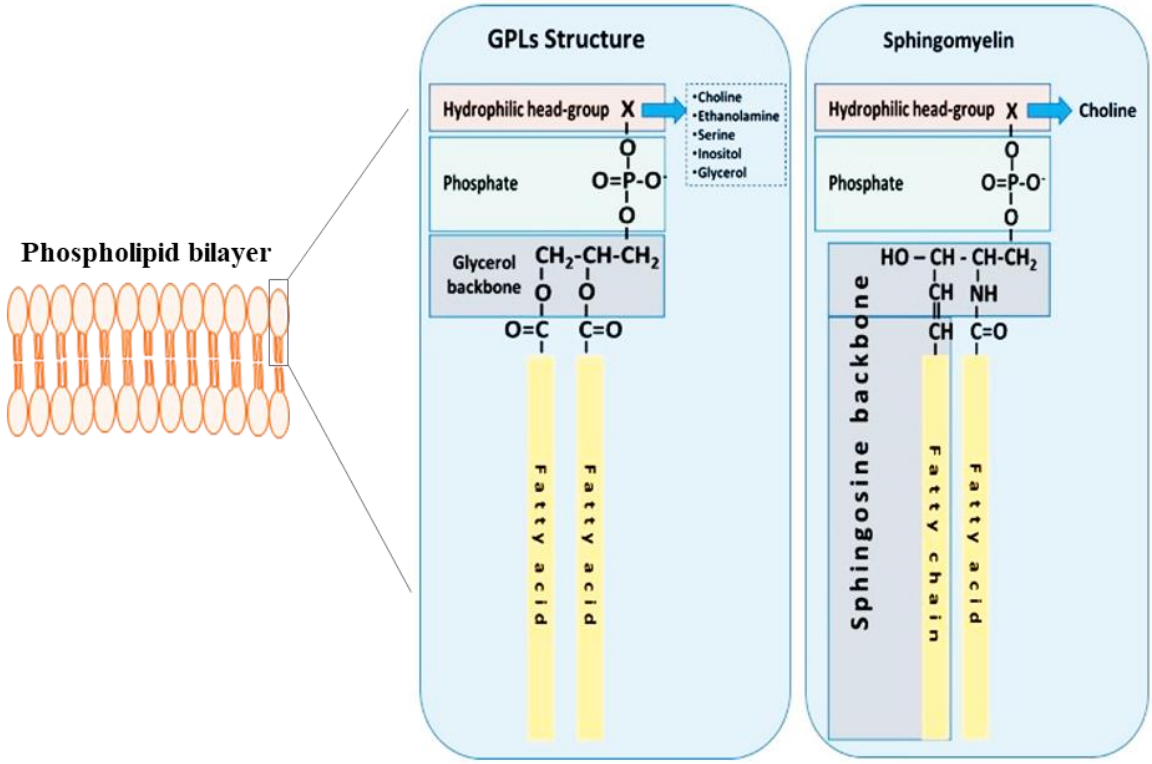

Figure 1.2: Common structures of glycerophospholipids (GPLs) with a glycerol backbone and sphingomyelin as a representative of a sphingophospholipid (SPLs). Modified from Lordan R *et al.*, 2017**,** *Molecules*, MDPI.

The phospholipids are asymmetrically distributed between the two leaflets of the membrane bilayer. The outer layer contains mainly PC and SM, whereas the inner leaflet consists mainly of PE and PS. The asymmetric lipid distribution between the two leaflets

contributes to curvature stress in biological membranes, which is useful for the membrane budding, fission and fusion [15] as well as the conformation of membrane proteins and modulation of their function. Polar lipid heads are involved with strong electrostatic interactions and hydrogen bonds with amino acid residues the interface surface of the membrane proteins and the charge and aqueous their microenvironment can affect the activity of peripheral membranes proteins [15-17]. The hydrophobic domain is a diacylglycerol (DAG) made of long fatty acid chains that usually range from 14 to 24 carbon atoms. The fatty acid tails can be either unsaturated (with one or more *cis* double bonds) or saturated (without any double bonds). Usually, within the hydrophobic domain, one chain is unsaturated and the second one saturated. Both the length and saturation degree of the fatty acid chains can influence the packing of the phospholipid molecules against one another, thus affecting the fluidity of the lipid bilayer. Considering the variety of phospholipids' headgroups and their combination with several different fatty acids, the content of individual phospholipid species can be relatively diverse. This results in increasing membrane's flexibility and may be needed for the numerous processes in which phospholipids have been reported to be involved [18].

1.1.1.2 Physicochemical properties

The plasma membrane is characterized by various physicochemical properties, such as the membrane thickness, lipid packing, fluidity, elasticity, permeability, flipflop, protein activity, fusion, blebbing and the structure and function of lateral and transmembrane domains. The kind of lipids building the biological membrane is a parameter that affecting most of these properties. However, it is reported that the physical properties of any lipid mixture are a collective property determined by the single lipid components [19]. The plasma membrane is constituted of a large variety of lipid molecules, each of them having different physical properties. As a result, every lipid moiety contributes collectively to the final properties of the membrane assembly. Several biophysical and biochemical studies on membrane lipids in parallel with genetic manipulation of membrane lipid composition have indicated that the L_α state of the membrane bilayer is required for cell viability and that cells adjust their lipid content in response to external factors in order that the collective property of the membrane exhibits the L_α state [19].

The physical and chemical properties of the membrane influence several cellular processes, thus suggesting that the lipids are not only structural components, but they also have a dynamic role in cell function [20, 21]. A key factor affecting the physicochemical properties of the membrane is the type of fatty acid moieties that are present to the phospholipid molecules [22]. The fluidity of the hydrophobic domains of the phospholipids is a function of the fatty acid chain structure and temperature [23], as depicted in Figure 1.3. At a given temperature the fluidity of the hydrocarbon core of the membrane bilayer increases with higher content of unsaturated alkyl chain or with smaller alkyl chain length. Most phospholipid molecules have one *cis*-unsaturated fatty acyl chain, which enables them fluid at room temperature. Higher temperature leads to increased mobility of the fatty acid chains, which in turn increases the fluidity and the space occupied by the hydrophobic domain of lipids.

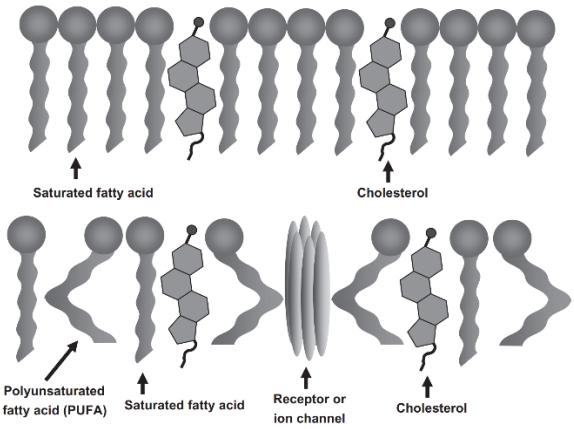

Figure 1.3: The structure of fatty acid chain influences the membrane fluidity. Saturated fatty acids form a more rigid and less fluid lipid bilayer due to the tight packing of the straight chains. The double bonds of unsaturated fatty acids create a bend in the fatty acid tail, thus leading to increased membrane fluidity. Modified from Jich et al. (2010) [24].

1.1.2 Membrane fatty acids

As mentioned above the major building block of membrane assembly is the phospholipid molecule whose hydrophobic tail contains usually two long fatty acid chains. The fatty acids (FA) are aliphatic chains with a carboxylic acid group (-COOH) at the end of the chain. Fatty acids naturally occurring in phospholipids commonly have a chain of 14 to 24 carbons (usually unbranched and even-numbered), which may be saturated or unsaturated.

Odd-numbered fatty acids are most frequent in bacteria and lower plants or animals [25]. In eukaryotes, the fatty acid chains are esterified to the positions C1 and C2 of the L-glycerol, as depicted in Figure 1.2. The acyl chain can vary in length and degree of unsaturation, thus affecting the properties of each moiety.

1.1.2.1 Nomenclature

For the precise description of a fatty acid molecule, the length of the alkyl chain, the number of double bonds and their exact position along the hydrocarbon chain must be defined. The exact annotation suggests the biological reactivity of each fatty acid moiety as well as of the lipid-containing the specific fatty acid molecule. There are several different naming systems used for the fatty acids [26, 27]. Amongst them are:

Trivial nomenclature

It involves the use of non-systematic historical names which are commonly used in literature. Most of the common FA have trivial names in addition to their systematic names. Trivial names do not contain any pattern or clue to the structure and they typically derive from a common source of the compound or the source from which it was originally isolated.

Systematic nomenclature

The systematic (or IUPAC) names follow the nomenclature rules of the International Union of Pure and Applied Chemistry. In the IUPAC system, carbon atoms numbering starts from the carboxylic acid end and the rest positions in the chain are denoted with reference to it. Double bonds are labelled with *cis*-/*trans*- or *E*-/*Z*- notation, respectively. These names describe the structures in detail and give a clear description of the FA chains. The systematic name used for a fatty acid is derived from the name of its parent aliphatic chain by substituting the suffix -e with -oic. For example, the C18 saturated fatty acid is called octadecanoic acid since its parent hydrocarbon is the octadecane. The C18 fatty acids that have one, two and three double bonds are named octadecenoic, octadecadienoic and octadecatrienoic acid, respectively. In the case of ionized or esterified fatty acids, it is more suitable to name them according to their carboxylate form: for instance, stearate or octadecanoate, instead of stearic or octadecanoic.

Shorthand nomenclature

This is another systematic way of naming the fatty acids. It is a carboxyl-reference system that indicates the number of carbons, the number of double bonds and the positions of the double bonds, counting from the carboxyl carbon (which is numbered 1, as in the IUPAC system). Lipid names take the form C:D, where C is the number of carbon atoms and D is the number of double bonds in the FA. For example, the notation 18:0 denotes a C18 fatty acid with no double bonds, whereas 18:2 signifies that there are two double bonds. This notation is sometimes puzzling since different FA can have the same shorthand nomenclature, like positional or geometrical isomers. Consequently, it is usually paired with an Δx term, where x is a number representing the position of the double bond (x^{th} carbon-carbon bond), counting from the carboxylic acid end. Each double bond is preceded by a *cis*-/*trans*- notation, indicating the configuration of the molecule around this bond. For instance, *cis*-Δ9 stands for a *cis* double bond between the carbon atoms 9 and 10; *trans*-Δ5 stands for a *trans* double bond between carbon atoms 5 and 6.

omega-reference system

The omega-x (ω−x or n-x) nomenclature does not provide names for individual compounds. It is applied when double bonds are present and indicates the position of the double bond closest to the omega carbon, which is numbered 1 in this case. According to the "omega nomenclature", as omega carbon is designated the terminal methyl carbon. This system is useful for the categorization of FA by their physiological properties since there are significant differences between omega-3 and omega-6 counterparts. For example, linoleic acid is classified as a ω−6 or omega-6 FA, and so it shares some properties with other members of the ω-6 family. The omega position of the first double bond is also helpful to avoid confusion in case of positional isomers (fatty acids differing just in the position of double bonds). Sometimes, the shorthand nomenclature contains the positioning of the first double bond from the omega end written in parenthesis, instead of the Δx term.

Table 1.1: List of main fatty acids naturally present in eukaryotic membranes, described by their shorthand, trivial and systematic nomenclature and their omega annotation. The melting point for each FA is also reported (values retrieved from https://pubchem.ncbi.nlm.nih.gov); na: not available.

C:D	Trivial name (x-acid)	IUPAC name (x-acid)	ω-n	Melting point (°)
Saturated Fatty Acids				
14:0	Myristic	Tetradecanoic	/	53.9
16:0	Palmitic	Hexadecanoic	/	61.8 - 63
18:0	Stearic	Octadecanoic	/	68.8 - 72
20:0	Arachidic	Eicosanoic	/	75.4
Monounsaturated Fatty Acids				
16:1	Sapienic	6*Z*-hexadecenoic	ω-10	na
16:1	Palmitoleic	9*Z*-hexadecenoic	ω-7	-0.1
18:1	Oleic	9*Z*-octadecenoic	ω-9	13.4 – 16.3
18:1	Vaccenic	11*Z*-octadecenoic	ω-7	39
20:1	Gondoic	11*Z*-eicosenoic	ω-9	na
Polyunsaturated Fatty Acids				
18:2	Linoleic	9*Z*,12*Z*-octadecadienoic	ω-6	-8.5
18:3	α-Linolenic	9*Z*,12*Z*,15*Z*-octadecatrienoic	ω-3	-16.5
18:3	γ-Linolenic	6*Z*,9*Z*,12*Z*-octadecatrienoic	ω-6	-11
20:3	Dihomo-γ-linolenic	8*Z*,11*Z*,14*Z*-eicosatrienoic	ω-6	na
20:4	Arachidonic	5*Z*,8*Z*,11*Z*,14*Z*-eicosatetraenoic	ω-6	-49
20:5	EPA	5*Z*,8*Z*,11*Z*,14*Z*,17*Z*-eicosapentaenoic	ω-3	-54
22:5	DPA	7*Z*,10*Z*,13*Z*,16*Z*,19*Z*-docosapentaenoic	ω-3	na
22:6	DHA	4*Z*,7*Z*,10*Z*,13*Z*,16*Z*,19*Z*-docosahexaenoic	ω-3	-44

1.1.2.2 Classification

In general, fatty acids can be divided according to a) the chain length into short (C2-8), medium (C8-10) and long (>C12), b) the degree of saturation into saturated and unsaturated, c) the biological value into essential and non-essential and d) the chain structure into aliphatic, branched and cyclic. Membrane fatty acids, which consist the hydrophobic domain of phospholipids, contain long aliphatic alkyl chains, with an even number of carbon atoms, typically atom ranging between 14 and 24. For this reason, further description of fatty acid classification in this chapter will concern only their saturation degree and their biological significance.

The hydrocarbon chain of membrane fatty acids can vary in the number of double bonds and thus be classified into saturated or unsaturated. The differences between saturated and unsaturated fatty acids, as well as the variation in geometry of unsaturated FA, determine the properties of membrane structure, thus influencing its microdomain organization and altering numerous cellular processes [21, 28].

Saturated fatty acids

Saturated fatty acids (SFA) do not contain any double bond along the alkyl chain. The term 'saturated' is used because all the carbon atoms contain as many hydrogen atoms as possible. The general formula of SFA is $CH_3(CH_2)_nCOOH$. The lack of any double bonds or other functional groups enable these fatty acids to be nearly chemically inert and thus subject to drastic chemical conditions, such as temperature and oxidation. In Figure 1.3, the structures of two representative members of the SFA family are depicted.

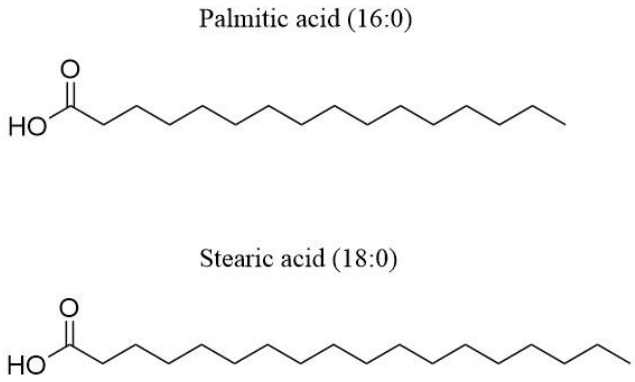

Figure 1.3: Molecular structure of representative members of saturated fatty acids (SFA) family. Palmitic (16:0) and stearic (18:0) acid are characterized by straight chains that differ in length by two carbon atoms.

Palmitic (16:0) and stearic (18:0) acid are the two most commonly occurring SFA. As shown in Table 1.1, the long SFA are characterized by high melting points, which means that they are in the solid state at room temperature. This physicochemical behavior is a consequence of their molecular structure (straight shape chains) that contributes to the high packing of SFA in phospholipid bilayer.

Unsaturated fatty acids

The hydrocarbon chain of unsaturated fatty acids (UFA) may contain one or more double bonds. Unsaturated fatty acids exhibit the positional and geometrical isomerism at the double bonds, which are characterized by *cis*-configuration in the majority of naturally occurring UFA. According to the number of double bonds, the unsaturated fatty acids can be further divided into mono- and polyunsaturated FA.

- Monounsaturated Fatty acids (MUFA)

  Monounsaturated FA contain only one double bond along the alkyl chain. The general formula of MUFA is $CH_3(CH_2)_xCH=CH(CH_2)_yCOOH$. The position of the unique double bond can vary a lot. The presence of the double bond increases the FA fluidity since a double bond in the *cis* configuration provokes a bend in the alkyl chain, as shown in Figure 1.4. This bending leads to a total spatial width of 0.72 nm for a *cis*-MUFA compared to the 0.32 nm one that characterizes the saturated structures.

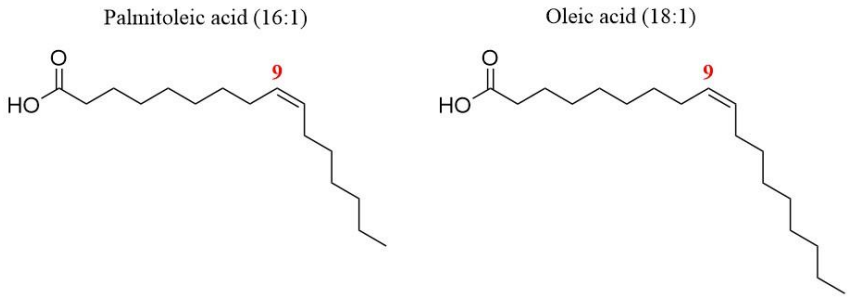

Figure 1.4: Molecular structure of representative members of monounsaturated fatty acids (MUFA) family. The formation of a double bond in Δ9 position creates a bend to the chain of palmitoleic (16:1-c9) and oleic (18:1-c9) acid.

Unlike the SFA that have the tendency to pack in a membrane structure, MUFA cause a higher molecular disorder due to their three dimensional shape. As a consequence, their presence in membrane assembly influences its fluidity and permeability [28]. MUFA have a lower melting temperature than SFA and they are in liquid state at normal temperature and semisolid or solid when refrigerated. Amongst the most common MUFA members are the palmitoleic acid (16:1,cis-Δ9), oleic acid (18:1,cis-Δ9) and vaccenic acid (18:1,cis-Δ11).

- Polyunsaturated Fatty acids (PUFA)

  Polyunsaturated FA contain two or more *cis* double bonds, which are usually separated from each other by a single methylene group (methylene-interrupted unsaturation) and have the general formula -C-C=C-C-C=C-. PUFA, as unsaturated fatty acids, have a more extended shape than SFA due to the presence of double bonds that increase the bending of the hydrocarbon chains. Therefore, PUFA have significantly lower melting points compared to other FA families, as presented in Table 1.1. PUFAs are important structural components and contribute to membrane fluidity and selective permeability [29]. The higher the degree of unsaturation in FA (more double bonds), the more susceptible they are to lipid peroxidation, whereas UFA can be protected from lipid peroxidation by antioxidants [30, 31]. Polyunsaturated fatty acids are usually divided into omega-6 (ω-6) and omega-3 (ω-3) series, based on the distance between the final methyl group and the closest double bond in the chain. Thus, starting the numbering from the omega carbon, the first double bond is at the position C6 and C3 for the ω6 and ω3 family, respectively. Figure 1.5 shows the molecular structure of representative members of each PUFA family.

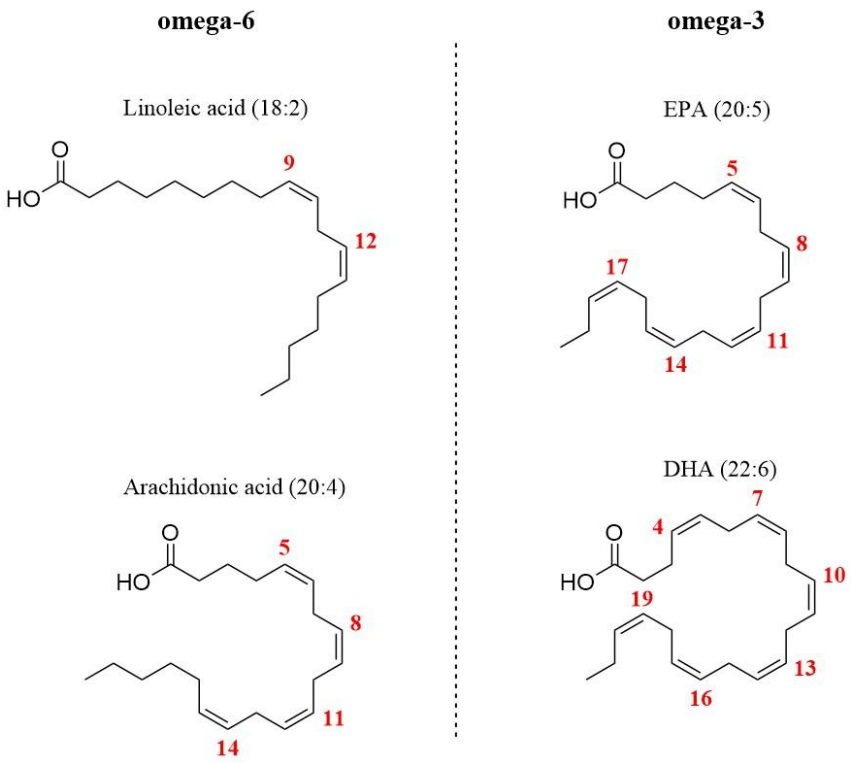

Figure 1.5: Molecular structure of representative members of polyunsaturated fatty acids (PUFA) family. PUFA have an extended shape due to the multiple double bonds and are generally divided into omega-6 and omega-3, based on the distance between the final methyl group and the closest double bond in the chain.

Geometrical isomerization

The double bond in unsaturated fatty acids can be either in *cis* or *trans* configuration (*Z*- or *E*-, respectively, according to IUPAC notation). In the *cis* configuration the two alkyl groups (R1 and R2) are on the same side of the double bond, where in *trans* geometry they are on the opposite sides (Figure 1.6). In eukaryotes, the double bond of unsaturated fatty acids has prevalently *cis* geometry. During fatty acid biosynthesis, the insertion of *cis* double bonds is catalyzed by desaturases, which act in a regioselective and stereospecific way [32]. The *trans* geometry is not naturally present since these eukaryotic enzymes are not capable to form *trans* double bonds or catalyze their *cis-trans* isomerization. The loss of the natural *cis* geometry changes dramatically the molecular shape of the fatty acid chain, thus affecting several membrane properties, such as the diameter, fluidity and permeability [33, 34]. For instance, elaidic acid (9*trans*-18:1), which is the geometrical isomer of oleic acid (9*cis*-18:1), is characterized by linear alkyl chain instead of the typical bending structure of MUFA, as shown in Figure 1.6.

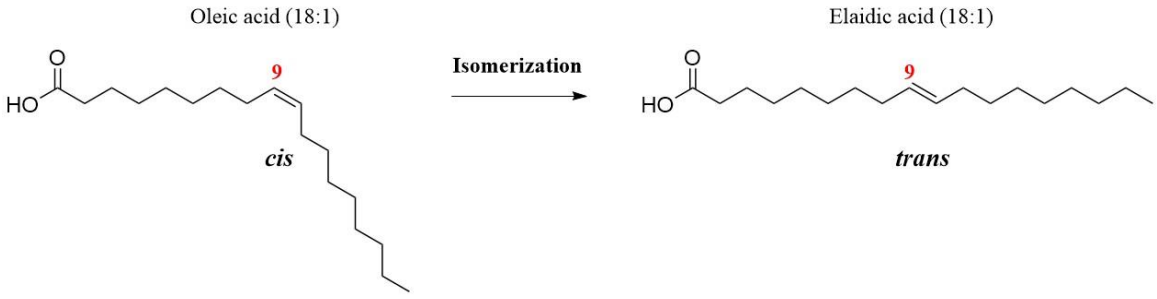

Figure 1.6: Example of geometrical *cis-trans* isomerization in fatty acids. The configuration of the double bond influences the shape of the alkyl chain; *cis* geometry produces a kink in the molecule, while *trans* geometry favors a linear carbon chain.

Trans fatty acids (TFA) usually originate from processed food products (deodorized or partially hydrogenated) [35, 36]. Another dietary source of TFA is the consumption of dairy products and meat due to the microbial biohydrogenation that takes place in the stomach

of ruminants [37]. Contrary to eukaryotes, some Gram-negative bacteria have the ability of endogenous *cis–trans* isomerization as a response to environmental stress conditions [38]. In eukaryotic cells, the conversion of the natural *cis* fatty acids to their *trans* isomers may occur endogenously under stress condition and involves a thiyl radical catalytic mechanism [39-41].

1.1.2.3 Biosynthetic vs essential fatty acids

Mammals can synthesize saturated and monounsaturated fatty acids, but they are unable to synthesize FA containing more than one double bond (PUFA). Indeed, they lack the enzyme system that is responsible for the introduction of a double bond in a monounsaturated alkyl chain. Consequently, the fatty acids not being synthesized by the organism should be supplied through diet and are known as essential or semi-essential FA.

De novo biosynthesis

In adult humans, the *de novo* synthesis of fatty acids is taking place mainly in the liver, adipose tissue and lactating breast [42]. The fatty acids that contain up to 16 carbon atoms are synthesized by the fatty acid synthase (FAS). FAS is a cytoplasmic enzyme that is composed of two similar subunits (~250 kDa each) and acts as a multifunctional complex. It is characterized by seven different enzymatic activities within two catalytic centers. Fatty acid synthesis by FAS is initiated by the condensation of an acetyl-CoA and malonyl-CoA molecule, while NADPH serves as the reductant in this process. The addition of a two carbon-unit from malonyl-CoA is repeated seven times in a cyclic manner, thus leading eventually to the production of the saturated C16 fatty acid (palmitic acid) [43-45]. Due to the mechanism of their *de novo* biosynthesis, most of the natural FA have an even number of carbon atoms. The palmitic acid is the starting point for the biosynthesis of other fatty acids, which is catalyzed by a set of microsomal enzymes generating modified alkyl chains; elongated or desaturated ones (see Figure 1.7). The fatty acids produced by FAS, as well as those originated from the diet, can be further elongated into very-long chain fatty acids (VLCFA) containing more than 18 carbon atoms. The overall elongation reaction takes place mainly in the endoplasmic reticulum (ER) by four membrane-bound enzymes. The enzymatic steps involved in this process are similar to the synthesis of palmitate since

malonyl-CoA and NADPH are respectively used as an intermediate and reductant. The proteins performing the successive steps of VLCFA extension are individual molecules, which could be physically associated, contrary to the FAS multi-enzyme complex [46, 47]. Three of the four enzymatic activities in VLCFA elongation are localized to the cytoplasmic side of ER membranes, while the enzyme performing the third step is suggested to be embedded in the membrane [48]. In humans, seven enzymes (ELOVL 1–7) have been identified with the ability to elongate the >16C fatty acid chains into VLCFA [49]. Despite the capability of all the seven elongation enzymes to catalyze the condensation reaction in the elongation cycle, they are characterized by differential substrate specificity and tissue distribution [50]. In addition, palmitate and other long FA can be further processed by acyl-CoA desaturases that can modify the structure and properties of long-chain fatty acids by introducing a double bond at a specific position on the acyl chain [51]. An ER-bound enzymatic complex including NADH-cytochrome b5 reductase, cytochrome b5 and a desaturase catalyzes the desaturation. These enzymes use molecular oxygen, as an electron acceptor, while in this case the NADH is the reducing agent. [52-54]. Mammalian cells express three different desaturases that are generally divided into two distinct families: stearoyl-CoA desaturases (SCDs) [55] and fatty acid desaturases (FADS) [56]. Human desaturases catalyze the introduction of a double bond at specific positions (Δ9, Δ6 and Δ5) into the saturated fatty acyl-CoA chain. SCDs, also known as Δ9 desaturases, catalyze the insertion of a single double bond at the carbon C9 (counting from the carboxylic acid group). The oleic and palmitoleic acids are the main products of SCDs synthesized by the desaturation of the SFA stearic and palmitic, respectively. In humans, two SCD isoforms (SCD1 and SCD5) have been identified, with the SCD1 being the most commonly expressed among tissues [57]. FADS1 and FADS2, which respectively have Δ5- and Δ6-desaturase activities are mainly involved in the PUFA biosynthetic pathways, as described later in this paragraph. However, FADS2 can potentially also act on palmitic forming the sapienic acid (*cis*-6 hexadecenoic), which is reported to be the most abundant fatty acid in human sebum [58]. The formed MUFA may undergo further elongation by the previously-mentioned elongation system. For example, palmitoleic (C16-Δ9) can be converted to the *cis*-vaccenic (C18-Δ11) and oleic (C18-Δ9) to gondoic acid (C20-Δ11). Consequently, this chain extension ‘shifts’ the position of the double bond by two carbon atoms, since the elongation occurs in the carboxyl terminus. Finally, it is worth mentioning that the intracellular fatty acid pool is enriched not only by

the endogenously synthetized FA but also by those obtained through the dietary habits of each individual.

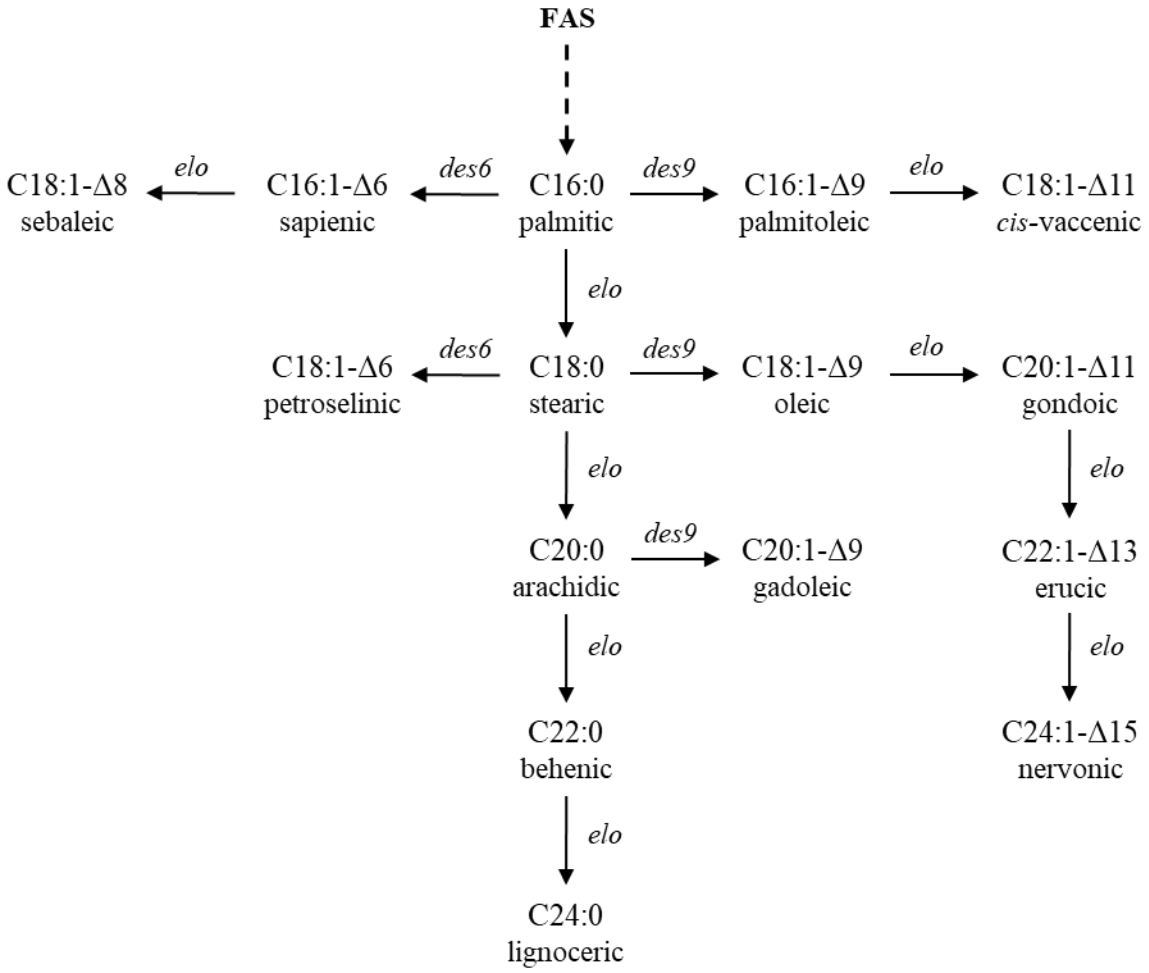

Figure 1.7: The biosynthesis pathways of SFA and MUFA family. Palmitic acid is synthesized by recurring reactions catalyzed by the enzymatic complex FAS. Elongases (*elo*) or desaturases (*des6/9*) can further modify the alkyl chain of palmitic acid and its downstream products. SFA: saturated fatty acids; MUFA: monounsaturated fatty acids; FAS: fatty acid synthase.

Essential fatty acids

Despite their ability to synthesize saturated and monounsaturated fatty acids, animals are not capable to produce *de novo* polyunsaturated FA because they lack the required enzyme system that further desaturases oleic acid (18:1-Δ9) into linoleic acid (LA, 18:2-ω6) and α-linolenic acid (ALA, 18:3-ω3) [59]. Therefore, these two PUFA moieties are considered as dietary essential fatty acids as they cannot be endogenously synthesized. However, they

themselves or their metabolic derivatives play an important role in human health and development by being involved in numerous biological functions [60, 61]. For instance, arachidonic acid (20:4-ω6), a metabolic derivative of linoleic acid, is the precursor molecule for the synthesis of prostaglandins by the cyclooxygenase enzyme system and leukotrienes by the lipoxygenase pathway in leucocytes [62]. The other members of PUFA family can be provided either through the dietary intake or synthesized from the nutritionally essential fatty acids (LA and ALA). LA and ALA are the starting points of PUFA biosynthesis in humans and can be further modified by the activity of desaturases and elongases, as depicted in Figure 1.8 [63]. As previously mentioned, PUFA can be divided into the omega-6 and omega-3 families, based on the position of the double bond closest to the methyl end of the alkyl chain. The precursors of these families (LA for ω-6 and ALA for ω-3) can be transformed to more highly unsaturated FA by a series of common elongation and desaturation reactions in ER [64]. FADS1, FADS2 are the key desaturases in PUFA biosynthesis. For example, arachidonic acid (ARA), a long-chain ω-6 PUFA, is synthesized from LA, through the following successive reaction steps: the addition of a double bond by Δ6-desaturase to form γ-linolenic acid (GLA, 18:3-ω6), the elongation of GLA to form dihomo-γ-linolenic acid (DGLA, 20:3-ω6) and finally the addition of another double bond by Δ5-desaturase to form eicosatetraenoic acid (ARA, 20:4-ω6) [65]. Similar desaturation and elongation steps are utilized for the formation of eicosapentaenoic acid (EPA, 20:5-ω3), a member of omega-3 family. In higher eukaryotes for the synthesis of DHA, a downstream derivative of EPA, the latter is elongated to DPA-ω3 which is further elongated into tetracosapentaenoic acid (TPA, C24:5-ω3) and then TPA is desaturated to form ω3-tetracosahexaenoic acid (THA, C24:6-ω3) by a Δ6-desaturase. Finally, the THA undergoes beta-oxidation in peroxisomes to form the DHA-ω3 [66, 67]. On the contrary, lower eukaryotes are able to elongate the EPA-ω3 into DPA-ω3 and then desaturate the latter into DHA-ω3 by the Δ4-desaturase, an enzyme that is not present in mammals [68]. PUFA family members, such as ARA and DHA are considered as semi-essential fatty acids, since they can be synthesized endogenously by their precursors (LA or ALA). Semi-essential FA turn into essential ones in case their precursors are missing from the diet. Interestingly, *in vitro* studies in glioma cells have shown that the occurrence of double bonds with *trans* configuration in PUFA influences the metabolic fate of the latter by affecting the processes of desaturation and elongation in the fatty acid chain [69, 70].

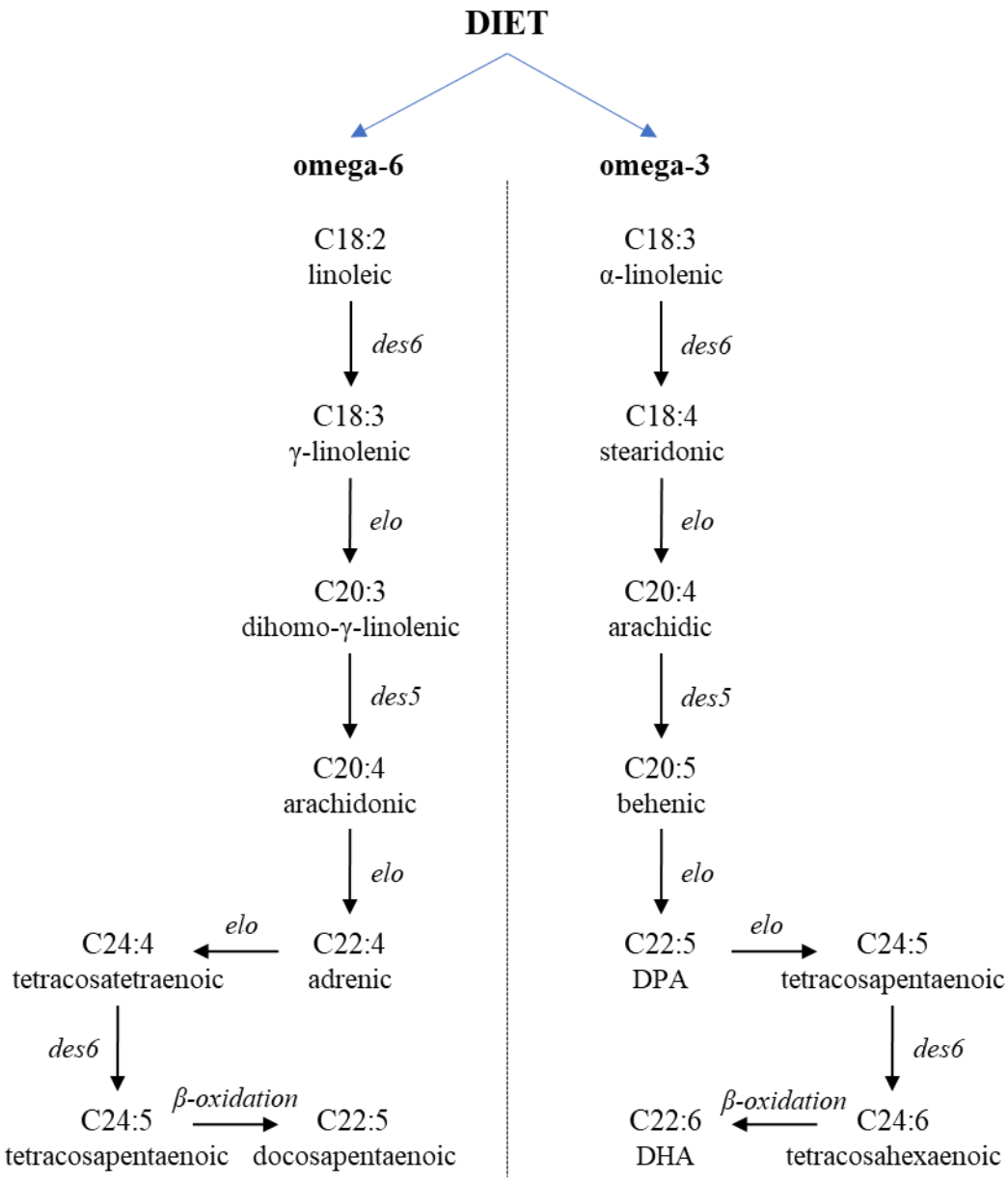

Figure 1.8: PUFA biosynthesis in mammals. Linoleic (LA) and α-linolenic (ALA) acids are respectively the precursors of omega-6 and omega-3 family. LA and ALA are further converted to long chain fatty acids using a series of desaturation and elongation reactions in the endoplasmic reticulum. The final products of omega-6 and omega-3 biosynthetic pathways, DPA-ω6 and DHA-ω3, respectively, are formed by β-oxidation in peroxisomes. Modified from Lauritzen et al. (2001) [71]. *elo*: elongase, *des5/6*: Δ5-/6-desaturase.

1.1.3 Membrane role in cell proliferation and survival related signaling

Membrane lipids can affect both the 3D structure and the function of membrane-associated protein molecules through the protein-lipid interactions and the lipids' self-association properties. The chemical and structural characteristics of phospholipids, such as the type of polar head, the alkyl chain length and unsaturation degree, can influence the specific protein-lipid interactions. Moreover, the lipids organization within the membrane assembly plays an important role regarding several of its properties, such as its fluidity, thickness and packing, also affecting the function of membrane proteins [19].

Besides serving as the building blocks of cellular membranes, fatty acids also contribute to the modulation of intracellular signaling pathways related to cell proliferation and survival [72]. Diverse external stimuli can induce the hydrolysis of sphingolipids or glycerophospholipids and lead to the formation of biologically active lipids, which can function as second messengers in the regulation of cell viability, mobility and inflammation [73]. Such examples of messenger lipids are the sphingosine 1-phosphate (S1P), lyso-phosphatidic acid (LPA), inositol-trisphosphate (IP3) and DAGs, amongst others [74, 75]. The lipid signaling molecules can either get easily released from the membrane and act through membrane-related receptors [76], or can remain in the membrane and recruit cytosolic proteins [77]. LPA can also be formed extracellularly by the secreted phospholipase A2 (PLA2) or the lysophospholipase autotaxin (ATX), thus exerting both autocrine and paracrine signals [73, 78]. Since the membrane remodeling process, known as Lands' cycle [79] takes place constantly, the composition of the intracellular lipid pool influences the phospholipids turnover and their fatty acid content. LPA contains one acyl chain that can belong to any family SFA, MUFA or PUFA, with the palmitoyl group (16:0-LPA) being the most prevalent [78]. However, the acyl chain's length and the unsaturation degree have been reported to affect the affinity of LPA receptor and its ligand [80], while only unsaturated FA containing-LPA was able to induce chemotaxis of immature dendritic cells [81].

The biological properties of the individual FA moieties also play significant role in the fatty acylation of proteins, such as the N-myristoylation and S-palmitoylation. Fatty acylation is a post-translational modification regulating protein function (protein-protein and protein-lipid interactions) as well as its intracellular trafficking and localization [82]. A profound example is the WNT proteins, which participate in the development and tissue homeostasis

related signaling [83]. The optimal function of WNT proteins requires their post-translational S-palmitoleoylation by the membrane-bound O-acyltransferase porcupine [84]. Interestingly, β-catenin, a downstream transcriptional factor of Wnt pathway, is protected from proteasomal degradation by unsaturated fatty acids [85].

PUFAs also serve as precursors for the eicosanoid synthesis [62]. Eicosanoids are lipid mediators that regulate a wide range of physiological processes [86, 87] and therefore have profound effects on various pathological conditions [88]. In particular, ARA and EPA are released from cell membrane by phospholipases (mainly cPLA2) and then serve as the substrates of cyclooxygenase 1 (COX1) and lipoxygenase1 (LOX1). COX and LOX enzymes are responsible for the synthesis of prostaglandins and leukotrienes, respectively [89]. Eicosanoids usually interact with plasma or nuclear membrane receptors and are key effector molecules in inflammation, autoimmunity and cancer [89, 90]. Furthermore, the release of ω-6 PUFA from membrane favors the activation of signaling pathways related to cell proliferation and apoptosis [91, 92].

Finally, cardiolipin is a dimeric phospholipid in the inner mitochondrial membrane that undergoes continuous remodeling. Its participation in signaling platforms during the induction of apoptosis has been indicated by influencing the activity of the pro-apoptotic Bcl-2 proteins as well as the autoprocessing of caspase-8 [93]. Cardiolipin's acyl chain composition is known to affect several aspects of mitochondrial function. In particular, the binding of cytochrome *c* in the inner mitochondrial membrane is influenced by the characteristics (length and saturation level) and oxidative state of cardiolipin's acyl chains [94].

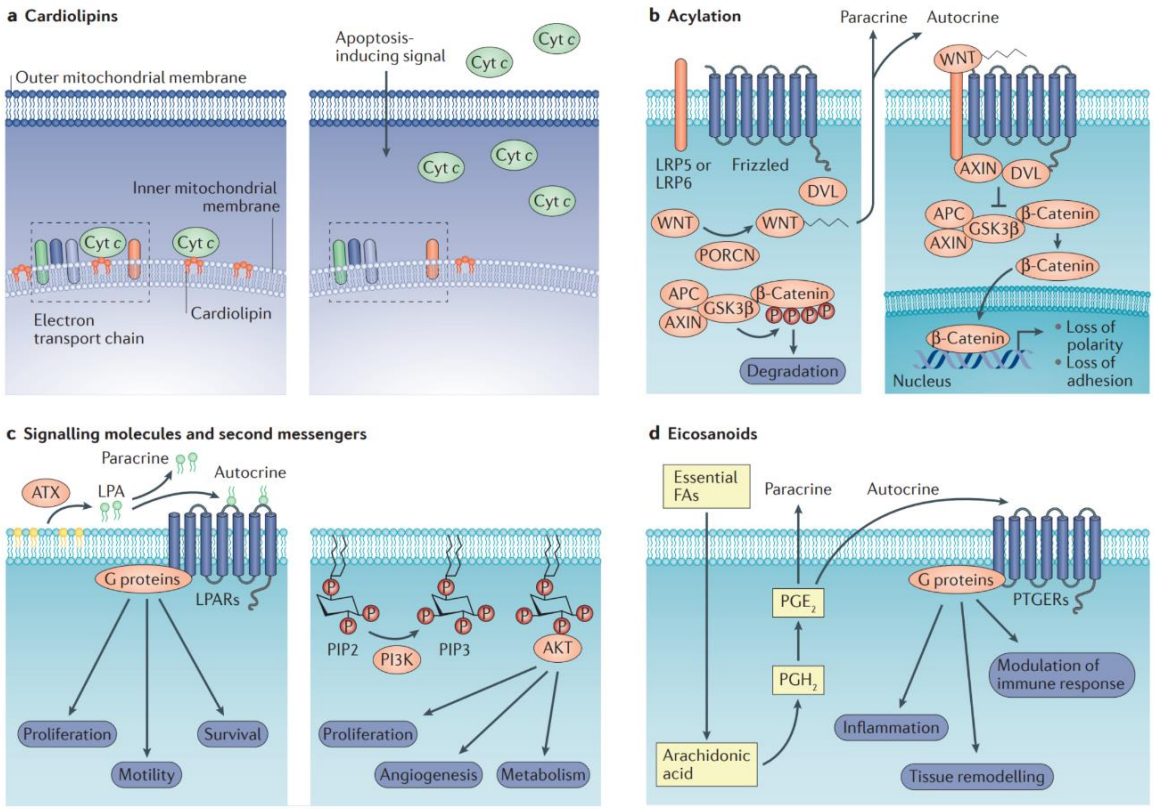

Figure 1.9: Examples of fatty acids' multifaceted contribution to intracellular signaling processes and regulation of apoptosis; (a) Mitochondrial membrane composition affects the sensitivity to apoptotic signals; (b) Acylation of WNT protein triggers its secretion and thus activates the WNT-β-catenin pathway; (c) Extracellular phospholipase autotaxin (ATX) releases lysophosphatidic acid (LPA) facilitating the autocrine signalling through LPA receptors (LPARs). Activation of the AKT signaling through the production of the second messengers PIP3 (phosphatidylinositol-3,4,5-trisphosphate); (d) Arachidonic acid serves as the substrate for prostaglandin E_2 production leading to the regulation of inflammation and immune response. Modified from Röhrig F. *et al.* (2016) [72]

1.2 Membrane lipidome in cancer

Metabolic reprogramming is an established hallmark of cancer that facilitates tumor growth [95, 96]. The deregulation of cellular metabolism and the acquisition of new metabolic features enable the cancer cells to sustain the continuous cellular growth and proliferation and effectively support their dissemination [97]. Cancer metabolic modifications include altered glucose metabolism, enhanced pentose phosphate pathway, elevated amino acid and lipid metabolism, increased mitochondrial biogenesis and macromolecules biosynthesis, amongst others [98-100]. Cancer cells are characterized by increased lipid metabolism due

to their elevated proliferation rate [101]. Lipids are the major building blocks of membrane and play an important role in energy storage and cell signaling. Consequently, the actively proliferating tumor tissues require higher amounts of lipids to satisfy their structural and functional needs [102, 103].

1.2.1 Altered fatty acid synthesis in cancer

Cancer development is characterized by a distinct lipid metabolism as well as a fatty acid one [95, 103]. It is well known that the transformation of membrane lipid composition affects its fluidity, permeability as well as membrane lipid-related signaling, and can give favorable signals for tumor growth, progression and metastasis [72, 96, 97]. Membrane remodeling is affected by the intracellular lipid pool, which depends on both the endogenous fatty acid biosynthesis and the dietary intake, especially for the essential polyunsaturated fatty acid (PUFA) supply. Thus, membrane fatty acid composition is influenced by a combination of stabilized nutritional conditions and metabolic status [104]. Tumor initiation and propagation are characterized by an altered activity of enzymes involved in lipid biosynthesis, such as fatty acid synthase (FASN) and desaturases (SCD1, FADS1, FADS2). Indeed, together with the corresponding fatty acids, the increased enzymatic activities are pointed as significant markers of tumor presence and growth [42, 72, 105, 106].

Fatty acid synthase (FASN) is the major lipogenic enzyme in humans since it is responsible for the *de novo* fatty acid synthesis. The upregulation of the endogenous fatty acid production has been reported by numerous studies [102, 103]. More particularly, overexpression and enhanced activity of FASN has been detected in various types of cancer, such as breast, ovarian, colorectal and prostate [42, 107, 108] [109-114]. Furthermore, elevated levels of FASN expression have been associated with poor prognosis and tumor aggressiveness [115-118]. Some studies support the hypothesis that the overexpression of *Fasn* gene may lead to neoplastic or malignant cell transformation by enhancing the lipogenesis along with increased cell growth and proliferation [119]. The expression of FASN is also elevated in proliferating fetal cells, thus suggesting that stimulated FASN activity might correspond to a less differentiated cell phenotype in tumor. [120]. Moreover, interaction between fatty acid synthase and human epidermal growth receptor 2 (HER2) in osteosarcoma cells has been reported [121]. FASN inhibition induces

programmed cell death in both in vitro and in vivo cancer models and suppresses the overexpression of the HER2/neu (erbB-2) oncogene and tyrosine-kinase activity in breast and ovarian cancer [122, 123]. FASN activity leads to the synthesis of the palmitic acid which besides its role in energy metabolism exerts pleiotropic effects on cellular function, as summarized in Figure 1.9 [42].

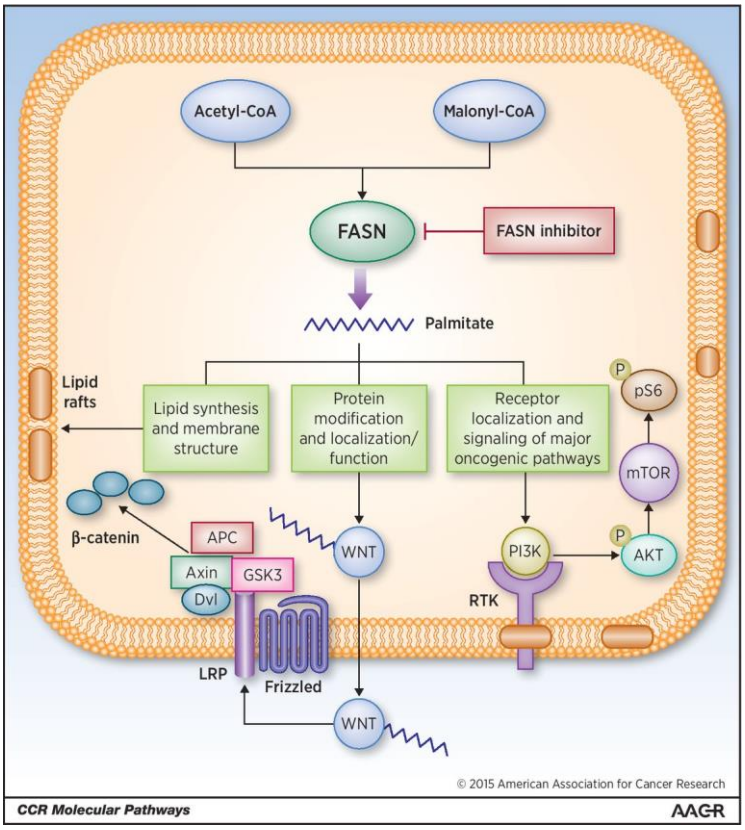

Figure 1.9: FASN-catalyzed synthesis of palmitic acid plays an important role in tumorigenesis. Palmitate is either incorporated in more complex lipid structures or conjugated to proteins. Its presence regulates the proper localization and function of several receptors that are involved in oncogenic signaling platforms. Modified from Jones *et al.* (2015) [124].

Palmitate can be incorporated to more complex lipids, such phospholipids, thus facilitating the membrane synthesis and cellular growth. In addition, it can be conjugated to proteins leading to their post-translational acylation, which in turn determines protein's localization and function [84, 125]. Correlation between palmitic acid occurrence and the proper function of important oncogenic signaling platforms, like the PI3K/AKT/mTOR pathway, has also been reported [124].

The significance of stearoyl-CoA (SCD1) in tumor development has also been thoroughly studied, since accumulation of monounsaturated fatty acids (MUFA) is a main feature in metabolic deregulation [126-129]. Being a key enzyme in lipogenesis regulation and responsible for MUFA synthesis, SCD1 activity supports the rapid cell growth and proliferation in cancer [42]. Furthermore, it contributes to the evasion of apoptosis, as well as to the tumor cell initiation and transformation, since it is involved in intracellular signaling, such as the PI3K-Akt and AMPK pathway [128, 130, 131]. Several studies have reported elevated expression levels of SCD1 desaturase in diverse types of cancer, such as breast, lung and prostate [132-136]. Inhibition of SCD1 activity not only reduces lipid biosynthesis, but also blocks cell cycle progression and induces cell apoptosis [137, 138]. On the contrary, dietary supplementation with oleic or palmitoleic, which are the metabolic products of SCD1, reversed cell proliferation blockage and restored intracellular lipids [137]. Examination of the mechanisms accompanying SCD1-mediated cancer progression by Chen *et al*. revealed a crosstalk between upregulated ceramide biosynthesis and SCD1 inhibition in *in vivo* models of colorectal cancer [126]. Aiming at revealing the mechanisms underlying the cancer stemness, Noto *et al.* proved that SCD1 interacts with the Hippo signaling pathway. In particularly, it regulates the activity of YAP and TAZ through the Wnt/β-catenin pathway, thus contributing to the propagation of lung cancer stem cells [127]. Spheroids formed in primary cell cultures derived from lung adenocarcinoma patients express higher levels of SCD1 in comparison to the adherent cells [128]. In line with these findings, higher levels of unsaturated lipids were detected in ovarian cancer stem cells compared to non-stem cancer cells and were positively correlated with *in vitro* sphere formation efficacy and *in vivo* tumor initiation [128, 139]. Desaturases expression is controlled by the nuclear factor kappaB (NF-kB) and in turn their activity affects the NF-kB pathway [139]. Moreover, Zhang *et al.* showed that the epidermal growth factor receptor (EGFR) binds and phosphorylates the SCD1 at Y55. This EGFR kinase activity is proved to be important for SCD1's protein stability, intracellular MUFA levels and lung cancer growth [129]. The same group also proved a positive correlation between EGFR activation, SCD1 protein expression, SCD1 Y55 phosphorylation and poor patient prognosis in patients with non-small cell lung cancer [129]. High levels of SCD1 expression have also been correlated with low overall survival in breast cancer and hepatocellular carcinoma patients [140, 141]. Overall, stearoyl-CoA desaturase-1 has been characterized as a central regulator in the orchestration of the complex metabolic and signaling events that govern cancer cells [131, 142]. Igal RA has reviewed numerous

experimental, clinical and epidemiological data on the role of SCD1 activity in tumor phenotype and has hypothesized a model for its implication in cancer, as presented in Figure 1.10.

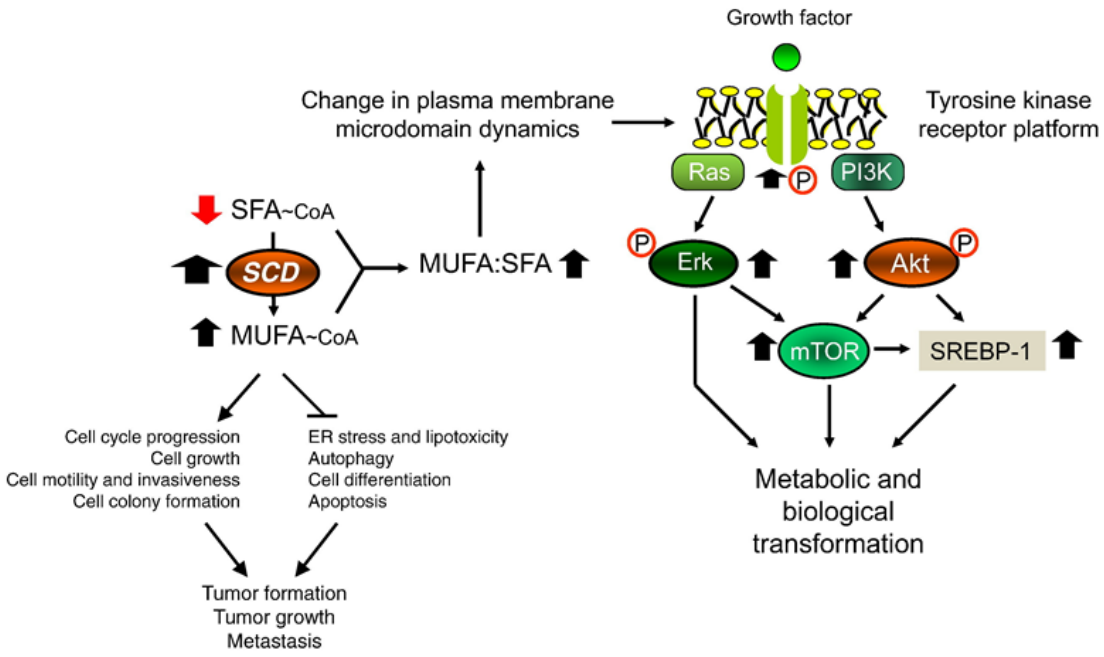

Figure 1.10: A hypothetical mechanism for the crosstalk between oncogenic signals and metabolic pathways controlled by SCD1 in cancer onset and progression. MUFA, monounsaturated fatty acids; SFA, saturated fatty acids; SCD, Stearoyl-CoA Desaturase. Modified from Igal RA (2016).

According to this hypothesis, SCD1 may regulate important signaling pathways that are involved in the survival and proliferation of tumor cells and supports the concept of the dynamic interplay between oncogenic signals and metabolic pathways. The enhanced desaturase activity leads to increased MUFA to SFA ratio in plasma membrane, thus influencing the fluidity of non-raft microdomains. These relatively more fluid membrane microdomains may favor the oncogenic transformation through the modulation of signaling platforms, such as the PI3K/Akt, mTORC, AMPK and Wnt pathways [143-146]. In addition, the conversion of SFA into MUFA by the SCD1 might have a protective impact on cancer cells by preventing lipotoxicity events caused by SFA excess that would lead to cell stress response and the consequent programmed cell death [147, 148].

Other enzymes, involved in endogenous FA biosynthesis, have been reported to be important in tumorigenesis. For instance, the ATP citrate lyase (ACLY), which is activated by Akt, has been proved to be crucial for tumor development and progression in *in vitro* and *in vivo* studies [149, 150]. The acetyl-CoA carboxylase (ACC) induces cancer growth in prostate cancer cells [151]. Furthermore, the sterol regulatory element-binding proteins (SREBPs), which are transcription factors controlling the expression of genes involved in FA synthesis, are overexpressed in cancer [42, 152]. Both SREBP and ACC are suppressed by AMPK [153]. Finally, cancer cells form more lipid droplets than normal cells [154].

Finally, it is worth noting that fatty acid synthesis in cancer cells is mainly regulated through hormones or oncogene signaling, and not by the diet like in the case of lipogenic tissues. Although cancer cells are able to incorporate exogenous fatty acids, they are characterized by a highly active *de novo* fatty acid biosynthesis. This increased FA production could be attributed to the limited availability of nutrients in tumor microenvironment.

1.2.2 Fatty acid composition of tumor patients' erythrocytes

As described previously, the fatty acids exert multifaceted roles on the development and progression of cancer [72]. In this regard, several studies have examined the association between the fatty acid composition in human tissues and the risk of tumor occurrence [133, 155, 156]. The families of SFA and MUFA may be considered as markers of FA metabolic turnover, since they are endogenously synthesized. On the other hand, PUFA could represent the dietary FA intake since they are either essential or semi-essential lipid species [104]. Being an easily withdrawn human tissue, blood has been often examined for its fatty acid composition. The Table 1.2. summarizes the results of studies analyzing the correlation between RBC membrane FA content and tumor risk. Although some controversies arised among the reported findings, some trends can be presumed in the FA composition of erythrocyte's phospholipids and cancer risk. Increased levels of oleic, SFA and omega-6 PUFA content show a positive correlation with tumor occurrence. In contrast, EPA, DHA and total omega-3 PUFA content are inversely associated to cancer risk.

Table 1.2: Summary of published studies examining the association between fatty acid composition in erythrocyte's membrane and tumor risk. DGLA, dihomo-γ-linolenic acid; DHA, docosahexaenoic acid; EPA, eicosapentaenoic acid; FA, fatty acids; GLA, γ-linolenic acid; LA, linoleic acid; MUFA, monounsaturated fatty acids; PUFA, polyunsaturated fatty acids; SFA, saturated fatty acids.

Cancer type	Positive correlation	Negative correlation	N	Country/ State	Reference
Breast	Oleic MUFA	PUFA total SFA/MUFA	71	Italy	Pala *et al.* [157]
Breast	Palmitic Palmitoleic Vaccenic GLA	EPA PUFA-ω3 SFA/MUFA	322	China	Shannon *et al.* [158]
Breast	SFA SFA/PUFA-ω3	EPA DHA PUFA-ω3	103	Japan	Kuriki *et al.* [159]
Breast	-	LA Arachidonic	46	Russia	Zaridze *et al.* [160]
Colorectal (adenoma)	Oleic DGLA	EPA DHA	328	France	Cottet *et al.* [161]
Colorectal (adenoma)	Arachidonic	EPA	904	Tennessee	Rifkin *et al.* [162]
Colorectal	-	PUFA-ω3	13	Italy	Coviello *et al.* [163]
Colorectal	Palmitic SFA SFA/PUFA	Arachidonic DHA PUFA total	74	Japan	Kuriki *et al.* [164]
Colorectal	-	EPA	61	Japan	Okuno *et al.* [165]
Gastric	-	DHA PUFA-ω3	179	Japan	Kuriki *et al.* [166]
Gastro-intestinal	Stearic DHA PUFA-ω3	Oleic LA MUFA	50	China	Lin *et al.* [167]
Multiple myeloma	SFA PUFA-ω6	MUFA PUFA-ω3 *trans* FA	43	Poland	Jurczyszyn *et al.* [168]
Ocular melanoma	-	Stearic/Oleic	19	UK	Aclimandos *et al.*[169]
Skin SCC	Arachidonic	Palmitic Palmitoleic	335	Arizona	Harris *et al.* [170]
Various	Oleic	Stearic	255	Kansas	Mikirova *et al.* [171]
Various	-	Stearic/Oleic	60	UK	Wood *et al.* [172]

A parallel analysis of breast tissue and erythrocytes FA composition of women with breast cancer indicated a positive association regarding the long-chain PUFA-ω3, while no significant correlation was revealed for their diet-derived precursor, alpha-linolenic acid [173]. Furthermore, the examination of the breast adipose tissue indicated that linoleic and arachidonic acid were increased in women with breast cancer compared to control group [174]. Another comparative study examined the differences on the tumor tissue's FA

content between patients with metastatic and non-metastatic colorectal cancer [175]. Notarnicola *et al.* showed that metastatic patients were characterized by lower levels of EPA and higher percentages of GLA in tumor tissues. However, no significant differences were revealed in their RBC membrane profiles. Finally, both the white blood cells (WBC) and the red blood cells of chronic leukemia patients presented lower saturation indices (stearic:oleic) than controls [176]. Similarly reduced saturation index has been also found in malignant liver neoplasms [177].

1.2.3 Antineoplastic agents affecting membrane's structure and properties

Like other xenobiotics, several antineoplastic agents have been recently reported to influence the physical and functional properties of the plasma membrane, such as fluidity and composition [178-181]. The changes in plasma membrane characteristics trigger the activation of signaling pathways that in turn influence the cell fate [179]. Since chemotherapy-induced cell death is mediated via signaling through plasma membrane (e.g. lipid rafts involving the death receptor pathway), attention has been given to the changes that membranes undergo upon cellular death [178, 181]. Therefore, affecting the metabolism of plasma membrane's building blocks might influence the tumor cellular growth and the related lipid signaling. For example, it has been reported that the regulated biosynthesis of SFA and MUFA can influence the biophysical properties of the tumor cell membrane and thus the signaling pathways related to cellular growth and survival [3, 182-185].

Cisplatin, a common antitumoral drug, has been proven to induce membrane fluidification and clustering of lipid rafts and Fas death receptors in human colon cancer cells [186, 187]. All these effects were reversed in cisplatin treated cells when membrane-stabilizing agents were used, without affecting the drug uptake and its DNA cleavage efficacy [187]. In addition to altered membrane fluidity, cisplatin as well as gemcitabine treatment promoted the intracellular acidification through the inhibition of NHE1 (Na+/H+ membrane exchanger-1), which led to the aSMase (acid sphingomyelinase) activation and the subsequent ceramides formation [187-189]. Liang *et al.* demonstrated a positive association between membrane saturation degree and resistance to cisplatin treatment in lung adenocarcinoma cells [190]. Many chemotherapeutics, such as doxorubicin, tamoxifen and 3,6-dihydroxyflavone, have been also indicated to influence membrane's

fluidity with consequent effects on their cytotoxicity [191-198]. Interestingly, a cross talk between chemical-induced cellular membrane effects and drug's main mechanism has been suggested to be important for the final outcome of chemical exposure [180].

Bleomycin is another widely known antineoplastic agent known to react with the membrane lipids [199-201]. Its therapeutic use is based, alike the famous cisplatin chemotherapy, on its ability to cleave DNA [202, 203]. However, such metallo-antibiotics mediate oxidation of other cellular molecules, such as lipid peroxidation [204, 205]. More specifically, bleomycin has been found to induce *in vitro* a profound membrane remodeling at the level of the fatty acid constituents, which includes an increase of saturated fatty acid (SFA) content with a parallel decrease of monounsaturated and polyunsaturated fatty acids (MUFA and PUFA) [199]. Furthermore, studies on liposomes made of SFA, MUFA and PUFA-containing phospholipids have shown the occurrence of lipid isomerization, as well as the PUFA consumption, under biomimetic conditions of free radical and oxidative stress [200]. Differential fatty acid distribution in phospholipids has been also observed in hepatocellular and colorectal cancer cells treated with non-toxic doses of 5-fluorouracil and doxorubicin. In particular, chemotherapeutics-treated cells showed lower levels of SFA and higher content of PUFA in both cell lines [206]. Modifications of the membrane structure have been reported in minerval (2-hydroxyoleic acid)-treated cells [207, 208]. Minerval is a potential antitumoral drug that, contrary to conventional strategies, serves as a membrane's structure modifier by increasing the propensity of phospholipid bilayer to assemble into nonlamellar phases [208]. This reorganization leads to the localization of PKC (protein kinase C) to the membrane and subsequent cellular growth arrest through p21 activation [208]. Llado *et al.* proposed that minerval-induced membrane reorganization induces the aggregation of Fas death receptors, thus leading to the activation of the extrinsic pathway of programmed cell death [207].

1.2.4 Fatty acid supplementation in cancer prevention and co-adjuvant treatment

According to the available epidemiological data, the elevated consumption of fish oil as well as the dietary PUFA-ω3 supplementation decrease the risk of various cancer types, such as breast, prostate, pancreatic and colorectal [209-213]. The low PUFA-ω3 to PUFA-ω6 ratio has also been associated to increased cancer incidence [214]. On the contrary, a meta-analysis of numerous epidemiological studies, including 900,000 subjects, proved

that the high consumption of total, saturated and trans fatty acids increase ovarian risk [215]. Several *in vitro* and *in vivo* studies have been carried out aiming to elucidate the mechanisms underlying PUFA's protective role against cancer [216, 217]. These mechanisms involve a big range of target molecules with various effects on cellular survival, proliferation and inflammation [218]. For instance, PUFA-ω3 supplementation alters the size and composition of membrane lipid rafts which in turn affects the function of lipid rafts proteins and the associated downstream signaling [219].

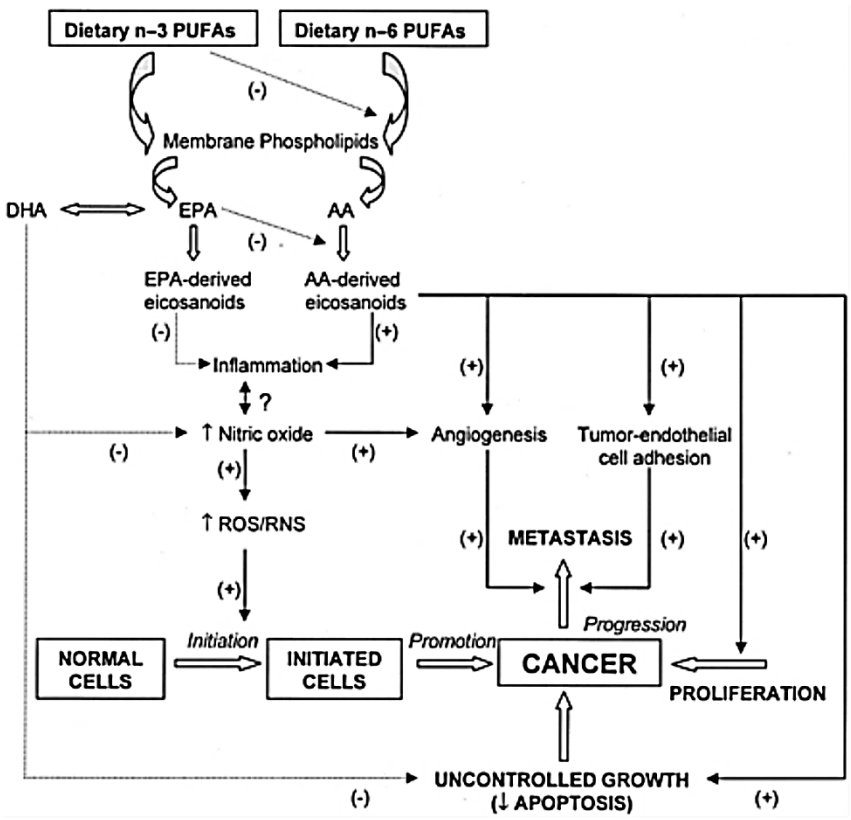

Figure 1.11: Hypothetical mechanisms for tumor promotion and suppression by PUFA-ω6 and PUFA-ω3, respectively. Dietary modulation of ω-6/ω-3 ratio may reduce the PLA2-catalyzed release of ARA and the production of the pro-inflammatory eicosanoids, that are involved in tumor initiation and progression. Modified from Larsson (2004) [218]

More particularly, DHA exerts its anti-proliferative properties by inducing the ROS production and subsequent apoptosis, suppressing the Wnt/β-catenin pathway, and decreasing the production of pro-angiogenic factors in pancreatic cancer cells [220-222]. Hawkins *et al.* have proved a positive correlation between the number of double bonds and PUFA-induced apoptosis of leukemic and pancreatic cancer cells [223]. In the case of colon

cancer, dietary fish oil supplementation is accompanied by limited synthesis of secondary bile acids, which are implicated in the colon carcinogenesis and their levels have been found increased in tumor patients [224, 225]. Furthermore, animal models that received a PUFA- ω3 enriched diet showed lower activity of PLA2 and COX-2 in colonocytes, thus limiting the ARA release and prostaglandins synthesis, respectively [224, 226, 227]. PUFA-ω3 have also been proved to suppress the expression and activity of proteins that are involved in cell proliferation and apoptosis, such as the protein kinase C, Ras, Bcl-2 and insulin-like growth factor-II in cell lines and animal models [217]. Based on the demonstrated protective effects of the essential PUFA-ω3 against cancer in animal and cell culture models and the fact that Western diet includes an unbalanced omega-6 to omega-3 ratio, the clinical use of ω-3 supplementation for tumor prevention has been suggested [228-230].

Furthermore, the consumption of PUFA-ω3 has been proposed as a potential adjuvant and nutritional support for the cancer patients since they exhibit a particular metabolism and have specific nutritional requirements [231, 232]. FA administration (mainly EPA and DHA) aims at weight loss stabilization, limitation of side effects, nutritional status improvement, as well as enhancement of tumor treatment outcome [228]. As far as the pharmacological success is concerned, PUFA-ω3 have gained attention thanks to their effect on inflammatory and immune response [233]. Furthermore, dietary enrichment of PUFA-ω3 may reduce the proportion of PUFA-ω6 and limit the synthesis of the pro-inflammatory eicosanoids [228]. DHA supplementation in breast cancer patients undergoing anthracycline treatment improved the overall survival and the side effects tolerance [234]. Lipid replacement therapy (LRT), as suggested by Nicolson, involves the use of membrane lipids along with antioxidants as food supplements to replace damaged lipids [235]. Cells have the ability of rapid membrane remodelling that gives them the opportunity to alter the phospholipid composition based on the intracellular FA pool [79]. Impaired lipids can originate from intracellular ROS reactivity and alter membrane properties, such as fluidity, thus impeding its proper function like ion exchange, transport, enzymatic activity [236]. The substitution of oxidatively damaged membrane lipids with unoxidized ones contributes to the repaired structure and function of cellular membranes. LRT has been proved efficient on patients with chronic fatigue and fibromyalgia syndrome [229, 237]. Colodny *et al.* conducted a clinical study that examined the efficacy of lipid replacement therapy on decreasing the chemotherapy-induced side effects. Human subjects

consumed Propax with NTFactor®, which is a commercially available food supplement that contains essential fatty acids and antioxidants, amongst others. Patients with advanced colon, pancreatic or rectal cancer that received Propax before and during chemotherapy demonstrated fewer incidences of fatigue, nausea and other quality life indicators [238].

2. Materials and methods

2.1 Materials

2.1.1 Reagents

Cu-TPMA-Phen was prepared by Fantoni N. *et al.* at School of Chemical Sciences, Dublin City University (DCU) according to published procedure [239]. Polymeric nanocontainers and encapsulated form of Cu-TPMA-Phen were prepared by Toniolo G. at the Institute of Nanoscience and Nanotechnology, N.C.S.R. "Demokritos". Cell viability was measured using the colorimetric CellTiter 96®Aqueous One Solution Cell Proliferation Assay (Promega). The CellTiter 96® Aqueous One Solution Reagent contains the tetrazolium compound 3-(4,5-dimethylthiazol-2yl)-5-(3-carboxymethoxyphenyl)-2-(4-sulfophenyl)-2Htetrazolium (MTS), and an electron coupling reagent (1methoxy phenazine methosulfate—PMS). The activity of caspases -8, -9, -3/7 was evaluated using the luminescent assays Caspase-Glo™ 8 and Caspase-Glo™ 9 Caspase-Glo™3/7 (Promega Corporation, Fitchburg, Wisconsin, USA). Morphological membrane changes were detected using Annexin V-EGFP/PI detection kit (Biovision, Mt. View, CA, USA). The human neuroblastoma-derived NB100 cell line [20] and the MCF7 cell line (ATCC number HTB-22™) were from long term culture in the Department of Experimental, Diagnostic and Specialty Medicine, University of Bologna, IT. U87MG brain glioblastoma was obtained from the American Type Culture Collection (ATCC). RPMI 1640, Fetal Bovine Serum (FBS), L-Glutamine and penicillin-streptomycin solution were purchased from Sigma-Aldrich (San Louis, MO, USA). Trypsin/EDTA was from BioWhittaker Europe, Verviers, Belgium. Trypan blue (BioWhittaker, Vervies, Belgium) was used for the cell viability evaluation during standard cell seeding. Flasks and plates were from Falcon (Franklin Lakes, NJ, USA). All the other cell culture reagents were from Sigma-Aldrich. The water used was prepared by the device Milli-Q (Millipore, Milford, MA USA) and was acquired at a resistance value of 18 MΩ at the source. Silica TLC plates were purchased from Macherey-Nagel. Chloroform, n-hexane, methanol and phosphate buffer were purchased from Sigma-Aldrich (San Louis, MO, USA). All compounds were used without further purification. Other reagents used were from Merck (Darmstadt, Germany), Carlo Erba (Milano, Italy) and Sigma-Aldrich.

2.1.2 Instruments

Cell viability was evaluated by measuring absorbance at 492 nm by a microtiter plate reader Multiskan EX (ThermoLabSystems, Basingstoke, UK). Phase contrast microscopy was carried out with a Wilovert Standard PH 20 (HUND, Wetzlar, Germany) and a digital camera from Motic Microscopes, China. Protein concentration and NADPH-cytochrome c reductase activity were measured by the spectrophotometer UVICON 860 (Kontron Instruments, Milano, IT). For the luminescence acquisition the luminometer Fluoroskan Ascent FL (Labsystem, FI) was used. Flow cytometry analysis was performed on a FACSaria BD Analyser using FACSDiva software (Becton, Dickinson and Company, Franklin Lakes NJ, USA). Fatty acid analysis was performed on a 6850 Series II gas chromatography apparatus using ChemStation software (Agilent 6850, Milan, IT).

2.2 Methods

2.2.1 Cell cultures

The activity of Cu-TPMA-Phen was assayed on NB100 cells that derived from a human primary neuroblastoma [20]. Cells were cultured as a monolayer at 37 °C in a humidified atmosphere at 5% CO_2 in complete medium (RPMI 1640 supplemented with 10% heat-inactivated FBS, 2 mM L-Glutamine, 100 units/mL Penicillin, 0.1 mg/mL Streptomycin). Cultures were maintained in the log phase of growth with a viability >95% and checked for the absence of Mycoplasma infection. The viability was checked before each experiment by Trypan blue dye exclusion. Before any treatment cells were incubated for 24 h.

2.2.2 Cell viability assay

Cell viability was evaluated using the colorimetric CellTiter 96® Aqueous One Solution Cell Proliferation Assay. Cells (2×10^4/well) were seeded in 96-well microtiter plates in 100 µL of complete medium. After 24 h, the cells were incubated in the absence or in the presence of Cu-TPMA-Phen at various concentrations in complete medium. After the indicated times, 20 µL/well of the kit solution was added. After 1-2 h of incubation at 37

°C, the absorbance at 492 nm was measured by a microtiter plate reader Multiskan EX (Thermo Labsystems, Helsinki, Finland). In continuous incubation experiments, cells were exposed to Cu-TPMA-Phen for 24, 48 and 72 h at a concentration ranging from 0.1 to 30 μM. In pulse and chase experiments, cells were treated with Cu-TPMA-Phen for 2 h at a concentration ranging from 0.1 to 100 μM and then incubated in complete medium for a total time of 24 and 48 h. Half-maximal effective concentration (EC_{50}) was determined by standard slope analysis without normalization.

2.2.3 Evaluation of apoptosis

The cell death pathway (apoptotic vs necrotic) was assessed using a flow cytometry AnnexinV/PI detection kit and by a luminescent reagent detecting caspase activity [240]. For flow cytometry experiments, cells (2×10^5/3ml) were seeded in 25-cm^2 flasks and, after 24 h incubation with 5 μM Cu-TPMA-Phen, the cells then, were treated with Annexin VEGFP and PI and analysed by flow cytometry. The apoptotic (AnnexinV+/PI−), necrotic (AnnexinV−/PI+) and late stage apoptotic cells (AnnexinV+/PI+) were counted by the instrument and reported on scatter plots. The caspase-3/7 activity was assessed by the luminescent Caspase-Glo™3/7 Assay. Briefly, cells (2×10^3/well) were seeded in 96-well microtiter plates in 100 μL of complete medium. After 24 h, cells were treated with 5 μM Cu-TPMA-Phen. After further 24 h incubation, 100 μL/well of caspase kit reagent was added. After 20 min the luminescence was measured by a Fluoroskan Ascent FL (Thermo Labsystems), and the values were normalized to cell viability. The morphological features of the treated cells were analyzed through phase contrast microscopy, directly in 96-well plate, using an inverted microscope Nikon Eclipse TS100 (Nikon, Melville, NY, USA).

2.2.4 Microsomes isolation

The microsomal membrane fraction was isolated by sequential centrifugation. For this purpose, $>2\times10^8$ NB100 cells were cultured in near confluent monolayer. The followed steps for the extraction and isolation of microsomes (crude endoplasmic reticulum) are described below:

<u>Sample homogenization</u>

1. Cell detachment with trypsin/EDTA using standard procedures.

2. Cell centrifugation at 600 × g for 5 min.
3. Washing of cell pellet with 1 mL ice-cold PBS.
4. Cell centrifugation at 600 × g for 5 min (at 4 °C) and measurement of packed cell volume (PCV).
5. Discard of the supernatant. Cell pellet resuspension in cold 1 × Hypotonic Extraction Buffer equivalent to 3 times the PCV and cell incubation for 20 min at 4 °C (cell swelling).
6. Cell centrifugation at 600 × g for 5 min. Supernatant removal by aspiration. Measurement of the new PCV.
7. Addition of a volume of the 1 × Isotonic Extraction Buffer equivalent to 2 times the «new» PCV volume and transfer to a 7 mL Dounce homogenizer.
8. Cell breakage with 10 strokes of the Dounce homogenizer.
9. Addition of more 1 × Isotonic Extraction Buffer (1.5 mL per mL of PCV). Pipetting of the cell slurry up and down several times for full suspension of the homogenate.

Endoplasmic reticulum isolation

1. Transfer of the homogenate to a microcentrifuge tube and vortex for 30 s, followed by incubation on ice for 1 min.
2. Centrifugation at 10.000 × g for 15 min, at 4 °C.
3. Transfer of the supernatant to a new, pre-chilled microcentrifuge tube and centrifugation at maximum speed (>100.000 × g) for 60 min, at 4 °C. Following centrifugation, discard of the supernatant, taking care to preserve only the light beige/pink opalescent (microsomal) pellet.
4. Washing of the pellet gently with 1× Isotonic Extraction Buffer (500 μL per mL of PCV) and discard of excess buffer.
5. Resuspension of the microsomal pellet in ice-cold 1× Isotonic Extraction Buffer (500 μL per mL of PCV) and determination of the total microsomal protein concentration.

The microsomal solution was aliquoted and stored at -80 °C.

Buffer Recipes

Isotonic Extraction Buffer 1×	Hypotonic Extraction Buffer 1×
HEPES, 10 mM (pH 7.8)	HEPES, 10 mM (pH 7.8)
Sucrose, 250 mM	EGTA, 1 mM
EGTA, 1 mM	KCl, 25 mM
KCl, 25 mM	Protease inhibitors (1%)
Protease inhibitors (1%)	

2.2.5 Protein concentration

Protein concentrations were determined by the method of Bradford. Protein calibration curve was prepared with known concentrations of bovine serum albumin (BSA) solution.

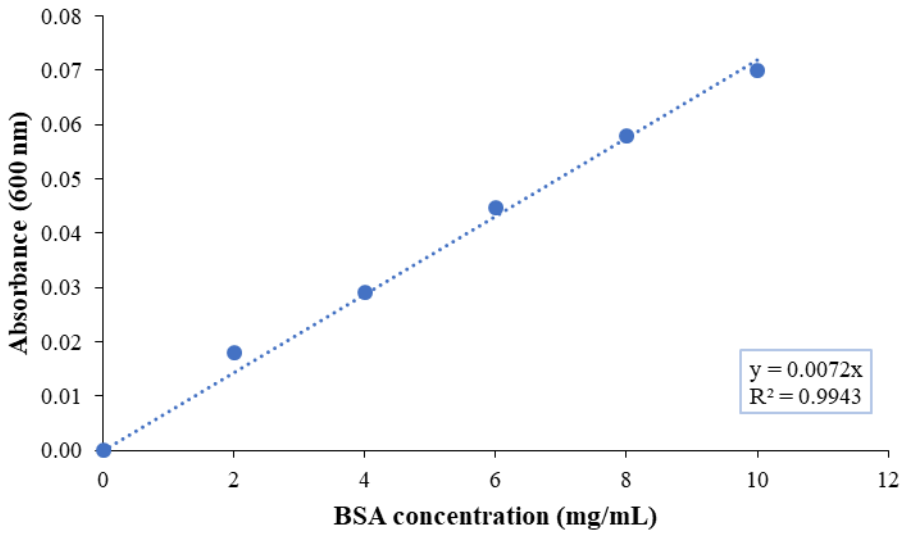

Figure 2.1: BSA calibration curve for the calculation of protein concentration.

2.2.6 Microsomes activity

The functionality of isolated microsomes was evaluated by measuring the activity of NADPH cytochrome c reductase, which is widely used as an endoplasmic reticulum marker. The activity of this enzyme in purified microsomes was determined using the Cytochrome c Reductase Assay Kit, SIGMA. It is a colorimetric method, which depends on the reduction of cytochrome c by NADPH-Cytochrome c reductase in the presence of NADPH. The reduced cytochrome c results in the formation of distinct bands at 550 nm

and the rate of absorbance (550 nm) increase is estimated. The calculated activity of NADPH cytochrome c reductase at the extracted microsomes was 0.261 units/mL.

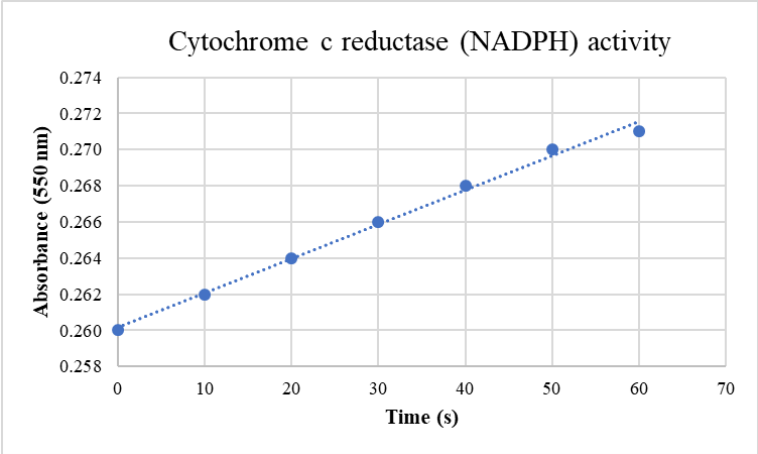

Figure 2.2: Cytochrome c reductase (NADPH) activity for the analysis of functionality of extracted crude endoplasmic reticulum (microsomes).

2.2.7 SCD1 activity assay

The reaction mixture for the stearoyl-CoA desaturase activity included the following: 60 µM stearoyl-CoA, 2 mM NADH in 10 mM potassium phosphate (pH 7.2), 0.1 M potassium phosphate (pH 7.2), and 100 µg of microsomal protein in a final volume of 100 µl. The microsomal fractions were incubated with the reaction mixture at 37 °C for 10 min under shaking. The reaction was terminated by the addition of isopropanol. The mixture was then evaporated, and the reaction products were trans-esterified for the consequent analysis with gas chromatography. SCD1 activity was estimated using the product-to-precursor fatty acid ratio, [oleic (18:1-Δ9) / stearic (18:0)] [241, 242].

2.2.8 Phospholipid Extraction

To analyze the effect of Cu-TPMA-Phen treatment on membrane fatty acids, 0.8×10^6 cells were seeded in 25 cm^2 flasks in 5 mL of complete medium. After 24 h of incubation, medium supplemented with 5 µM Cu-TPMA-Phen was added. Cells were harvested and washed twice with ice-cold PBS. The cell pellet was resuspended in 1 mL milli-Q H_2O and centrifuged at 14.000 rpm for 15 min at 4 °C. For mice RBC analysis, blood was withdrawn from deeply ether-anaesthetized animals and collected in K_2EDTA treated tubes. 200 µL whole blood from mice were centrifuged at 4.000 rpm for 5 min at 4 °C to remove plasma

fraction. The red blood cell (RBC) pellet was then resuspended in pure water and centrifuged at 14.000 rpm for 15 min at 4 °C. In both cases, membrane pellets were dissolved in chloroform:methanol (2:1) and Folch extraction method followed.

2.2.9 Thin layer chromatography

Lipid extract was examined by thin layer chromatography to determine the purity of the phospholipid fraction. Silica plates were used as the stationary phase, while the solvent system n-hexane/diethyl ether/acetic acid (70:30:1) consisted the mobile phase. Standard reference molecules were used for the recognition of phospholipids, cholesterol, triglycerides and cholesteryl esters in the lipid extract. TLC plates were stained with ceric ammonium molybdate solution (CAM) and spots were formed after heating.

2.2.10 Gas chromatographic fatty acid analysis

Fatty acid derivatization

The phospholipid extracts were treated with 0.5 M KOH in methanol for 10 min at room temperature under stirring for the derivatization of fatty acid residues of the phospholipids into their corresponding fatty acid methyl esters (FAME). The acyl-CoA moieties were treated with trimethylsulfonium hydroxide (TMSH) in methyl *tert*-butyl ether (MTBE) anhydrous (1:2) at 120 °C for 3 min [243]. After transesterification, FAME were extracted with n-hexane; n-hexane phase was dehydrated with anhydrous Na_2SO_4, evaporated and analyzed in GC.

GC parameters

FAME were analyzed by gas chromatography (Agilent 6850, Milan) equipped with a 60 m x 0.25 mm x 0.25 μm (50%cyanopropyl)-methylpolysiloxane column (DB23, Agilent, USA), a flame ionization detector (FID), with injector temperature at 230 °C and split injection 50:1. Oven temperature started from 165 °C, held for 3 min, followed by an increase of 1 °C/min up to 195°C, held for 40 min, followed by a second increase of 10 °C/min up to 240 °C, and held for 10 min. A constant pressure mode (29 psi) with helium

as a carrier gas was used. Methyl esters were identified by comparison with the retention times of commercially available standards or trans fatty acid references, obtained as described elsewhere [244]. The list of the examined FAME (corresponding to chromatographic peak areas >97%) in membrane PL are reported as % relative percentages of GC area.

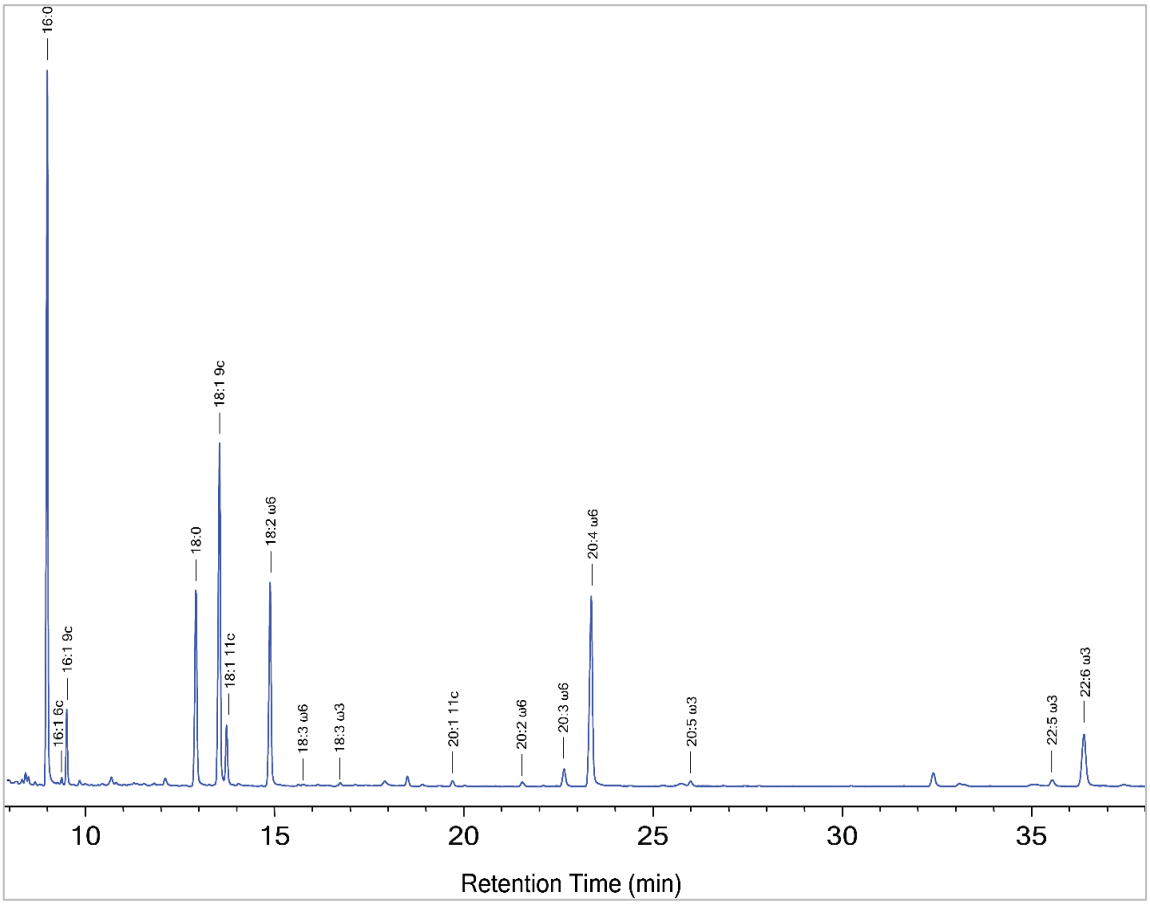

Figure 2.3: Representative GC chromatogram of FAME for fatty-acid based membrane lipidomic analysis.

The detection and quantitation limit were determined by comparing measured signals from the chromatograms of samples with known low concentrations of analyte with those of blank samples. For the detection limit, the acceptance criterion was a signal/noise ratio of minimum 3:1, while for the quantitation limit the acceptance criterion was a signal/noise ratio of minimum 10:1.

Fatty acid indices calculation

Membrane's desaturation degree and susceptibility to peroxidation were estimated using the Unsaturation Index (UI) and Peroxidation Index (PI), respectively. The indices were calculated using the following formulas [245, 246]:

Unsaturation Index (UI) = (% monoenoic × 1) + (% dienoic × 2) + (% trienoic × 3) + (% tetraenoic × 4) + (% pentaenoic × 5) + (% hexaenoic × 6)

Peroxidation Index (PI) = (% monoenoic × 0.025) + (% dienoic × 1) + (% trienoic × 2) + (% tetraenoic × 4) + (% pentaenoic × 6) + (% hexaenoic × 8)

Quantification

The external standardization method was applied for the GC quantification and it was performed within the linear range of response. Calibration curves (GC area vs FA concentration) were obtained using standard solutions of known concentration for each FA moiety. Calibration curves were considered linear when the coefficient factor R^2 was equal to or greater than 0.995. Representative calibration curves are depicted below:

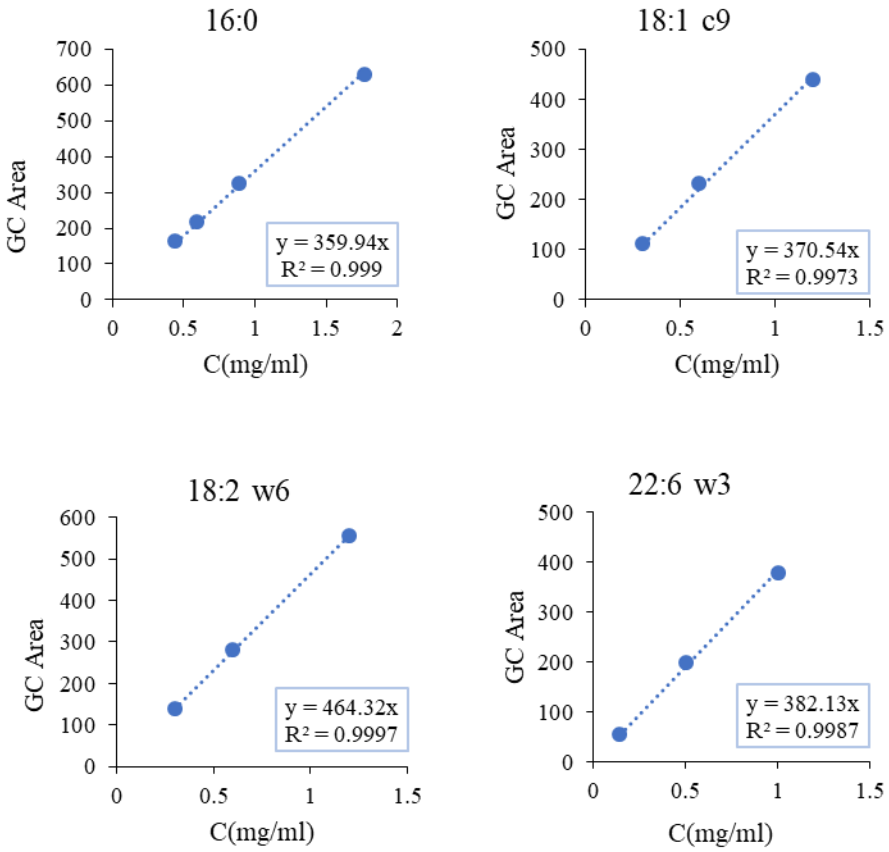

Figure 2.4: Calibration curves of four representative fatty acid methyl esters (FAME): (A) the saturated methyl palmitate (16:0); (B) the monounsaturated methyl oleate (18:1 c9); (C) the ω6 polyunsaturated methyl linoleate (18:2 ω6) and (D) the ω3 polyunsaturated methyl-(22:6 ω3).

Analyte's concentration was calculated by the following expression:

$$Cx = \frac{Cstd \times Ax}{Astd}$$

where,

Cx: the concentration of the x-FA in the sample

Cstd: the concentration of the x-FA in the standard solution

Ax: the area of the x-FA from the sample chromatogram

Astd: the area of the x-FA from the standard chromatogram

2.2.11 Animal studies

Mice were housed at SOL-GEL laboratory, Institute of Nanoscience and Nanotechnology at the National Centre for Scientific Research "Demokritos". Female severe combined immunodeficient (SCID) mice and normal healthy Swiss mice were housed in groups of three per cage under positive pressure in polysulfone type IIL individual ventilated cages (Sealsafe, Tecniplast, Buguggiate, Italy). Room temperature and relative humidity were 24 ± 2 °C and 55 ± 10 % respectively. All animals in the facility were screened regularly according to the Federation of European Laboratory Animal Science Associations' recommendations and were found free of the respective pathogens. Mice had ad libitum access to water and food. SCID mice were inoculated with U87MG human brain glioblastoma cells as previously described [247]. Humane endpoints were predetermined (tumor volume over 1,2 cm, severe compromise of the welfare of the animals, and body weight loss over 20%). The tumor volume and mice weight were monitored once a week with an automatic caliper and scale. The tumor volume, body weight, and the survival rate were calculated at different time intervals. Ethical statement: All protocols were approved by the General Directorate of Veterinary Services Athens, Greece according to Greek legislation (Presidential Degree 160/1991) in compliance with the European Economic Community Directive 609/1986, and Law 2015/1992 for the protection of vertebrate animals used for experimental or other scientific purposes, 123/1986.

2.2.12 Xenografts model construction

U87MG brain glioblastoma cells were cultured as monolayers at 37 °C in a humidified atmosphere of 5% (v/v) CO_2 and 95% relative humidity. Cells were seeded in 75 cm^2 plastic tissue culture flasks and cultured in DMEM supplemented with 10% FBS, washed with phosphate buffered saline (PBS) and were harvested by trypsinization with 0.05% (w/v) trypsin in PBS containing 0.02% (w/v) EDTA. SCID mice were xenografted at two weeks of age with U87MG cells subcutaneously on the right side of the thorax. Tumors were inoculated after injection of $6x10^6$ U87MG cells in SCID mice, which were previously grown in DMEM.

2.2.13 Statistical analysis

Statistical analysis was conducted using GraphPad Prism 7.02 software for Windows, GraphPad Software, La Jolla California USA. All measurements were performed in replicates and the data were expressed as the mean ± standard deviation (SD). Statistical significance was based on 95% confidence intervals ($p \leq 0.05$).

Comparison of two groups

For the comparison of two groups, an unpaired Student's t-test was employed to analyze the data.

Comparison of three or more groups

For the comparison of three or more groups, data were analyzed by one-way analysis of variance (ANOVA) combined with either Tukey's posthoc test or Dunnett's multiple comparison tests for the statistically significant results.

Curve fitting and EC_{50} calculation

For cell viability curves, experimental values were fitted to a nonlinear regression model. Half-maximal effective concentration (EC_{50}) was determined by standard slope (Hill factor 1.0) analysis without normalization using *log[concentration] vs response* equation.

Cell viability curves comparison

Comparison of diverse cell viability curves was conducted with F test (sum-of-squares). The statistically significant difference between the EC_{50} values was evaluated based on the obtained *p*-value.

3. The copper complex: Cu-TPMA-Phen

3.1 Background and Objectives

The project described in the present chapter was performed in collaboration with the groups of Prof. Dr. A. Kellett at School of Chemical Sciences, Dublin City University (DCU) and Dr. E. Efthimiadou at the Institute of Nanoscience and Nanotechnology, N.C.S.R. "Demokritos". The overall goal of this research project was to develop novel copper complexes and study their cytotoxic properties in relation with their effect on cell membrane lipidome. The chemical compound here studied and its encapsulated form in a drug delivery system were respectively provided by our collaborators at DCU and at the NCSR "Demokritos". The below-described research activities were carried out in the laboratory of Prof. Dr. A. Bolognesi in the Department of Experimental, Diagnostic and Specialty Medicine (DIMES) at University of Bologna and in the CNR/spin-off company Lipinutragen.

The novel copper complex developed at DCU was envisioned to be a gene silencing agent by acting as a chemical nuclease. Thanks to their intrinsic redox properties, the copper complexes are interesting compounds for oxidative-based therapeutic strategies [248, 249]. Among antitumoral active metallodrugs, copper(II)-complexes are of particular interest since they can become redox-active upon their *in vivo* reduction to Cu(I) [250, 251]. In parallel, when combined with DNA binding properties, they can mediate oxidatively-induced DNA-strand breaks and eventually result in genome damage and instability [252-254]. Although copper is essential for cellular redox metabolism, its homeostasis must be fine-tuned since free copper ions can catalyze the generation of reactive oxygen species (ROS), such as superoxide ($O_2^{\cdot -}$) and hydroxyl (·OH) radicals. Indeed, Cu(I) is unstable under physiological conditions and it is oxidized into Cu(II) by O_2 or H_2O_2 via the Fenton reaction (Figure 3.1). As a consequence, the formed ROS cause oxidative stress to cells thus resulting in the damage of various biomolecules such as DNA, proteins and lipids [255]. Among the non-specific strategies for cancer chemotherapy, chemical agents with the ability to cleave DNA are widely used, such as cisplatin (metal-containing compound) and bleomycin (metal-binding site containing compound) [256, 257]. Based on their biological and chemical properties, copper complexes can act as artificial metallo-

nucleases (AMNs) for specific gene disruption and therefore represent promising anticancer agents [254, 258].

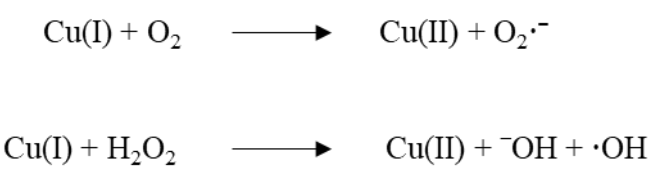

Figure 3.1: Fenton reaction; copper(I) is oxidized by oxygen to copper(II), forming superoxide and hydroxyl radicals in the process.

Like other xenobiotics, AMNs have been recently reported to influence the characteristics of the plasma membrane, such as fluidity and composition [188, 259]. The changes in plasma membrane characteristics trigger the activation of signaling pathways that in turn influence the cell fate [179]. Since chemotherapy-induced cell death is mediated via signaling through plasma membrane (e.g. lipid rafts involving the death receptor pathway), attention has been given to the changes that membranes undergo upon cellular death [178, 181]. Moreover, it has been suggested that a cross talk between chemical-induced cellular membrane effects and DNA damages may be important for the final outcome of chemical exposure [180]. Cell membranes are built by phospholipids, which are fatty acid-containing lipid species responsible for the membrane's structural, organizational and functional properties. The fatty acids and their metabolism are of vital significance for cancer cells [105, 260]. Indeed, because of their active proliferation, cancer cells need a substantial amount of newly biosynthesized lipids. Consequently, affecting the metabolism of these building blocks might influence the tumor cellular growth and the related lipid signaling. For example, it has been reported that the regulated biosynthesis of SFA, such as palmitic acid (16:0) or stearic acid (18:0), and their subsequent desaturation to MUFA (palmitoleic acid (delta-9 16:1) and oleic acid (delta-9 18:1)), can influence the biophysical properties of the tumor cell membrane and thus the signaling pathways related to cellular growth and survival [3, 182-185]. Since the fatty acids are part of our dietary intakes, their balance can also impact the drug outcomes and interactions with other organelles. In this regard, fatty acid-based membrane lipidomics could in principle represent a valuable tool

in cancer therapy by providing insights on how the rearrangement of cell membranes of a tumor cell population might enhance the outcome of a given treatment [185, 235].

In the present research project, the novel Cu(II) complex $[Cu(TPMA)(Phen)](ClO_4)_2$ was studied being used both as a free compound and under an encapsulated form within polymeric nanoparticles, thus allowing for the comparison with the free drug. In vitro experiments were carried out in the neuroblastoma derived cell line NB100 and in the breast carcinoma cell line MCF7. The cytotoxicity of both free and encapsulated complex was determined and the cell death pathways were analyzed with parallel monitoring of caspase activation. NB100 cells were treated with EC_{50} (half maximal effective concentration) doses of copper complex and membrane fatty acids were analyzed by gas chromatography. Inhibitors of apoptosis and necroptosis and scavengers of oxidative stress were tested to evaluate their protective effect against copper's cytotoxicity and membrane remodeling. Finally, we were interested to test whether fatty acid supplementation could influence the cell response to copper complex exposure.

3.2 Molecular structure

In the current project, we studied the biological effects of the synthetic chemical nuclease $[Cu(TPMA)(Phen)](ClO_4)_2$ (Cu-TPMA-Phen)], where TPMA = tris-(2-pyridylmethyl)amine and Phen = 1,10-phenanthroline) (Figure 3.2). The above-reported complex was synthesized and characterized by Fantoni *et al.*, following a rational design so that it combines the following characteristics: a) the catalytic stabilizing effect of TPMA for effective intercalation to DNA [261-263] and b) the oxidation properties of copper(II) phenanthroline for potent DNA scission [263-265]. Since Cu-TPMA-Phen is a metal-containing chemical that induces DNA cleavage, it may belong to the group of AMNs that exert cytotoxic effects against human cancer cells [266, 267].

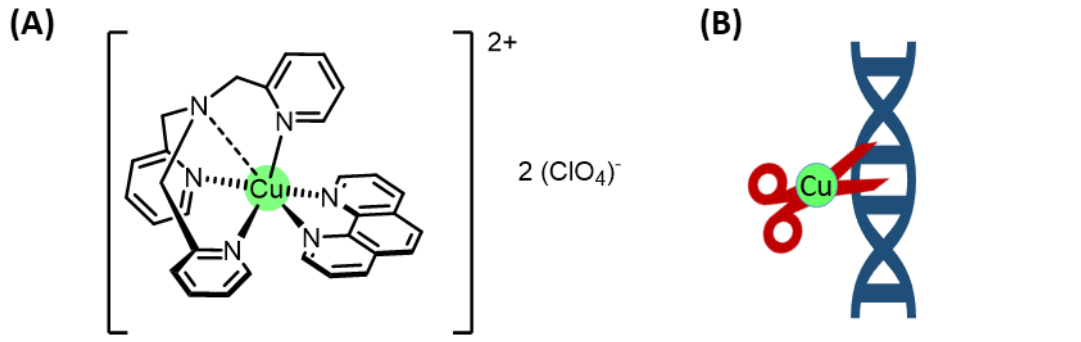

Figure 3.2: (A) Molecular structure of [Cu(TPMA)(Phen)]$(ClO_4)_2$ (Cu-TPMA-Phen)], where TPMA = tris-(2-pyridylmethyl)amine and Phen = 1,10-phenanthroline), synthesized by Fantoni *et al*., (B) Schematic representation of DNA cleavage by the copper complex.

3.3 Effects on cell viability

3.3.1 Cytotoxicity

Neuroblastoma cells (NB100) were exposed to different concentrations of the complex Cu-TPMA-Phen (0.1-30 μM) for 24, 48 and 72 h. Cell toxicity of free Cu-TPMA-Phen was determined using an MTS cell viability assay. Dose-dependent curves were derived (Figure 3.3A) and the half maximal effective concentration (EC_{50}) values were calculated (Figure 3.3C). The EC_{50} was 4.2 μM (R^2 = 0.97) after 24 h of continuous incubation with the complex. Longer incubation times resulted to slightly lower EC_{50} values, 3.0 μM and 2.8 μM for 48 and 72 h, respectively. Cell viability was also evaluated in a pulse and chase experiment, in which NB100 cells were treated for 2 h with various concentrations of Cu-TPMA-Phen (1-100 μM), then washed and incubated with complete medium for 24, 48 and 72 h (Figure 3.3B). The concentrations effective to reduce cell viability by 50% are reported in Figure 3.3C. It should be noted that 2 h of exposure to the complex can be enough to ensure a strong cytotoxicity. In fact, the comparison of EC_{50} calculated for continuous and pulse and chase experiments shows only one log difference.

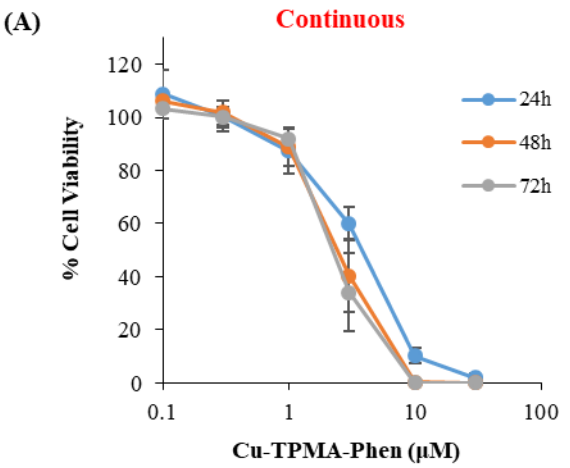

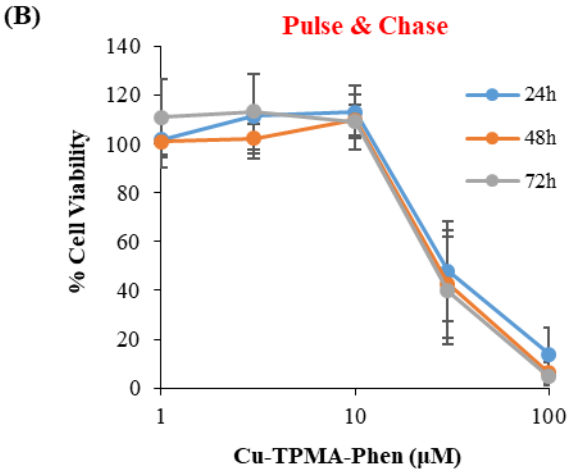

(C)

	Continuous Incubation	Pulse & Chase
	EC_{50} (µM)	
24 h	4.2	63.3
48 h	3.0	65.7
72 h	2.8	46.0

Figure 3.3: Cytotoxic effect of Cu-TPMA-Phen on NB100 cells; (A) Cell viability curves for NB100 cells continuously exposed to different doses of Cu-TPMA-Phen for 24, 48 and 72 h; (B) Cell viability pulse and chase curves of NB100 cells exposed at various doses of Cu-TPMA-Phen for 2 h and then incubated in complete medium for 24, 48 and 72 h. Cell viability was measured by MTS assay and expressed as a percentage of untreated cells. The results in A and B panels are presented as the means ± SD of three independent experiments performed in triplicate; (C) Half maximal effective concentration (EC_{50}) values were calculated by non-linear regression with standard slop analysis.

3.3.2 Evaluation of cell death

To further study the induced cell death pathway, cytofluorimetric analysis through Annexin V/PI double staining of NB100 cells treated with Cu-TPMA-Phen was carried out. This analysis indicated that NB100 cells treated for 24 h with 5 μM Cu-TPMA-Phen underwent apoptotic cell death. Treated and untreated cells were stained with Annexin V-EGFP and Propidium Iodide (PI) to differentiate apoptosis versus necrosis. Annexin V-EGFP detects the externalization of phosphatidylserine in apoptotic cells, while PI stains necrotic cells. After treatment with 5 μM Cu-TPMA-Phen for 24 h, 59% of the cell population was in late apoptosis (Annexin V+/PI+) and 5% of cells underwent necrotic death (Annexin V−/PI+), as depicted in Figure 3.4A. The low number of necrotic cells measured in our experiments can represent an advantage for a possible therapeutic use of this complex. In fact, necrosis, contrary to apoptosis, causes inflammation that can be responsible for unwanted toxicity towards surrounding normal tissue [268]. In parallel, cell morphology was analyzed by phase-contrast microscopy on NB100 cells incubated with 5 μM Cu-TPMA-Phen for 24 h. Treated cells showed typical apoptotic morphological features, as shown in Figure 3.4B. Finally, to confirm the apoptotic cell death pathway, the caspase 3/7 activity was assessed in NB100 cells treated with 5 and 10 μM Cu-TPMA-Phen for 24 h in comparison with untreated (control) cells (Figure 3.4C). At both concentrations, caspases 3/7 were strongly activated in Cu-TPMA-Phen treated cells, reaching values higher than 300% of that of control cells.

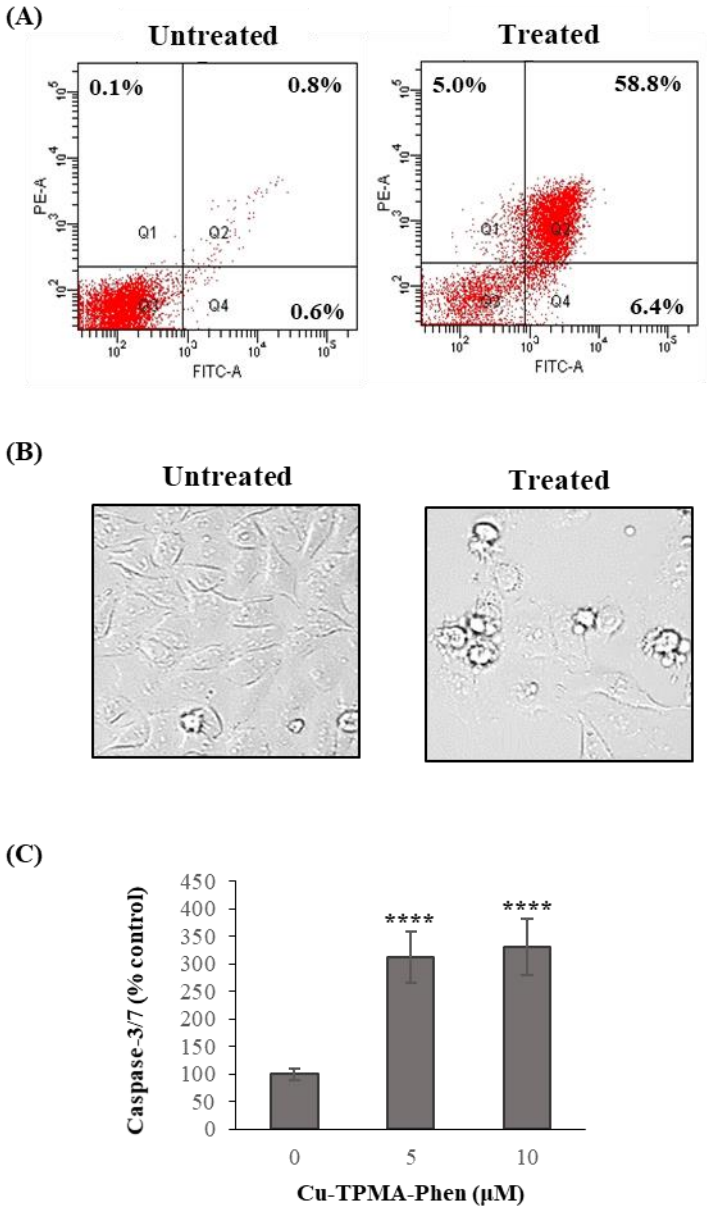

Figure 3.4: Cytotoxic effect of Cu-TPMA-Phen on NB100 cells; (A) The cell death pathway triggered by 5 µM Cu-TPMA-Phen was evaluated on NB100 cells after 24 h of treatment by AnnexinV/PI staining and flow cytometry analysis. FITC-A channel is used for the detection of Annexin V-EGFP fluorescence. PE-A channel is used for the detection of PI fluorescence. Representative plots of AnnexinV/PI staining of are shown; apoptotic cells (Q4, AnnexinV+/PI−), necrotic cells (Q1, AnnexinV−/PI+) and late-stage apoptotic cells (Q2, AnnexinV+/PI+); (B) Morphological analysis of NB100 cells treated with 5 µM Cu-TPMA-Phen for 24 h, using phase-contrast microscopy (400×); (C) Caspase 3/7 activation in NB100 cells exposed to 5 and 10 µM Cu-TPMA-Phen for 24 h. The expression of activated caspases is reported as a percentage of untreated cell values. Means ± S.D. of three independent experiments, each in triplicate, are given. Statistical significance was determined by unpaired t-test (**** $p < 0.0001$).

3.3.3 Caspase activation

Caspases are proteolytic enzymes with an important role in the regulation of apoptosis [269]. To further characterize the cell death induced by Cu-TPMA-Phen, the initiator caspases -1, -2, -8 and -9 and the executioner caspases -3, -7 were evaluated at different time points (2, 4, 8, 16 and 24 h) after Cu-TPMA-Phen treatment. Interestingly, the activation of all tested caspases was increased only after 8 h of cell incubation with the copper complex compared to untreated cells (Figure 3.5).

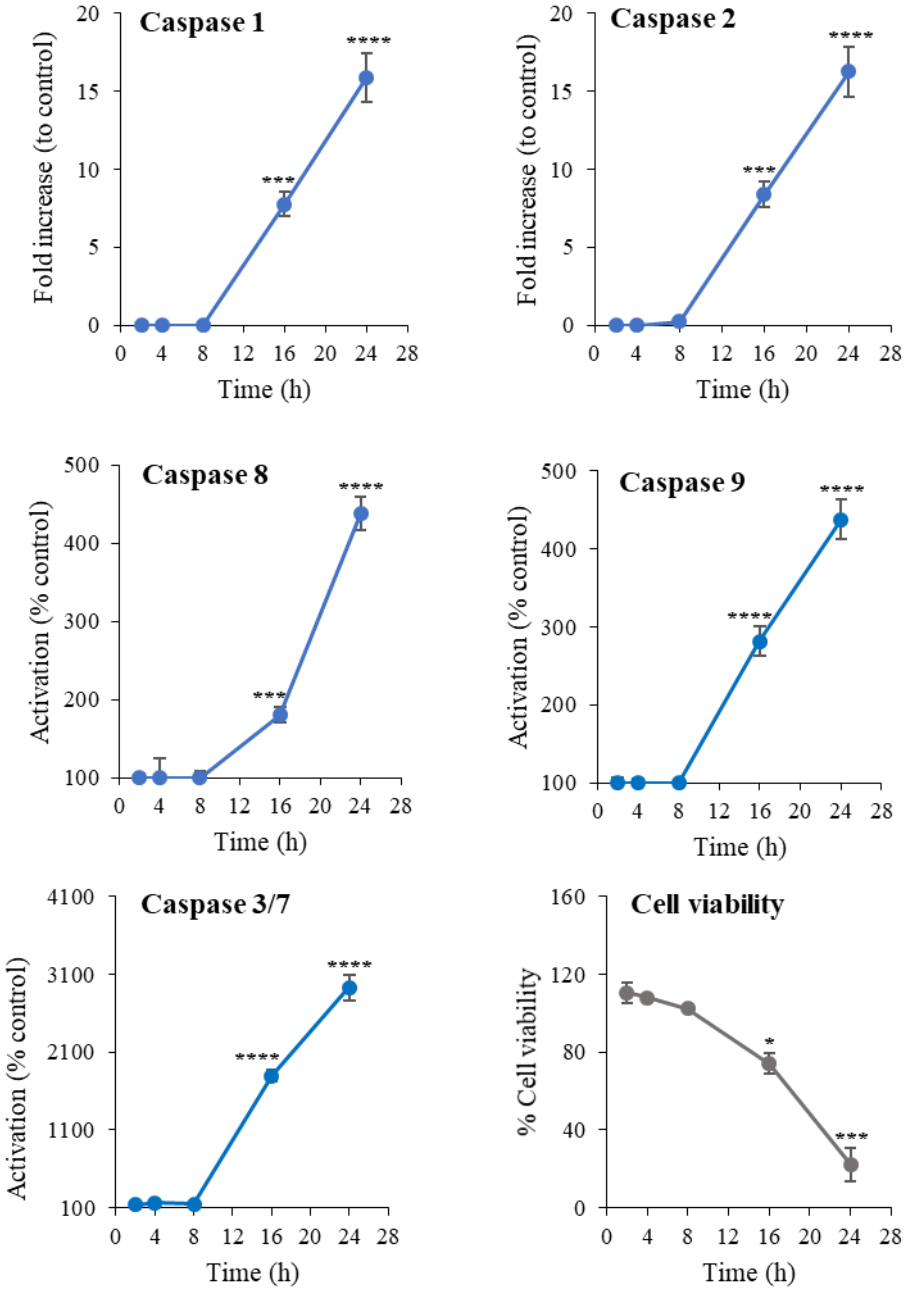

Figure 3.5: Caspase activation in NB100 cells treated with 5 µM Cu-TPMA-Phen. Caspase-1, -2, -8, -9 and -3/7 activation was determined at 2, 4, 8, 16 and 24 h as described in Materials and

Methods. Caspase activity is expressed as fold increase to control for caspase-1 and -2, and as percentage of control for caspase-8, -9 and -3/-7. Control values were obtained from cultures grown in the absence of copper complex. Mean values ± SD are reported. Cell viability was evaluated at the same time points. Statistical significance was determined by unpaired t-test (* $p < 0.05$, ** $p < 0.01$, *** $p < 0.001$, **** $p < 0.0001$).

In particular, Cu-TPMA-Phen induced a strong activation of all the apical caspases (-1, -2, -8 and -9) in a linear manner, reaching about 1600% (for caspase -1, -2) and 440% (for caspase -8, -9) of controls after 24 hours of incubation. Caspase -8 and -9 represent the initiator caspases for the extrinsic and intrinsic apoptotic pathway, respectively. The extrinsic pathway of apoptosis is activated through the binding of a ligand to the membrane death receptor which in turn leads the dimerization and activation of caspase-8. The intrinsic pathway is activated by various cellular stresses and involves the mitochondrial release of cytochrome c and the formation of the apoptosome, which leads to the activation of caspase-9 [270]. The activated form of both caspases (-8, -9) cleave and activate in turn the executioner caspases, such as caspase -3 and -7 (Figure 3.6). In the present case, Cu-TPMA-Phen treatment led to notable augmentation of caspase -3/-7 activity compared to untreated cells (~2900%). Besides its categorization to the group of apical caspases, caspase-2 is not involved in the cleavage and activation of downstream executioner caspases. The activation of caspase-2 has been attributed to diverse stress signals, such as DNA damage, metabolic imbalance, endoplasmic reticulum (ER) stress and others [271, 272]. Caspase -1 is known to be activated by inflammasomes and trigger pyroptosis; a process of programmed cell death that involves cell lysis and extracellular release of cytosolic contents, thus leading to the activation of an inflammatory cascade [273]. ROS have been recently reported as activating signals for inflammasomes, through MAPK-ERK1/2 pathway [274].

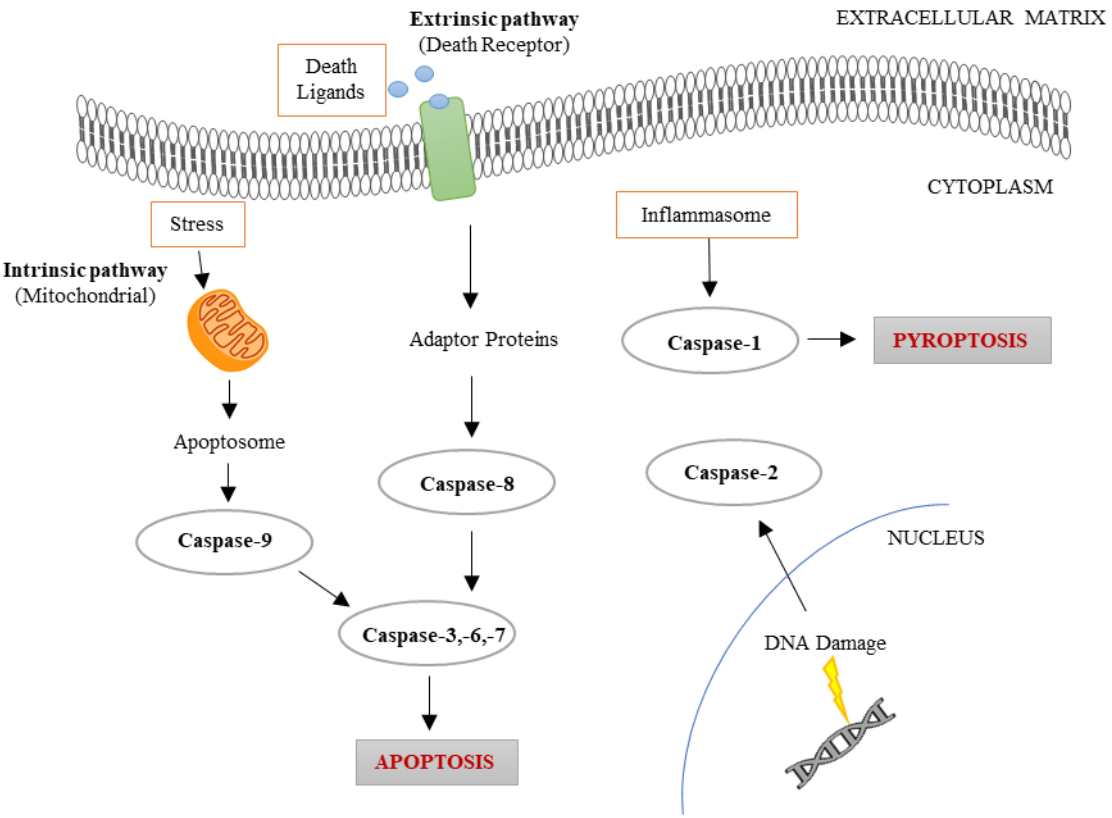

Figure 3.6: Molecular pathways of caspases activation in programmed cell death, such as apoptosis and pyroptosis. Intrinsic apoptotic pathway is activated by various stress signals and involves cytochrome c release from mitochondria and apoptosome formation, thus leading to activation of initiator caspase-9. Extrinsic apoptotic pathway is activated by the binding of death ligand to the receptor and leads to initiator caspase-8 activation. Activation of effector caspase-3, -6, and -7 follows. Inflammasome formation induces caspase-1 activation, which leads in pyroptosis.

3.3.4 Protection by inhibitors/scavengers

Inhibitors of apoptosis, necroptosis and oxidative stress were tested to evaluate their protective effect against Cu-TPMA-Phen cytotoxicity. Cell viability was evaluated using NB100 cells pretreated for 3h with 100 µM pan-caspase inhibitor Z-VAD, 100 µM necrostatin-1 (Nec-1), 1000 U/ml catalase (CAT), 1 mM sodium pyruvate (NaPyr), 1 mM N-acetyl-cysteine (NAC) and then treated with 5 and 10µM Cu-TPMA-Phen for 24 h. The inhibitor Z-VAD exerted a protective role against copper complex's cytotoxicity since we observed almost full recovery of cell viability when cells were pre-treated with it. Similar protective effect was observed when cells were treated with the necroptotic inhibitor Nec-1 (Figure 3.7A). In these experiments, Nec-1 was able to protect NB100 cells from the damage induced by the Cu-TPMA-Phen at a similar level as Z-VAD, thus suggesting that

both apoptosis and necroptosis are involved in its cytotoxic mechanism. Necroptosis is a recently identified programmed cell death and consists a form of regulated necrosis, which depends on the receptor-interacting serine-threonine kinase RIPK1 and RIPK3. Nec-1 inhibits necroptosis through the inhibition of RIPK1 [275]. It has been demonstrated that ROS have a highly important role in the process of necroptosis downstream of RIPK1 activation [276]. Moreover, necroptotic cell death has been associated with the occurrence of excessive DNA damage [277]. Catalase, that enzymatically reduces the hydrogen peroxide, protects the cell fate. Sodium pyruvate, which is known to have protective effects against hydrogen peroxide toxicity in human neuroblastoma cells [278], showed no protection in this case. On the other hand, N-acetyl-cysteine (NAC), which increases glutathione levels and thus its antioxidant effects [279], protects the cell viability (Figure 3.7B). These results suggest that cytotoxicity of copper complex is mediated mainly through oxidative stress and subsequent apoptosis and necroptosis in neuroblastoma cells. Phase-contrast microscopy was applied for the morphological analysis of NB100 cells treated under the conditions described above (Figure 3.7C). While 24-h incubation with Cu-TPMA-Phen at EC_{50} doses, induces cellular death and the formation of apoptotic bodies, the pre-treatment with inhibitors of apoptosis/necroptosis and scavengers of oxidative stress, rescues the cells from the complex's cytotoxic effects and cell morphology remains similar to untreated cells.

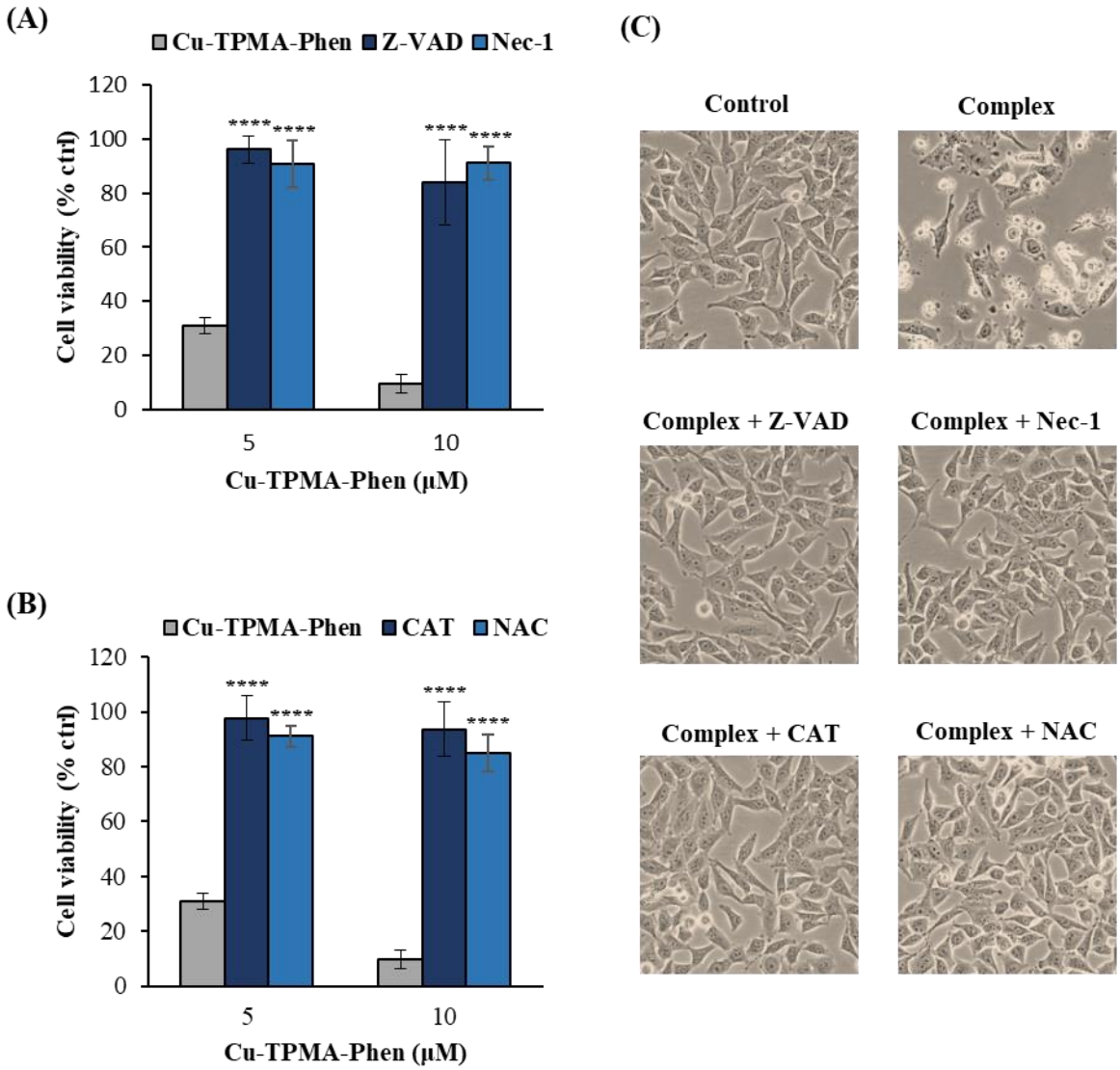

Figure 3.7: Protective effect against copper complex's cytotoxicity by inhibitors of apoptosis and necroptosis and scavengers of oxidative stress; (A) NB100 cells were pretreated for 3h with 100 µM pan-caspase inhibitor (Z-VAD), 100 µM necrostatin-1 (Nec-1),) and then treated with 5 and 10 µM Cu-TPMA-Phen for 24 h; (B) NB100 cells were pretreated for 3h with 1000 U/ml catalase (CAT), 1 mM N-acetyl-cysteine (NAC), and then treated with 5 and 10 µM Cu-TPMA-Phen for 24 h; (C) Morphological analysis of NB100 cells treated under the with conditions mentioned above, using phase-contrast microscopy (400×). Values represent mean ± SD of three independent experiments, each in triplicate. Statistical significance was determined by unpaired t-test (**** $p < 0.0001$).

3.4 Effects on membrane lipidome

3.4.1 Membrane fatty acid analysis of copper treated cells

Based on the cytotoxicity parameters identified above, NB100 cells were treated with 5 μM of Cu-TPMA-Phen for 24 h (N=6) and underwent fatty acid-based membrane lipidomic analyses. The fatty acid residues present in membrane phospholipids were isolated, derivatized to fatty acid methyl esters (FAME) and analyzed by gas chromatography (GC). GC separation led to the identification and quantification of fatty acid isomers. Membrane fatty acid-based lipidomics analysis on NB100 after 24-h treatment revealed a significant increase of saturated fatty acids (SFA) ($p<0.0001$) accompanied by a parallel decrease of their monounsaturated (MUFA) counterparts ($p<0.0001$) (Figure 3.8A). The family of polyunsaturated fatty acids (PUFA) did not show significant alterations between treated and untreated cells. In particular, the main members of the SFA family, palmitic (16:0) and stearic (18:0) acids, are significantly increased (Figure 3.8B), whereas the main members of the MUFA family, palmitoleic (9c-16:1), vaccenic (11c-18:1) and oleic (9c-18:1) acids showed significantly decreased levels in NB100 cells exposed to Cu-TPMA-Phen (Figure 3.8C). The enzymatic activity of stearoyl-CoA desaturase (SCD1) can be estimated by the product-to-precursor fatty acid ratio [241, 242]. SCD1, also named as delta-9 desaturase, catalyzes the conversion of saturated fatty acids (palmitic acid 16:0, or stearic acid 18:0) into monounsaturated fatty acids (palmitoleic acid 16:1, or oleic acid 18:1). In Cu-TPMA-Phen treated NB100 cells, the SCD1 activity was 2-fold decreased ($p<0.0001$) (Figure 3.8D). The detailed values of the analyzed fatty acid methyl esters (FAME) and the corresponding indices are presented later in this chapter in Tables 3.1 and 3.2, respectively.

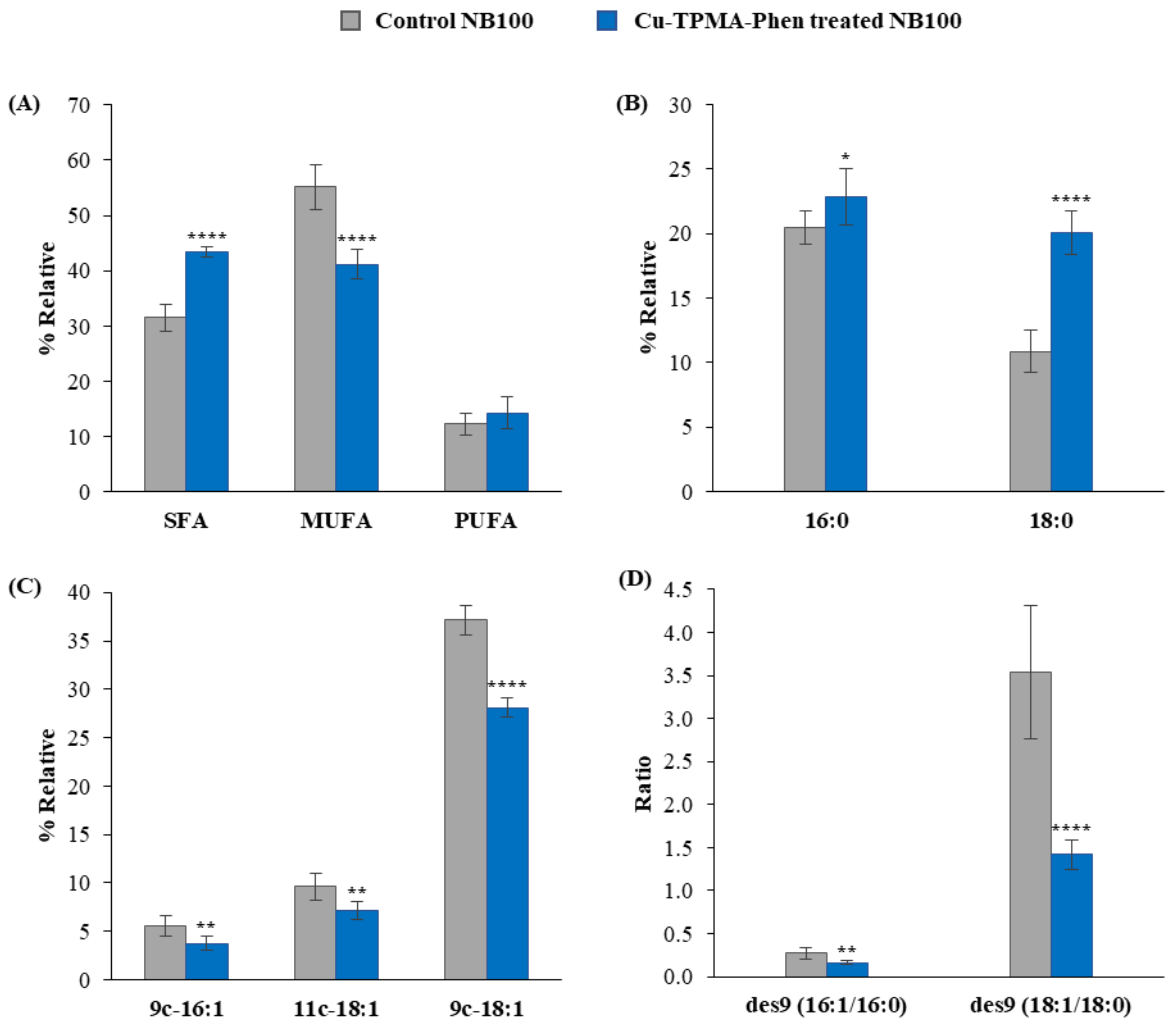

Figure 3.8: Fatty acid-based membrane lipidomics on NB100 cells treated with 5 µM free Cu-TPMA-Phen for 24 h; (A) Relative distribution of fatty acid families, SFA: saturated fatty acids, MUFA: monounsaturated fatty acids, PUFA: polyunsaturated fatty acids; (B) Palmitic (16:0) and stearic (18:0) acids trends in treated cells; (C) Palmitoleic (9c-16:1), vaccenic (11c-18:1) and oleic (9c-18:1) patterns in treated cells; (D) Estimation of delta-9 desaturase (des9) activity by the ratio palmitoleic/palmitic and oleic/stearic. Values represent mean ± SD (n=6). Statistical significance was calculated with unpaired t-test * ($p < 0.05$), ** ($p < 0.01$), **** ($p < 0.0001$).

The membrane lipidomic experiments were carried out also in the breast cancer-derived MCF7 cell line. The aim of this was to ascertain that the above-described membrane remodeling is not specific for the neuroblastoma cell line NB100 but can be extended to other cancer models. MCF7 cells were exposed to 10 µM Cu-TPMA-Phen (~ EC_{50} value) and membrane fatty acid analysis followed. Interestingly, Cu- TPMA-Phen showed a similar effect on cell membrane for both cell lines, although MCF7 and NB100 are cells of different origin, carcinoma, and neuroblastoma, respectively (Figure 3.9).

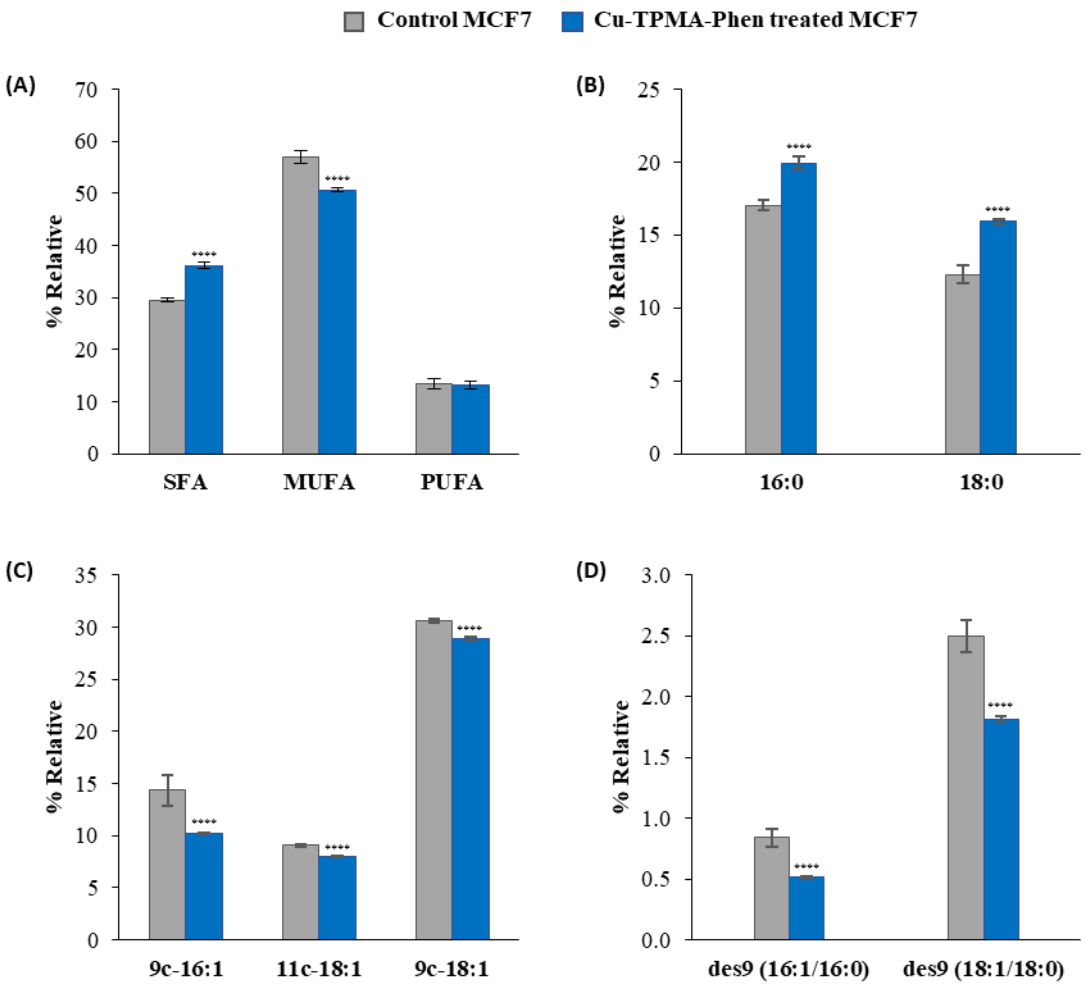

Figure 3.9: Fatty acid-based membrane lipidomics on MCF7 cells treated with 10 μM free Cu-TPMA-Phen for 24 h; (A) Relative distribution of fatty acid families, SFA: saturated fatty acids, MUFA: monounsaturated fatty acids, PUFA: polyunsaturated fatty acids; (B) Palmitic (16:0) and stearic (18:0) acids trends in treated cells; (C) Palmitoleic (9c-16:1), vaccenic (11c-18:1) and oleic (9c-18:1) patterns in treated cells; (D) Estimation of delta-9 desaturase (des9) activity by the ratio palmitoleic/palmitic and oleic/stearic. Values represent mean ± SD (n=6). Statistical significance was calculated with unpaired *t*-test * ($p < 0.05$), ** ($p < 0.01$), *** ($p < 0.001$), **** ($p < 0.0001$).

The results obtained from the cell viability experiments and death pathways analysis together with the values obtained from membrane fatty acid-based lipidomics suggested an interesting behavior arising from oxidative conditions typically associated with copper complex exposure [254, 280]. In fact, cell membranes exposed for 24 h to the free Cu-TPMA-Phen did not show a diminution of the PUFA residues of phospholipids. Lipid peroxidation and the subsequent PUFA decrease is the typical response of cellular membranes to such oxidizing molecules [204, 281]. Thus, the expected chemical reactivity

of Cu-TPMA-Phen towards lipid molecules was not observed. Instead, the increase of SFA was associated with MUFA diminution, which is distinct from oxidative response. Indeed, MUFA decrease cannot be induced by oxidation while the PUFA levels remain unchanged. Therefore, our hypothesis is that this MUFA diminution may be attributed to a "metabolic" rather than a "chemical" oxidative effect of Cu-TPMA-Phen. Since SFA are less susceptible to peroxidation, higher saturation degree in membrane contributes to higher protection from ROS [282]. Furthermore, the increase of SFA in membrane phospholipids is known to change membrane properties toward less permeability and fluidity [23]. Such changes can in turn trigger several signals that lead to programmed cell death, as reported in the case of supplementation with palmitic acid of NB100 cells [20]. Our interest was further focused to get a deeper insight into the reasons of such a membrane remodeling upon cell treatment with toxic concentrations of the copper complex (Figure 3.10). SFA and MUFA are metabolically connected through the enzyme stearoyl-CoA desaturase (SCD1), which is responsible for the insertion of a double bond at C9 position by catalyzing the reduction of SFA to MUFA [241].

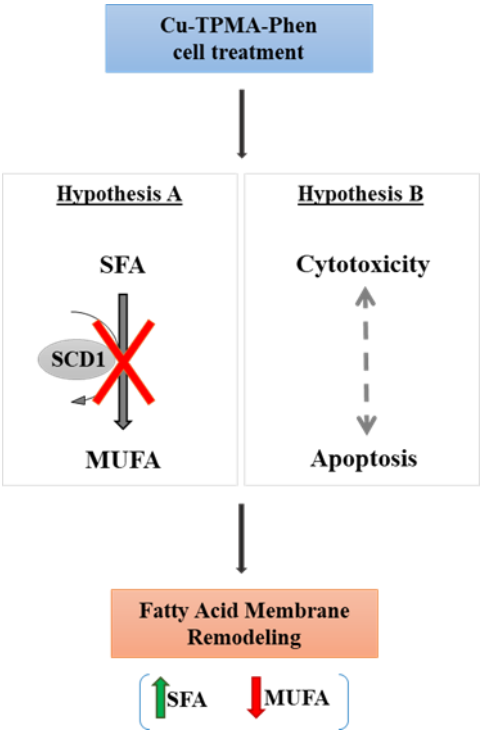

Figure 3.10: Hypotheses for the molecular base of membrane remodeling upon cell treatment with EC_{50} value of Cu-TPMA-Phen; Hypothesis A: enzymatic inhibition of stearoyl-CoA desaturase (SCD1) that catalyzes the conversion of SFA to MUFA; Hypothesis B: Association of membrane remodeling with cytotoxic effects of the copper complex and the consequent induction of apoptosis.

The inhibition of desaturase is known to induce cancer cell death and is indeed inspiring new pharmacological strategies in anticancer therapy [138]. On the other hand, the molecular basis of such membrane remodeling could be possibly associated with the observed apoptotic fate, since the interplay between cell membrane composition and cellular death is well known [178].

3.4.2 Time-course lipidomics

To better evaluate the connection between the cytotoxic events and membrane fatty acid remodelling, we performed time course membrane lipidomics in copper complex-treated cells and correlated these results with the cell viability and caspase activation in a time-dependent manner. More specifically, NB100 cells were treated with 5 μM Cu-TPMA-Phen for 2, 4, 8, 16 and 24 h. Cells were harvested at these time points and membrane lipidomic analysis was carried out. The fatty acid content of treated cells was compared to the one obtained from untreated cells at the same incubation periods. The results are presented as % difference of control cells. Time-course membrane lipidomics revealed a gradual membrane remodelling upon copper complex treatment (Figure 3.11). The relative distribution of total SFA increased significantly in Cu-TPMA-Phen treated NB100 cells at the time point of 16 h ($p<0.0001$). However, stearic (18:0) acid was characterized by a significant increase after 4 h-treatment ($p<0.05$). Moreover, the treated cells showed higher % difference for stearic than palmitic (16:0) acid. Total MUFA content was significantly lower after 8 h-treatment ($p<0.05$), reaching a 25% decrease after 24 h-treatment ($p<0.0001$). All the members of MUFA family followed the same decreasing trend, thus indicating a global alteration pattern. Although not significant, the PUFA were characterized by a slightly increasing trend along treatment time. Interestingly, the membrane remodeling was observed even at the very early time points, having an evident trend after 8 h incubation. Comparison of the time-course lipidomic changes with the corresponding curves for cell viability and caspase activation drives to the conclusion that membrane remodelling takes place prior to the detected cytotoxic effects of Cu-TPMA-Phen. Indeed, cell viability at 8 h is still 100% compared to control cells and caspases activation is detected only after 8 h-monitoring.

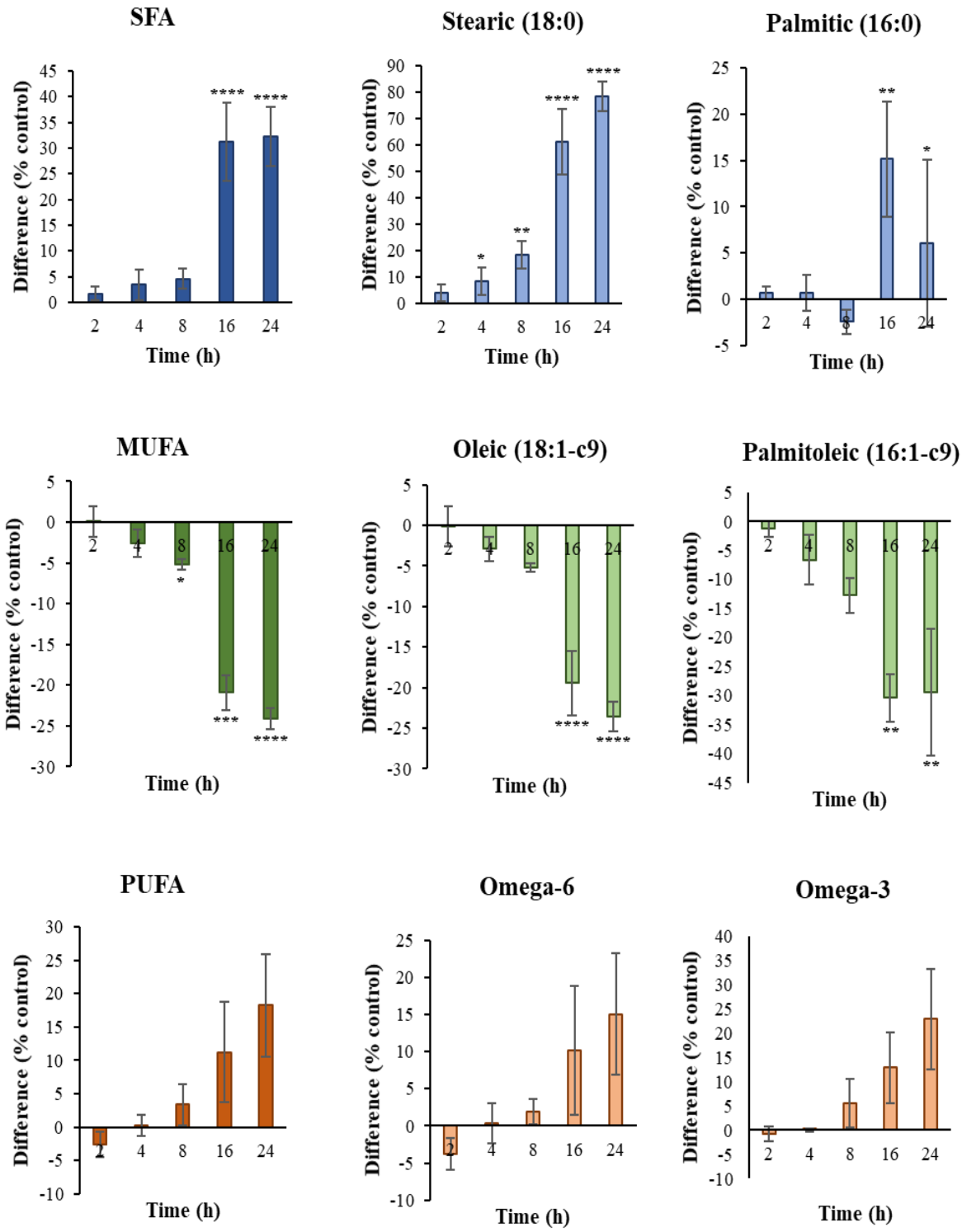

Figure 3.11: Time-dependent membrane remodeling in NB100 cell line treated with 5 μM Cu-TPMA-Phen. Values are expressed as % difference to untreated cells and represent mean ± SD, (N=3). Statistical significance was calculated with unpaired *t*-test * ($p < 0.05$), ** ($p < 0.01$), *** ($p < 0.001$), **** ($p < 0.0001$). SFA: saturated fatty acids, MUFA: monounsaturated fatty acids, PUFA: polyunsaturated fatty acids.

3.4.3 Membrane fatty acid analysis after inhibitors/scavengers pre-treatment

The observed membrane remodeling could be indirectly caused because of the complex's cytotoxicity since it is well known the interplay between membrane remodeling and cell death. To examine a possible connection between the cytotoxic events and fatty acid changes, we performed lipidomic analysis in the presence of Cu-TPMA-Phen in cells that were pre-treated with apoptosis inhibitor (Z-VAD) and oxidative stress scavengers (catalase and N-acetyl-cysteine). Previous results showed that the Z-VAD and the scavengers (catalase and NAC) had a protective effect against Cu-TPMA-Phen cytotoxicity (Figure 3.7). In these experiments, NB100 cells were pretreated for 3 h with Z-VAD/catalase/NAC and then incubated for 24 h in the presence of the copper complex at the EC_{50} concentration. Fatty acid analysis revealed that cell viability protection by apoptosis inhibitor and catalase prevented the membrane remodeling, which is induced in NB100 cell line after Cu-TPMA-Phen treatment. On the contrary, pre-incubation with NAC led to significant differences in fatty acid composition in copper complex treated cells. In particular, total MUFA were slightly decreased ($p<0.05$), while PUFA family showed a similar decrease ($p<0.05$). However, the observed differences in membrane lipidome were not so profound compared to the changes characterizing the NB100 cells incubated with the Cu-TPMA-Phen without any pre-treatment. Furthermore, the different effect on fatty acid composition, after cell pre-treatment with NAC, could be attributed to the fact that NAC shows slightly lower protection of cell viability compared to Z-VAD and CAT (Figure 3.7). The above results lead us to the conclusion that the membrane remodeling is possibly correlated to the cytotoxic mechanism of the copper complex.

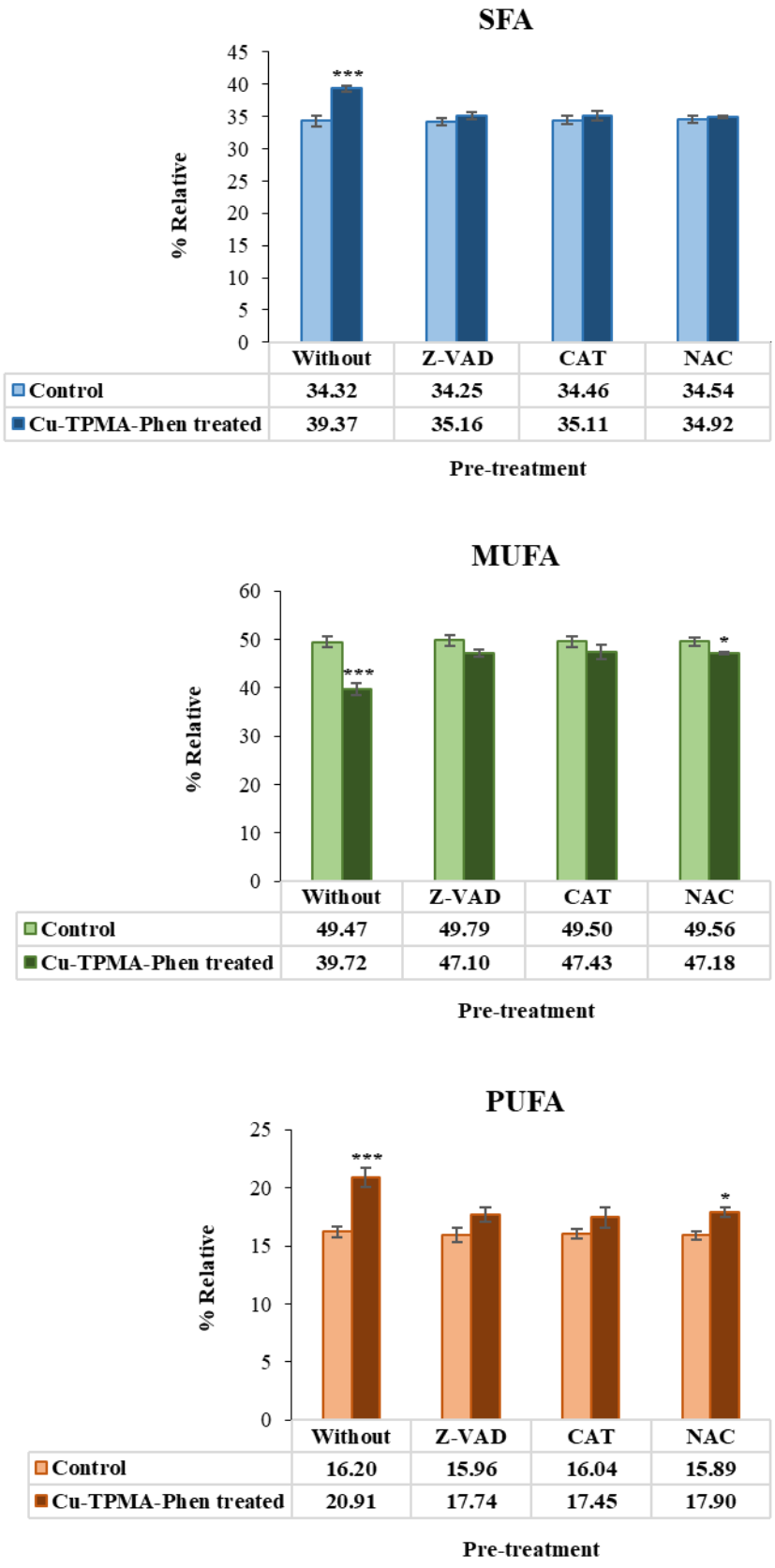

Figure 3.12: Changes of membrane fatty acids after pre-treatment with inhibitor of apoptosis and ROS scavengers. NB100 cells were pretreated for 3 h with 100 µM pan-caspase inhibitor (Z-VAD),

1000 U/ml catalase (CAT), 1 mM N-acetyl-cysteine (NAC) and then treated with 5 μM Cu-TPMA-Phen for 24 h. Fatty acid-based membrane lipidomics followed for treated and untreated cells. Values represent mean ± SD (n=3). Statistical significance was calculated with unpaired *t*-test * ($p < 0.05$), *** ($p < 0.001$).

3.5 Cell-free SCD1 activity assay

The plasma membrane remodeling, which took place after cell treatment with Cu-TPMA-Phen, could suggest a possible inhibition of stearoyl-CoA desaturase (SCD1). Since SFA and MUFA are metabolically connected through the SCD1 desaturase, we hypothesized that the copper complex could provoke the inhibition of this enzyme. Indeed, within the catalytic area of the desaturase, there is a highly conserved histidine-box that coordinates with a di-iron center. Thus, the copper of the complex could, in theory, substitute the iron in the active site. To test this hypothesis, we developed a cell-free assay to assess the SCD1 enzymatic activity in the presence of Cu-TPMA-Phen. SCD1 is a transmembrane enzyme, located on the endoplasmic reticulum (ER), with its catalytic area towards the cytoplasm. For the assay, we isolated microsomes (extracted forms of ER) from NB100 cell line by sequential centrifugation and resuspension in 0.1 M potassium phosphate buffer (pH 7.2). Protein concentrations were determined by the method of Bradford. The reaction mixture for the stearoyl-CoA desaturase activity included the following: 60 μM stearoyl-CoA, 2 mM NADH in 10 mM potassium phosphate (pH 7.2), 0.1 M potassium phosphate (pH 7.2), and 100 μg of microsomal protein in a final volume of 100 μl. Reactions were performed at 37 °C for 10 min under shaking. The positive control included all the above-mentioned components. As a negative control, this reaction was performed in the presence of the commercially available inhibitor of the desaturase, MF-438 (Calbiochem). Finally, another reaction including the copper complex was performed. The enzymatic activity was estimated by the ratio of oleic (18:1c9) to stearic (18:0), representing the conversion rate of the saturated fatty acid to its monounsaturated counterpart [241, 242]. In the presence of Cu-TPMA-Phen, it was calculated a ratio of 1.16, which was identical to the control sample (ratio 1.18). In the presence of MF-438 inhibitor, the ratio was decreased to 0.72, proving the SCD1 enzyme's inhibition, since less oleic but more stearic were observed at the end of the reaction compared to control sample. The above result suggests that the previously

noted increase of SFA of Cu-TPMA-Phen-treated cells cannot be attributed to a specific inhibition of this desaturase.

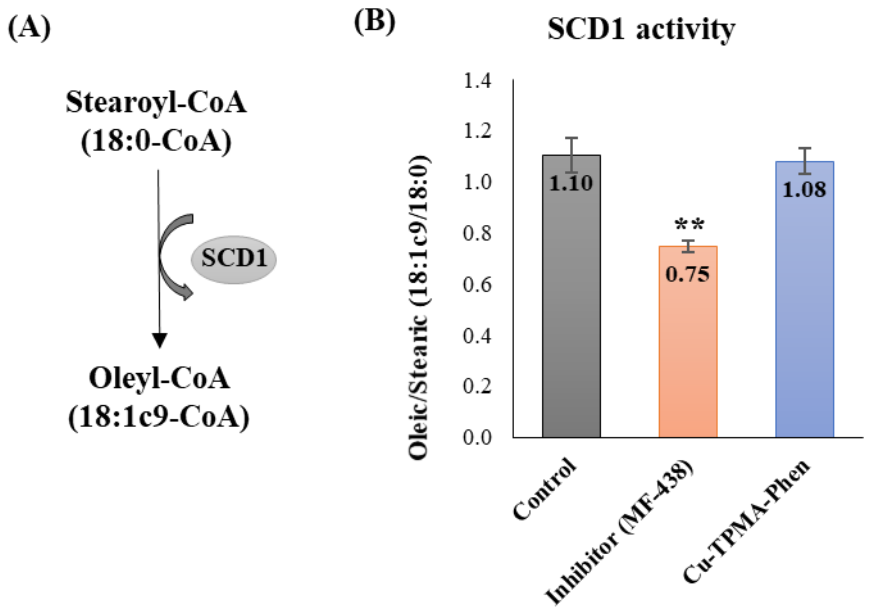

Figure 3.13: Cell-free assay for SCD1 activity; (A) Scheme of the enzymatic reaction catalyzed by stearoyl-CoA desaturase (SCD1); (B) SCD1 activity was tested in microsomes extracted from NB100 cell line in the presence of 5 μM Cu-TPMA-Phen. The commercial inhibitor (MF-438) for SCD1 was used as a negative control. SCD1 activity was estimated using the product-to-precursor fatty acid ratio (oleic/stearic). Values represent mean ± SD (N=3). Statistical significance was calculated with unpaired *t*-test ** ($p < 0.01$).

3.6 Fatty acids supplementation

Finally, based on the above-mentioned membrane lipidomics results, we were interested to test whether a tailored fatty acid supplementation can influence the cell response to Cu-TPMA-Phen exposure. We used palmitic and oleic acid since the previous membrane lipidomics results showed that both fatty acids were significantly changed upon copper complex treatment. Fixed concentrations of 50 μM palmitic and 100 μM oleic acid, which are non-toxic doses [20], were used for simultaneous cell treatment with increasing concentrations of Cu-TPMA-Phen (0.3-100 μM). Cell viability was determined 24 h after cell treatment (Figure 3.14). The obtained results suggest that palmitic acid supplementation may have an additive, but not synergistic, cytotoxic effect with Cu-

TPMA-Phen on NB100 cells, since co-treatment results in slightly higher cytotoxicity (p=0.0189). In the case of oleic acid supplementation, the cell viabilities curves showed no significant difference (p=0.0905).

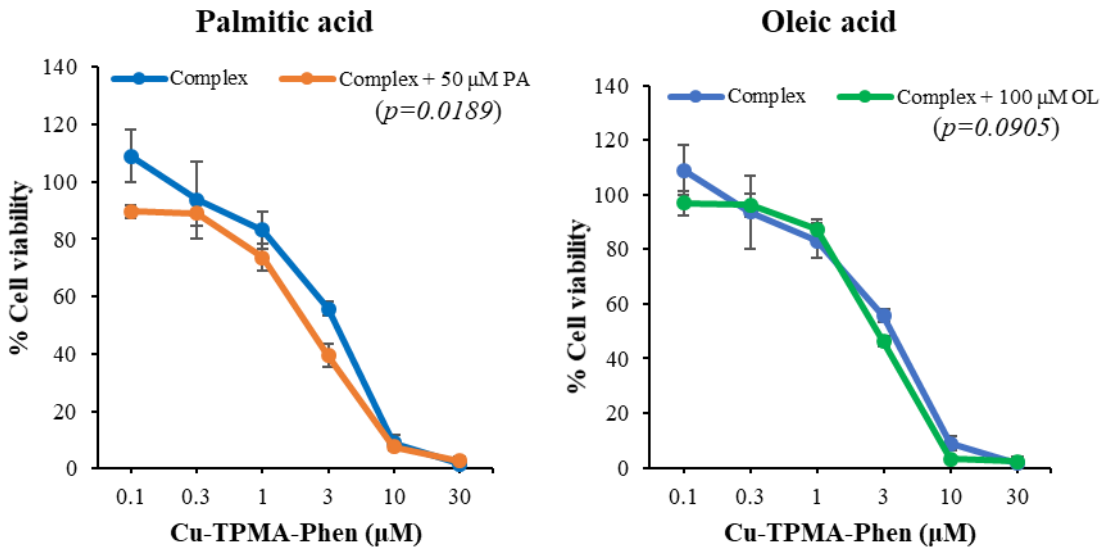

Figure 3.14: Effects of fatty acid supplementation on Cu-TPMA-Phen induced cytotoxicity. NB100 cells were exposed to different doses of Cu-TPMA-Phen for 24 h. Culture medium was supplemented with either 50 µM palmitic acid (PA) or 100 µM oleic acid (OL). Cell viability was measured by MTS assay and expressed as a percentage of untreated cells. The results are presented as the means ± SD of three independent experiments performed in triplicate. Comparison of cell viability curves was conducted with F test (sum-of-squares).

Subsequently, we were interested to study the effect of 100 µM oleic acid supplementation on the fatty acid content of NB100 cells, which were co-treated with 5 µM Cu-TPMA-Phen (Figure 3.15A). However, in this case we determined the total fatty acid content of the cells, which represents not only the membrane phospholipid fatty acid content but also the one of triglycerides (TG), that were formed upon oleic acid supplementation as shown by thin layer chromatography (TLC) (Figure 3.15B). Interestingly, oleic acid shows higher levels in the case of co-treatment compared to its administration alone. A hypothesis could be drawn that the increased levels of oleic acid detected in the supplemented cells treated with the copper complex could belong mostly to TG, thus not affecting either the membrane content and cell viability.

(A)

	Control		Cu-TPMA-Phen	
FAME (%rel)	**w/o oleic**	**+ oleic**	**w/o oleic**	**+ oleic**
16:0	21.9 ± 0.6	12.5 ± 0.1	19.2 ± 1.0	8.5 ± 0.1
16:1 c6	2.1 ± 0.1	2.3 ± 0.0	2.2 ± 0.1	1.9 ± 0.1
16:1 c9	5.0 ± 0.5	1.3 ± 0.0	2.4 ± 0.1	1.0 ± 0.0
18:0	10.9 ± 1.4	7.5 ± 0.2	16.1 ± 0.1	6.5 ± 0.4
18:1 c9	33.9 ± 0.1	61.1 ± 0.4	28.5 ± 0.7	66.8 ± 0.6
18:1 c11	7.9 ± 0.1	3.5 ± 0.1	6.6 ± 0.1	3.0 ± 0.1

(B)

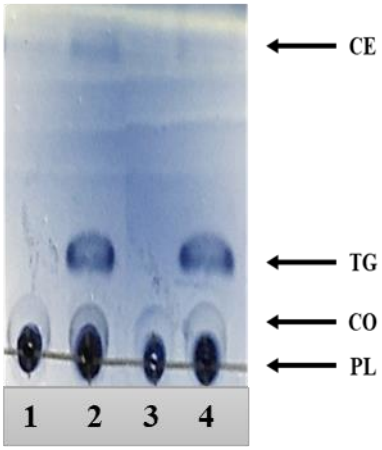

Figure 3.15: (A) Saturated and monounsaturated fatty acid analysis of NB100 cells co-treated with 5 μM Cu-TPMA-Phen and 100 μM oleic acid. Values represent mean ± SD (N=3); (B) Formation of triglycerides as revealed by thin layer chromatography (TLC) when oleic acid is present. Lane 1: untreated cells, lane 2: 100 μM oleic acid, lane 3: 5 μM Cu-TPMA-Phen and lane 4: 5 μM Cu-TPMA-Phen plus 100 μM oleic acid. CE: cholesteryl esters; CO: cholesterol; PL: phospholipids; TG: triglycerides.

3.7 Drug encapsulation in pH-sensitive polymeric nanoparticles

3.7.1 Cytotoxicity of encapsulated Cu-TPMA-Phen

Cell viability assays were performed to assess the toxicity effect of Cu-TPMA-Phen when the latter is encapsulated in pH-sensitive nanocarriers. The encapsulation of this complex in nanocontainers was carried out as described in by Toniolo *et al*. (2018). The resulting viability curves were compared to those obtained after treatment with free Cu-TPMA-Phen in the same concentration range, 0.1-30 μM, as shown in Figure 3.16A. Incubation with 3, 10 and 30 μM Cu-TPMA-Phen for 24 h results in significantly different viability between cells treated with free and encapsulated complex ($p < 0.0001$, 3 and 10 μM and $p < 0.01$, 30 μM). Analogous experiments were carried out for 48 h, resulting also in significant changes between the free and encapsulated form of the complex (Figure 3.16B). However, it should be considered that these differences do not indicate a lower activity of the NCs because the maximum release is at pH 4.0, which is a condition easily obtainable in cancer

microenvironment, but quite far from cell culture conditions. These differences in cytotoxicity can be attributed to the less amount of bioavailable drug. In fact, as described by Toniolo *et al.*, only 1/3 of Cu-TPMA-Phen is released from nanocontainers at the physiologic pH 7.4, which is similar to cell culture conditions.

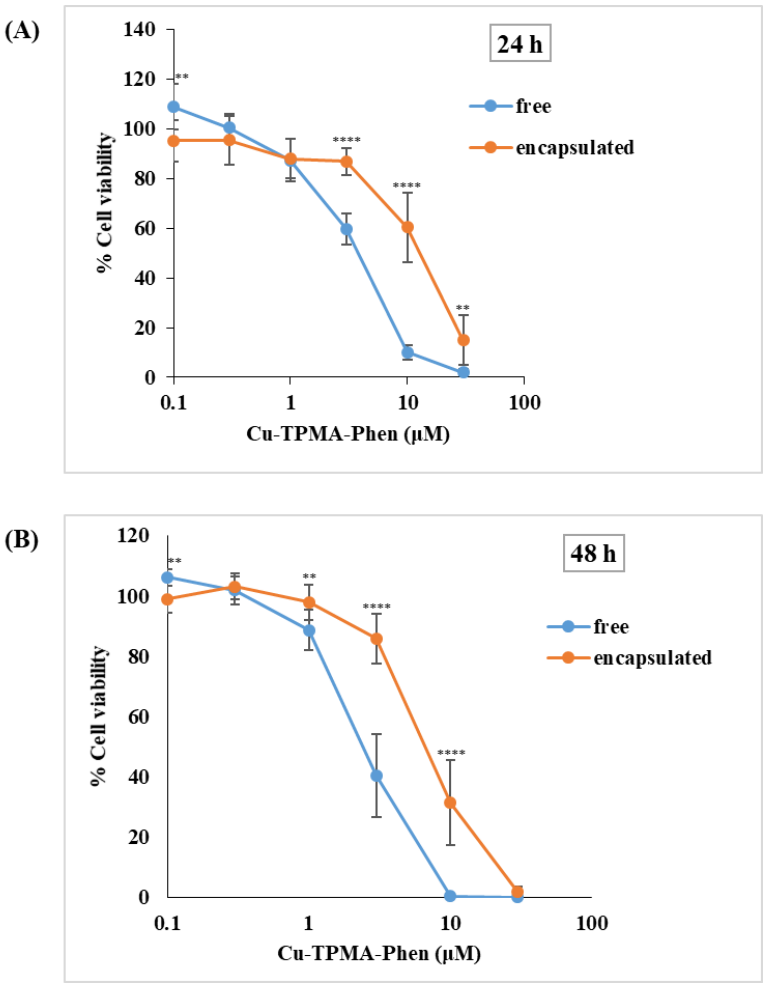

Figure 3.16: Dose-dependent response of NB100 cells treated with free or encapsulated Cu-TPMA-Phen for 24 and 48 h, panel A, and B, respectively. Cell viability was estimated with MTS assay. The results are presented as the means ± S.D. of three independent experiments performed in triplicate, representing the percentage of control values obtained from cultures grown in the absence of the complex. Statistical analysis was performed with unpaired t-test ** ($p < 0.01$), **** ($p < 0.0001$).

3.7.2 Membrane lipidomics of encapsulated Cu-TPMA-Phen

Membrane lipidomics analysis was also performed on NB100 cells treated with 5 µM of encapsulated Cu-TPMA-Phen in pH-sensitive nanocarriers. In this case, the impact on membrane lipidome presents no significant differences between untreated and treated cells (Figure 3.14A, B, C, D).

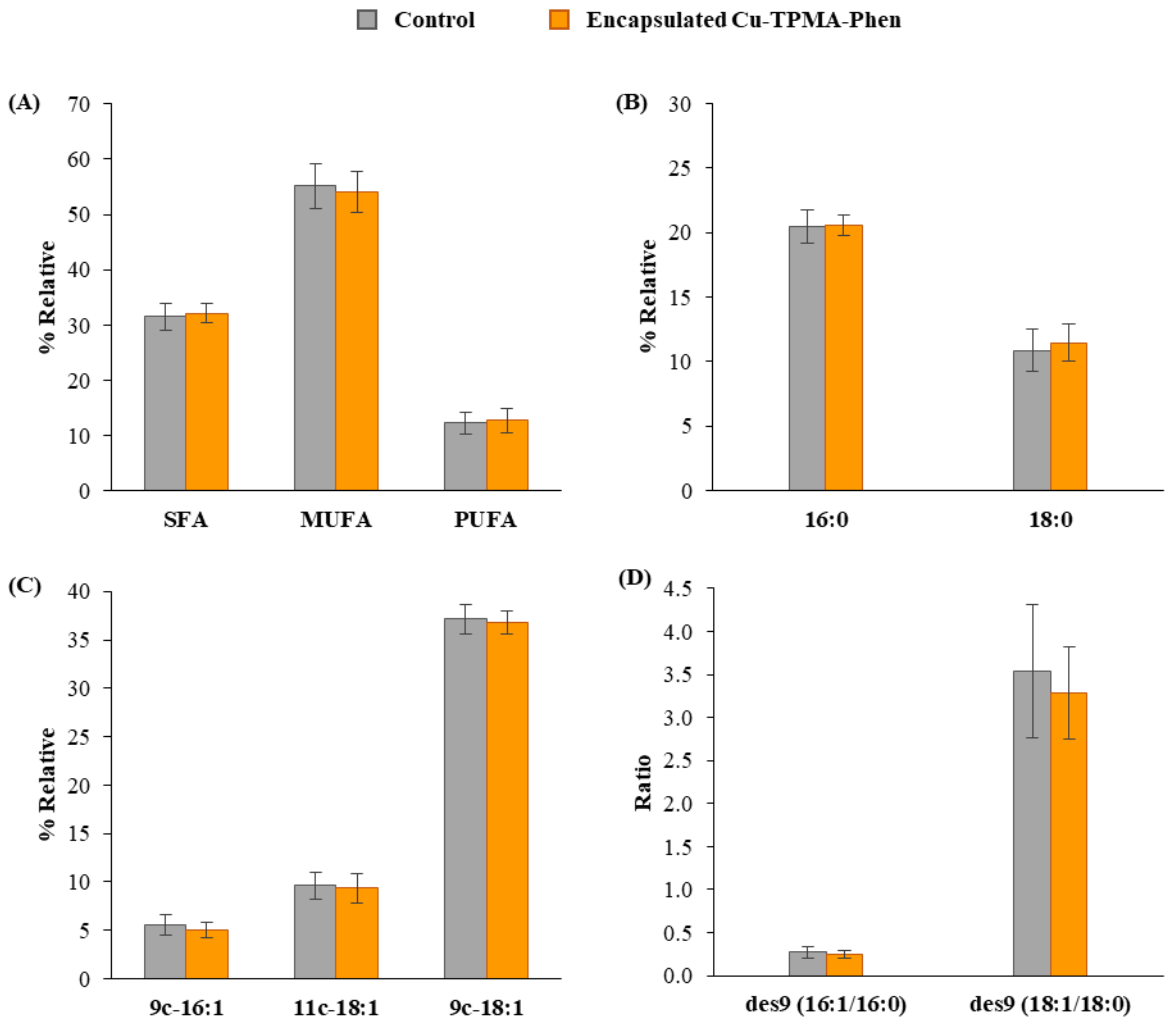

Figure 3.17: Fatty acid-based membrane lipidomics on NB100 cells treated with 5 µM encapsulated Cu-TPMA-Phen for 24 h; (A) Relative distribution of fatty acid families, SFA: saturated fatty acids, MUFA: monounsaturated fatty acids, PUFA: polyunsaturated fatty acids; (B) Palmitic (16:0) and stearic (18:0) acids trends in treated cells; (C) Palmitoleic (9c-16:1), vaccenic (11c-18:1) and oleic (9c-18:1) patterns in treated cells; (D) Estimation of delta-9 desaturase (des9) activity by the ratio palmitoleic/palmitic and oleic/stearic. Values represent mean ± SD (n=6). Statistical significance was calculated with the unpaired t-test. des9: Δ9-desaturase activity.

In this work, we observed the absence of effects of the copper complex when encapsulated in pH-sensitive nanocarriers, which do not release sufficient drug doses for membrane remodeling, but also suggests further studies on the control of oxidative effects by drug delivery in sense of enhanced tumor targeting [283]. In Tables 3.1 and 3.2, the detailed values of the analyzed fatty acids and their indices are presented, respectively.

Table 3.1: Relative percentages (% rel) and indices of membrane fatty acids methyl esters (FAME) of NB100 cells treated with 5 μM free or encapsulated Cu-TPMA-Phen. *P*-value represents the comparison among all the groups after conducting one-way ANOVA test. Stars indicate the statistically significant difference (Dunnett's multiple comparison test) between each treated group and the control cells (n=6); * ($p < 0.05$), ** ($p < 0.01$), *** ($p < 0.001$), **** ($p < 0.0001$).

FAME	Control	Free Cu-TPMA-Phen	Encapsulated Cu-TPMA-Phen	*p*-value
SFA				
16:0	20.43 ± 1.28	22.86 ± 2.21*****	20.54 ± 0.78	**0.0412**
18:0	10.85 ± 1.64	20.05 ± 1.71********	11.45 ± 1.42	**< 0.0001**
20:0	0.27 ± 0.20	0.46 ± 0.04*****	0.19 ± 0.02	**0.0060**
MUFA				
16:1c6	1.52 ± 0.09	1.32 ± 0.10******	1.47 ± 0.07	**0.0065**
16:1c9	5.54 ± 1.05	3.72 ± 0.73******	5.08 ± 0.81	**0.0133**
18:1c9	37.17 ± 1.52	28.13 ± 0.99********	36.80 ± 1.20	**< 0.0001**
18:1c11	9.62 ± 1.34	7.10 ± 0.92******	9.35 ± 1.52	**0.0138**
20:1c11	1.29 ± 0.29	0.94 ± 0.20	1.35 ± 0.32	0.0700
PUFA ω6				
18:2	2.20 ± 0.23	2.40 ± 0.43	2.29 ± 0.34	0.6369
20:2	0.39 ± 0.06	0.43 ± 0.08	0.40 ± 0.07	0.5248
20:3	0.58 ± 0.06	0.81 ± 0.12******	0.61 ± 0.08	**0.0021**
20:4	4.06 ± 0.73	4.51 ± 1.08	4.13 ± 0.78	0.6950
PUFA ω3				
18:3	0.09 ± 0.02	0.12 ± 0.03	0.09 ± 0.02	0.0840
20:5	0.81 ± 0.20	0.99 ± 0.26	0.85 ± 0.17	0.3822
22:5	1.94 ± 0.12	2.22 ± 0.22*****	2.01 ± 0.16	**0.0485**
22:6	2.23 ± 0.64	2.78 ± 0.83	2.35 ± 0.63	0.4525
Total *trans*				
18:1	0.63 ± 0.10	0.66 ± 0.06	0.64 ± 0.06	0.8524
18:2	0.22 ± 0.04	0.25 ± 0.04	0.22 ± 0.04	0.5132
20:4	0.16 ± 0.04	0.23 ± 0.06*****	0.17 ± 0.02	0.0583

Table 3.2: Indices of membrane fatty acids methyl esters (FAME) of NB100 cells treated with 5 μM free or encapsulated Cu-TPMA-Phen. *P*-value represents the comparison among all the groups after conducting one-way ANOVA test. Stars indicate the statistically significant difference (Dunnett's multiple comparison test) between each treated group and the control cells (n=6); * ($p < 0.05$), ** ($p < 0.01$), **** ($p < 0.0001$). des9: Δ9-desaturase activity.

Index	Control	Free Cu-TPMA-Phen	Encapsulated Cu-TPMA-Phen	*p*-value
SFA	31.55 ± 2.48	43.38 ± 0.92****	32.17 ± 1.82	**< 0.0001**
MUFA	55.14 ± 4.05	41.22 ± 2.60****	54.05 ± 3.71	**< 0.0001**
PUFA	12.29 ± 1.99	14.27 ± 2.94	12.74 ± 2.18	0.4137
PUFA ω6	7.22 ± 1.06	8.16 ± 1.72	7.43 ± 1.26	0.5408
PUFA ω3	5.07 ± 0.94	6.12 ± 1.24	5.31 ± 0.92	0.2789
SFA/MUFA	0.58 ± 0.08	1.06 ± 0.06****	0.60 ± 0.07	**< 0.0001**
ω6/ω3	1.44 ± 0.07	1.33 ± 0.05*	1.40 ± 0.03	**0.0219**
total trans	1.01 ± 0.13	1.13 ± 0.13	1.04 ± 0.10	0.2812
des9 (16:1/16:0)	0.27 ± 0.07	0.16 ± 0.02**	0.25 ± 0.04	**0.0062**
des9 (18:1/18:0)	3.54 ± 0.77	1.42 ± 0.17****	3.28 ± 0.53	**< 0.0001**

3.8 Conclusions

In the present research project, the novel Cu(II) complex $[Cu(TPMA)(Phen)](ClO_4)_2$ was studied being used both as a free compound and under an encapsulated form within polymeric nanoparticles, thus allowing for the comparison with the free drug. In vitro experiments were carried out in the neuroblastoma derived cell line NB100 cell line and breast carcinoma cell line MCF7. The cytotoxicity of both free and encapsulated complex was determined and the cell death pathways were analyzed with parallel monitoring of caspase activation. Inhibitors of apoptosis, necroptosis and scavengers of oxidative stress were tested to evaluate their protective effect against copper's cytotoxicity. NB100 cells were treated with EC_{50} doses of copper complex and membrane fatty acids were isolated, derivatized and analyzed by gas chromatography. As expected, membrane remodeling took place upon treatment with the copper complex prior to cell viability decrease. The observed changes in fatty acid composition included significant increase of SFA and diminution of MUFA, while PUFA levels did not alter. Since, SFA and MUFA are metabolically connected through the SCD1 desaturase activity, we hypothesized that the copper complex could provoke the inhibition of this enzyme. To test this hypothesis, we developed a cell-

free assay to assess the SCD1 enzymatic activity in the presence of copper complex. On the other hand, the observed membrane remodelling could be indirectly caused because of complex's cytotoxicity since it is well known the interplay between membrane remodelling and cell death. To examine a possible connection between the cytotoxic events and fatty acid changes, we performed lipidomic analysis in the presence of complex in cells that were pre-treated with apoptosis inhibitor and ROS scavengers. To further study this phenomenon, we performed time course lipidomics in complex-treated cells and correlated these results with the cell viability and caspase activation at the same time points. Finally, we were interested to test whether a tailored fatty acid supplementation could influence the cell response to copper complex exposure.

The main results include: i) oxidative stress-mediated cytotoxicity of copper complex and subsequent apoptosis and necroptosis in neuroblastoma cells, ii) membrane remodeling of treated cells with a specific increase of saturated fatty acids (SFA) and a decrease of MUFA, but not PUFA in both NB100 and MCF7 cell lines; iii) possible correlation of membrane remodeling with the cytotoxic mechanism of the copper complex, iv) elimination of the drug's effects on cell viability and membrane lipidome when Cu-TPMA-Phen is encapsulated in pH-sensitive polymeric nanoparticles, due to drug's delayed release and reduced bioavailability.

4. Membrane remodeling in tumor-bearing mice models

4.1 Background and Objectives

The project described in the present chapter was performed in collaboration with the group of Dr. E. Efthimiadou at the Institute of Nanoscience and Nanotechnology, N.C.S.R. "Demokritos". The overall goals of this research project were to a) evaluate the erythrocyte membrane fatty acid remodeling in normal and tumor-bearing mice at different stages of tumor occurrence and b) study the erythrocyte membrane fatty acid composition in normal and tumor-bearing mice, after administration of iron oxide nanoparticles and bleomycin. The mice models here studied were constructed, hosted and treated by our collaborators at the NCSR "Demokritos". Whole blood was collected in EDTA-treated tubes and shipped within 2 days in the laboratory of the CNR/spin-off company Lipinutragen where the erythrocyte membrane fatty acid analysis was carried out.

Lipid metabolic reprogramming is an established hallmark of cancer development [96], which among others includes a distinct fatty acid biosynthesis due to the rapid proliferation of cancer cells [103, 105]. Indeed, key enzymes that are involved in lipid biosynthesis, such as fatty acid synthase (FASN) and desaturases (SCD1, D5D, D6D), show increased activity in tumor development and propagation. These elevated enzymatic activities along with the corresponding fatty acids are thus pointed as markers of tumor presence and growth [42, 72, 105, 106]. It is well known that the fatty acid composition of the cellular membrane affects its fluidity, permeability as well as membrane lipid-related signaling. Alterations to the fatty acid content and consequently to the membrane properties might give favorable signals for tumor growth, progression and metastasis [72, 142, 284]. The membrane remodeling is highly affected by the intracellular lipid pool, which in turn depends on both the endogenous fatty acid biosynthesis and their dietary intake, especially in the case of the essential polyunsaturated fatty acids (PUFA) [285]. Several independent studies have revealed apparent correlations between the erythrocyte membrane phospholipid fatty acid concentrations and tumor risk [157, 158, 161-163]. Furthermore, differences on the fatty acid composition of tumor colorectal tissues has been reported between patients with and without metastasis, suggesting that membrane lipid remodeling could affect the cellular function and influence tumor cell metastasis [175].

One of the first discovered antitumoral drugs known to react with the membrane lipids was bleomycin (BLM) [199-201]. Bleomycin is a widely known antineoplastic agent, used to treat Hodgkin's lymphoma, non-Hodgkin's lymphoma, testicular, ovarian, head and cervical cancer among others [202]. Its therapeutic use is based, alike the famous cisplatin chemotherapy, on its ability to cleave DNA [202, 203]. Inhibition of DNA, RNA and protein synthesis by bleomycin has also been reported [203]. Studies have proved that DNA strand breaks induced by bleomycin rely on oxygen and metal ions. More specifically, it has been suggested that bleomycin chelates metal ions (mainly iron), producing a pseudoenzyme that reacts with oxygen to produce superoxide and hydroxide free radicals, as shown in Figure 4.1 [286, 287]. Its abilities to chelate redox-active metal-centers (i.e. Fe(III) or Cu(II)) as well as binding to DNA, enable metallo-bleomycin to the artificial metallo-nucleases (AMN) category [202]. Moreover, such metallo-antibiotics mediate oxidation of other cellular molecules, such as lipid peroxidation [204, 205].

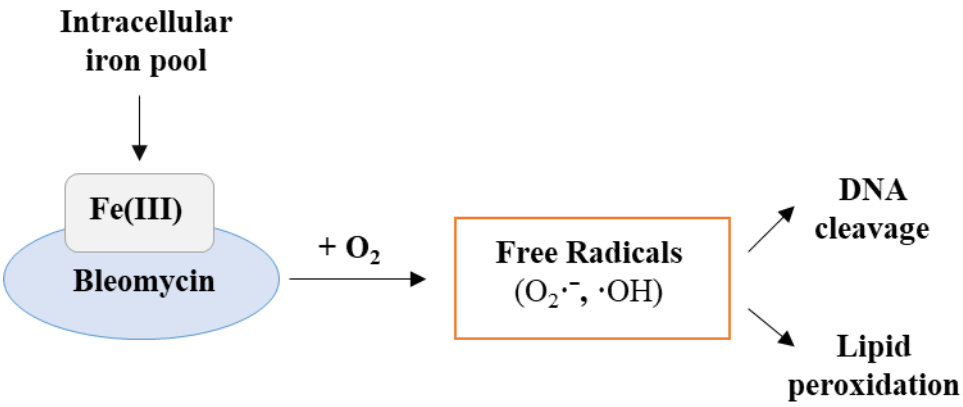

Figure 4.1: The free radical pathway generated by iron-bleomycin complex induces DNA and lipid damage**.**

Iron oxide nanoparticles find several medical applications, such as in the field of diagnostics (e.g. Magnetic Resonance Imaging - MRI) and therapeutics (e.g. hyperthermia-based cancer treatment) [288]. They may also serve as drug carriers for specific drug delivery, as well as nano-adjuvant for vaccine and antibody production [289]. Despite their low toxicity, iron nanoparticles can be degraded *in vivo*, thus leading to increased iron

levels in tissues [290]. The biodistribution of these biodegradation-produced iron ions can be then regulated by either ferritin or transferrin, which are the two main iron–binding proteins [291, 292]. High levels of intracellular iron have been implicated in the iron-induced lipid peroxidation, since the free iron ions can react with superoxide or hydrogen peroxide to form hydroxyl radicals [293].

In the present project, we used a mouse xenograft model, consisting of a severe combined immunodeficient (SCID) female mouse, inoculated with the human glioblastoma U87MG cell line. Fatty acid composition of erythrocyte membrane was monitored: a) at different stages of tumor occurrence and b) at early points of tumor occurrence after administration of iron nanoparticles, bleomycin or combination of the latter two. Non-xenografted SCID mice that underwent the same treatment with the xenografted ones served as the control sample. In parallel, healthy Swiss mice were used for comparison with the tumor-bearing SCID mice.

4.2 Erythrocyte membrane fatty acid analysis

4.2.1 Healthy Swiss *vs* control SCID mice

Comparison of healthy Swiss and control SCID mice was performed to evaluate the impact of the immunodeficiency to the obtained results, later presented in this chapter. Although it was not among the main aims to deepen into the differences between these two mice models, an initial evaluation of the distribution of the RBC membrane fatty acid families in these two animal models was carried out, prior to the examination of the membrane fatty acid distribution during the tumor progression in the immuno-deficient model of SCID mice. To our knowledge, the erythrocyte membrane fatty acid composition of SCID mice has not been evaluated before. For this reason, we performed an initial RBC fatty acid analysis aiming at a) the monitoring of fatty acid composition during ageing in both control SCID and normal Swiss mice and b) the comparison between these two animal models. The % relative distributions of the analyzed fatty acid moieties are reported in Table 4.1.

Table 4.1: Relative percentages (% rel) of fatty acids methyl esters (FAME) from red blood cell (RBC) membrane of normal healthy Swiss mice and control SCID mice at different age points (4 weeks and 17 weeks). *P*-value represents the comparison between young (4 weeks) and old (17 weeks) mice of each group after conducting unpaired t-test (n=3 for normal Swiss and n=2 for SCID mice).

FAME	Normal Swiss-4w	Normal Swiss-17w	*p*-value	Control SCID-4w	Control SCID-17w	*p*-value
SFA						
14:0	0.09 ± 0.13	0.61 ± 0.18	*0.3270*	0.57 ± 0.06	0.55 ± 0.14	*0.9075*
15:0	0.75 ± 0.36	0.56 ± 0.24	*0.9054*	0.15 ± 0.04	0.15 ± 0.02	*>0.9999*
16:0	28.63 ± 0.75	28.38 ± 0.80	*0.9994*	35.38 ± 0.46	31.78 ± 0.55	***0.0377***
17:0	0.29 ± 0.21	0.43 ± 0.10	*>0.9999*	0.17 ± 0.00	0.16 ± 0.02	*>0.9999*
18:0	13.15 ± 0.58	10.57 ± 1.01	*0.2690*	10.73 ± 0.09	12.11 ± 0.47	*0.1022*
MUFA						
16:1c6	0.57 ± 0.15	0.27 ± 0.02	*0.0713*	0.23 ± 0.02	0.23 ± 0.05	*>0.9999*
16:1c9	1.82 ± 0.66	3.09 ± 0.55	*0.2269*	1.66 ± 0.36	2.89 ± 0.38	*0.1426*
18:1c9	15.03 ± 0.96	18.06 ± 1.66	*0.4361*	15.87 ± 0.95	19.09 ± 1.20	*0.1701*
18:1c11	2.67 ± 0.08	3.26 ± 0.03	***0.0012***	2.70 ± 0.06	2.46 ± 0.07	*0.1213*
20:1c11	0.54 ± 0.12	0.39 ± 0.02	*0.2181*	0.48 ± 0.02	0.39 ± 0.04	*0.1425*
PUFA ω6						
18:2	10.63 ± 0.32	12.27 ± 1.28	*0.6759*	11.22 ± 0.30	11.67 ± 0.25	*0.3683*
18:3	0.10 ± 0.14	0.16 ± 0.04	*0.9999*	0.05 ± 0.05	0.16 ± 0.02	*0.1462*
20:2	0.59 ± 0.09	0.39 ± 0.04	*0.2793*	0.55 ± 0.02	0.39 ± 0.07	*0.1386*
20:3	1.44 ± 0.18	1.35 ± 0.05	*0.8947*	1.22 ± 0.01	1.14 ± 0.13	*0.5880*
20:4	14.50 ± 1.07	13.34 ± 1.51	*0.9082*	11.53 ± 0.99	10.40 ± 0.95	*0.4968*
PUFA ω3						
18:3	0.25 ± 0.20	0.24 ± 0.07	*0.9286*	0.18 ± 0.04	0.18 ± 0.00	*0.8995*
20:5	0.63 ± 0.04	0.52 ± 0.14	*0.7063*	0.43 ± 0.03	0.42 ± 0.03	*0.9098*
22:5	0.82 ± 0.15	0.70 ± 0.11	*0.8803*	0.89 ± 0.05	0.67 ± 0.04	*0.0663*
22:6	6.46 ± 0.30	5.35 ± 0.48	*0.2110*	5.70 ± 0.08	4.84 ± 0.30	*0.1091*
trans						
18:1	0.22 ± 0.31	nd	*0.6568*	nd	nd	-
18:2	0.26 ± 0.37	nd	*0.6611*	0.10 ± 0.00	0.10 ± 0.01	*0.6985*
20:4	0.56 ± 0.41	0.20 ± 0.04	*0.5000*	0.20 ± 0.03	0.24 ± 0.04	*0.6513*

The comparison between young (4 weeks) and old (17 weeks) mice of each model showed no significant difference on the RBC membrane fatty acid composition during ageing. A significant change found concerns the 17-weeks old control SCID mice, whose palmitic acid (16:0) was slightly decreased (p=0.0377) in contrast to the 4-weeks old SCID mice. Despite this diminution of palmitic acid, the fatty acid families and indexes were not

influenced. Furthermore, 17-weeks old Swiss mice have higher levels of vaccenic acid (18:1c11) opposite to the young ones (p=0.0012). Based on the few alterations detected, we consider that the ageing process is not the main factor for potential changes on membrane lipidome in the present case. As already mentioned, it was not the scope of this project to detail the differences between healthy Swiss and control SCID mice, however some interesting information was obtained related to the immunodeficient phenotype. The examined mice models (control SCID and healthy Swiss) are characterized by different erythrocyte membrane fatty acid profiles. Palmitic (16:0), stearic (18:0) and arachidonic (20:4ω6) are among the fatty acids with the most notable variation among the two models (Table 4.1), thus affecting the total SFA and PUFA values (Table 4.2). These differences could indicate that the immunodeficient phenotype may contribute to the final erythrocyte membrane remodeling. For following comparisons, the fatty acid families and indices that characterize normal healthy Swiss and control SCID mice at different age points (4- and 17-weeks old) are presented in Table 4.2.

Table 4.2: Relative percentages (% rel) of fatty acid methyl esters (FAME) families and indices of normal healthy Swiss and control SCID mice at different age points (4 weeks and 17 weeks). *P*-value represents the comparison between young (4-weeks) and old (17-weeks) mice of each group after conducting unpaired t-test (n=3 for normal Swiss and n=2 for control SCID mice). SFA: saturated fatty acids; MUFA: monounsaturated fatty acids; PUFA: polyunsaturated fatty acids; UI: unsaturation index; PI: peroxidation index.

	Normal Swiss-4w	**Normal Swiss-17w**	***p*-value**	**Control SCID-4w**	**Control SCID-17w**	***p*-value**
SFA	42.91 ± 1.41	40.55 ± 1.69	*0.3594*	46.99±0.35	44.75±0.93	*0.1529*
MUFA	20.63 ± 1.49	25.07 ± 2.18	*0.3192*	20.94±1.20	25.06±1.60	*0.1756*
PUFA	35.42 ± 1.15	34.18 ± 0.69	*0.9623*	32.07±0.85	30.00±0.48	*0.1685*
PUFA ω-6	27.26 ± 0.97	27.46 ± 0.42	*>0.9999*	24.86±0.65	23.89±0.77	*0.4339*
PUFA ω-3	8.17 ± 0.21	6.73 ± 0.53	*0.1602*	7.21±0.20	6.11±0.29	*0.0891*
ω-6/ω-3	3.34 ± 0.07	4.11 ± 0.32	*0.6196*	3.45±0.01	3.93±0.31	*0.2671*
SFA/MUFA	2.10 ± 0.22	1.64 ± 0.21	*0.7962*	2.25±0.15	1.80±0.15	*0.1625*
total trans	1.56 ± 0.05	0.20 ± 0.04	***0.0006***	0.30±0.03	0.34±0.05	*0.5636*
UI	152.47 ± 5.58	146.79 ± 4.57	*0.8856*	135.06±3.01	128.63±0.47	*0.1692*
PI	133.73 ± 5.94	119.99 ± 8.77	*0.5387*	114.39±4.76	101.76±1.50	*0.1268*

4.2.2 Tumor-bearing mice at different stages

We used an experimental animal model, which was the severe combined immunodeficient (SCID) mouse xenografted with a human tumor cell line (glioblastoma U87MG). Such human xenografts are widely used in clinical research for the assessment of anticancer therapeutics [294, 295]. The diseased model was followed up at different ages (4-, 5- and 17-weeks old) and was compared with no tumor-diseased SCID mice. Particularly, the erythrocyte membrane fatty acid profiles of these animals were monitored at different ages in order to track potential RBC membrane profile changes that could mirror the fatty acid remodeling and metabolism.

The flowchart of the protocol used in this study is described in Figure 4.2. Human tumor xenograft was obtained by inoculating U87MG human brain glioblastoma cells subcutaneously in two weeks old SCID mice. Approximately 2 weeks post-injection, the first set of animals was sacrificed (group 3, four-weeks-old). The second set of tumor-bearing mice was sacrificed one week later (group 4, five-weeks-old) and the third set after 84 days (group 5, seventeen-weeks old). The group 3 and 4 are referred as the early stage of tumorigenesis hereinafter, while the group 5 as the final stage of tumor presence when all tumor-bearing mice are characterized by very poor conditions. In parallel, we evaluated the fatty acid content of membrane phospholipids in control SCID mice without tumor implantation, four-weeks-old (group 1) and seventeen-weeks old (group 2), to identify potential differences with tumor-bearing animals. Since in the present study human xenograft are selected and tumors originate by exogenously inoculation with human cancer cells, tumor tissues were not analyzed, following an approach described for a genetically engineered mouse [295]. The fatty acid-based membrane lipidomic study was performed using membrane phospholipids isolated from red blood cells (RBCs) with published procedures [296]. As shown in Figure 4.2, the extracted RBC phospholipids were transformed into fatty acid methyl esters (FAME) under known conditions [297]. FAMEs were analyzed by gas chromatography (GC) in order to identify saturated (SFA) and unsaturated (MUFA and PUFA) fatty acids, the latter being recognized as positional and geometrical isomers [246].

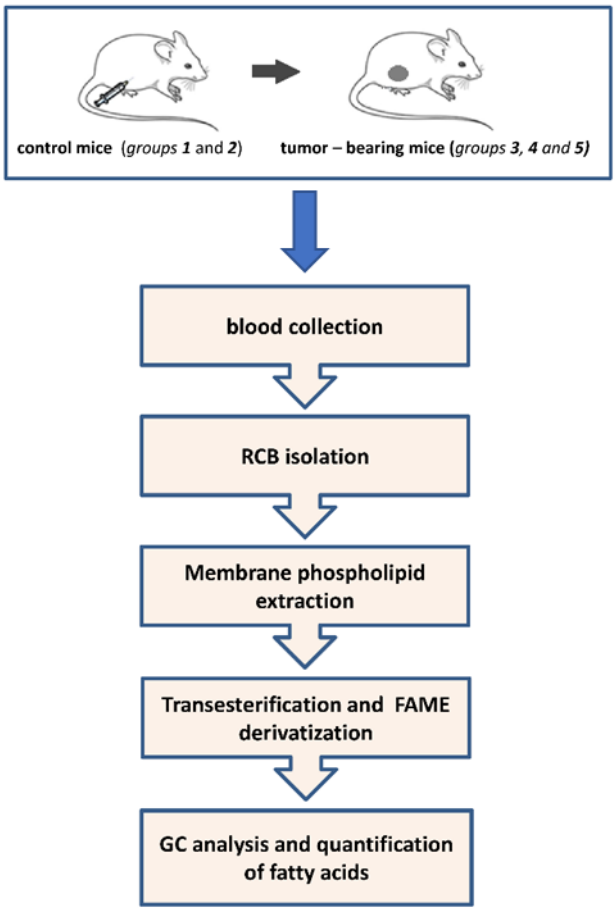

Figure 4.2: Flowchart for the analysis and quantification of membrane fatty acid moieties in erythrocytes of control SCID mice; **group 1**: 4-weeks old; **group 2**: 17-weeks old; and tumor-bearing SCID mice; **group 3**: 4-weeks old; **group 4**: 5-weeks old; **group 5**: 17-weeks old.

After better understanding the present experimental model (described in section 4.2.1), we proceeded with the membrane lipidomic analyses in tumor-bearing mice at an early stage of tumorigenesis (4- and 5-weeks old mice) and at a final stage of tumor progression (17-weeks old tumor-bearing mice). In the present study, the erythrocyte membrane was utilized for the examination of fatty acid composition, since it is an easily withdrawn biological specimen. Red blood cells are increasingly gaining attention as an interorgan communication system, since their crosstalk with other tissues has been revealed [298, 299]. RBCs structure and function are affected by the presence of ROS, but they also participate in the control of redox regulation [91, 299-301]. Recent works suggest that the RBC, as a "circulating" cell that is sensing the microenvironment found in all tissues, could be considered as a "reporter cell" for the antioxidant status of the other tissues [302-304]. Indeed, it has been reported that erythrocyte and liver cells have similar membrane fatty

acid composition [305] and mean lifetime (120 and 180 days, respectively). Thus, the fatty-acid based membrane lipidomics of erythrocytes can serve as a useful tool for the extrapolation of information, especially when combined with other relevant metabolic and cellular assays [306].

In Table 4.3, the fatty acids are grouped into families of SFA, MUFA and PUFA (graphically represented in Figure 4.3A), *trans* fatty acids (TFA) (graphically represented in Figure 4.3B), as well as into PUFA ω-3, PUFA ω-6 and their ratio. In Table 4.3 the calculated indices of unsaturation (UI) and peroxidation (PI) are also reported [246, 307].

Table 4.3: Relative percentages (% rel) of fatty acid families and indices of erythrocytes obtained from control SCID mice (4 weeks and 17 weeks) and tumor-bearing mice at different age points (4 weeks, 5 weeks and 17 weeks). *P*-value represents the comparison among all the groups after conducting a one-way ANOVA test among all the groups (n=3).

	Control SCID-4w	**Control SCID-17w**	**Tumor SCID-4w**	**Tumor SCID-5w**	**Tumor SCID-17w**	***p*-value**
SFA	46.99±0.35	44.75±0.93	42.16±0.03	42.54±1.07	57.86±0.44	***<0.0001***
MUFA	20.94±1.20	25.06±1.60	20.08±0.08	19.53±0.77	15.54±3.34	*0.0658*
PUFA	32.07±0.85	30.00±0.48	37.09±0.13	36.58±0.01	26.60±3.58	***0.0190***
PUFA ω-6	24.86±0.65	23.89±0.77	28.56±0.04	27.48±0.04	21.21±3.47	*0.0960*
PUFA ω-3	7.21±0.20	6.11±0.29	8.54±0.09	9.11±0.03	5.39±0.94	***0.0054***
ω-6/ω-3	3.45±0.01	3.93±0.31	3.35±0.03	3.02±0.01	4.05±1.02	*0.5875*
SFA/MUFA	2.25±0.15	1.80±0.15	2.10±0.01	2.18±0.14	3.89±0.76	***0.0281***
Total *trans*	0.30±0.03	0.34±0.05	0.55±0.11	1.36±0.32	0.32±0.07	***0.0074***
UI	135.06±3.01	128.63±0.47	159.61±0.53	156.82±0.63	109.00±10.19	***0.0014***
PI	114.39±4.76	101.76±1.50	142.52±0.60	140.68±0.24	92.10±13.59	***0.0053***

The following differences emerged from the comparison between control and tumor-bearing SCID mice at different time points:

i. Erythrocyte membrane lipidome profiles showed increased levels of SFA during tumor propagation. In particular, the relative percentage of SFA reached *ca* 58% over the total fatty acid composition in late-stage tumor-bearing mice, which is the highest SFA percentage found compared to both control SCID and early-stage

tumor-bearing mice (*ca* 42%, $p<0.0001$). As shown in Table 4.4, all the members of the SFA family follow this increasing trend in late-stage diseased SCID mice. On the contrary, the fatty acid moieties of MUFA family were decreased in the same animals, however not significantly. Consequently, the ratio of SFA/MUFA was increased at the erythrocytes of late-stage tumor mice, while the same ratio was decreased in the corresponding control SCID mice ($p=0.028$).

ii. In addition to the above membrane remodeling, PUFA levels were significantly decreased in 17-weeks old tumor-bearing SCID mice ($p=0.0019$). Late stage diseased mice were characterized by smaller PUFA content in RCB membrane phospholipids compared to the young (4- and 5-weeks old) tumor-bearing age mice ($p=0.0071$ and $p=0.0085$, respectively). Notably, the PUFA levels in 4-weeks old control SCID mice were found much lower compared to corresponding tumor-bearing and they were even fewer in 17-weeks old control mice, not significantly though. Both the families of omega-6 and omega-3 PUFA showed a decreasing pattern for late-stage tumor mice, without alterations at their in-between ratio (ω6/ω3).

iii. ARA and DHA (members of the ω-6 and ω-3 PUFA families, respectively) show also significant depletion in tumor-bearing SCID mice after 17-weeks disease progression ($p=0.0333$ and $p=0.0027$, respectively), as represented in Figures 4.3D and 4.3E. Remarkably, in all cases, the PUFA changes did not involve the ω-6 precursor linoleic acid (LA: 9cis, 12cis-C18:2), showing only a decreasing trend at the late-stage tumor-bearing mice (Tables 4.1 and 4.4 for control and tumor-bearing SCID mice, respectively).

iv. The indexes of unsaturation and peroxidizability are significantly decreased (UI and PI; $p=0.0014$ and $p=0.0053$, respectively) (Table 4.3). It is worth mentioning that the neither in SCID mice nor in healthy Swiss mice the UI and PI indexes were found significantly affected by the age (Table 4.1).

v. The level of TFA show also an interesting trend for tumor-bearing SCID mice, as they increase significantly in 5-weeks old tumor-bearing mice and then they

decrease again in 17-weeks old ones (p=0.0074) (Table 4.3 and Fig. 4.3B). No significant changes were revealed regarding the control SCID mice.

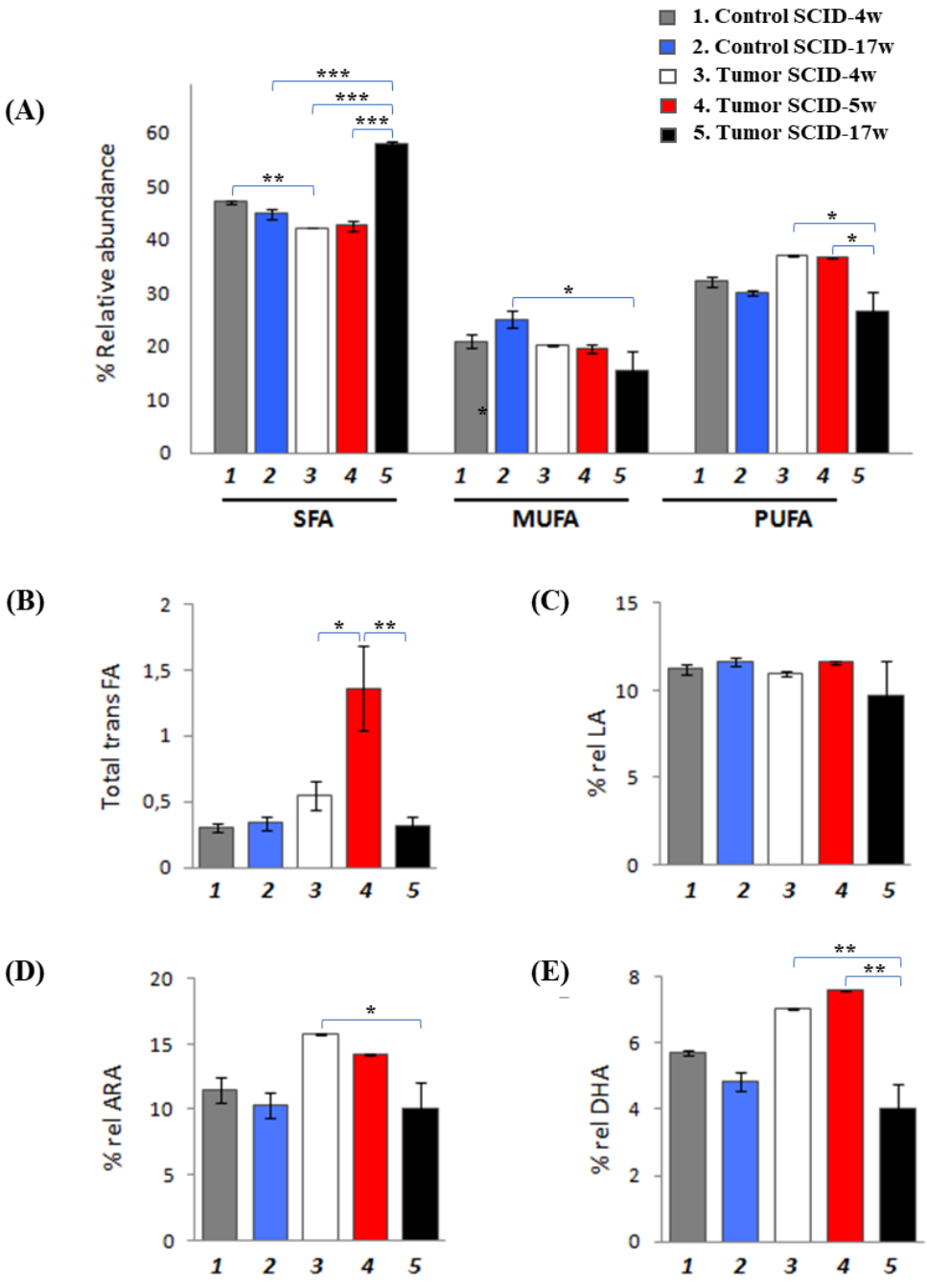

Figure 4.3: (**A)** Fatty acid composition grouped into families SFA, MUFA and PUFA of erythrocyte membrane at early and late stage of control SCID and tumour-bearing mice; comparison among control (4 weeks and 17 weeks old; group *1* and group *2*, respectively) and diseased mice (4 weeks old, 5 weeks old and 17 weeks old; group 3, group 4 and group *5*, respectively); **(B**) Total *trans* fatty acids isomers of erythrocyte membrane among control SCID

(group ***1*** and group ***2***) and tumour-bearing mice (group ***3***, group ***4*** and group ***5***); (**C**) LH (18:2 ω-6) levels for the five distinct mice groups; (**D**) ARA (20:4 ω-6) levels for the five distinct mice groups; (**E**) DHA (22:6 ω-3) levels for the five distinct mice groups. Values represent mean ± SD (n=3). * ($p< 0.05$), ** ($p < 0.01$), *** ($p < 0.001$), **** ($p < 0.0001$).

As far as the comparison between tumor diseased and healthy Swiss mice is concerned, we observed the following:

i. 4-weeks old tumor-bearing mice showed an erythrocyte membrane lipidomic profile quite similar to the one characterizing the healthy Swiss mice at early age points (comparison between Table 4.3 with Table 4.2, respectively). The relative distribution of fatty acid families (SFA, MUFA and PUFA) was rather comparable in the RBC membrane obtained from young mice of both models.

ii. The UI and PI indexes of 4-weeks old diseased SCID mice were more comparable to the ones of Swiss healthy than to those of control SCID mice (Tables 4.3 and 4.2).

iii. The total TFA were decreased during aging only in the case of healthy Swiss mice (p=0.0006, Table 4.2).

During tumor progression, the levels of erythrocyte membrane SFA increase, indicating their availability from the *de novo* fatty acid biosynthesis machinery. Indeed, many studies report an enhanced fatty acid synthase (FASN) activity in tumor progression [308-311], accompanied by an increase of desaturase activity [142], although this latter process was not observed in our animal model. In late stage tumor-bearing SCID mice, the SFA increase is accompanied by a diminution of PUFA, which are essential or semi-essential molecules and are not produced by endogenous biosynthetic pathways. The variation in PUFA levels among the different SCID mice (group 1 vs 3 and group 3 vs 5) is interesting, since there are numerous original publications and literature reviews discussing the role of PUFA in cancer risk [312] and tumor progression [313]. According to the above results, we could consider a significant distinction of PUFA levels during tumor progression; increased at early stages in tumor-bearing SCID mice and then lowered as the tumor progresses (Table 4.3). This PUFA diminution could be probably attributed to lipid peroxidation in cell

membranes [104, 314], since tumor tissue is characterized by enhanced oxidative stress [315]. ARA (20:4-ω6) and DHA (22:6-ω3), which are the major long chain PUFA counterparts in the membrane, are prone to oxidation and showed a significant decrease in late-stage tumor-bearing mice. However, it is notable that the levels of LA, which is the ω-6 precursor, were not significantly altered (Table 4.4). Thus, the hypothesis that oxidative processes are localized to tissues rich in ARA and DHA, which are more oxidizable molecules, can be fostered. PUFA play also an important role in lipid signaling. For instance, the arachidonic acid moieties are removed from membrane phospholipids by the enzyme PLA2, giving rise to signaling cascades that are known to lead to apoptosis evasion and tumor progression [312, 316]. Overall, both oxidative and signaling processes may contribute to the lower quantity of PUFA observed in membrane remodeling during cancer progression.

Another process that is correlated with the oxidative stress and particularly the reactivity of the free radicals is the geometrical *cis-trans* lipid isomerization [314, 317]. As observed in the membranes of our animal models of study, the *trans* fatty acid levels changed significantly in the 5-week old tumor-bearing mice and this could be related to an increased radical -induced fatty acid isomerization. On the contrary, at the early (4-weeks) and late (17-weeks) tumor stages, a lesser isomerizing effect was detected (Table 4.3 and Figure 4.3b). Indeed, the involvement of *trans* fatty acids (TFA) in cancer is still controversial [318] and no conclusive explanation can be given to this point for the pattern observed. The similarities found between tumor-bearing SCID and healthy Swiss mice cannot be currently explained, and further investigation has to be carried out for the elucidation of this observation.

Table 4.4. Relative percentages (% rel) of fatty acids methyl esters (FAME) from red blood cell (RBC) membrane of tumor-bearing mice at different age points (4 weeks, 5 weeks and 17 weeks). *P* value represents the comparison among all the groups after conducting one-way ANOVA test in parallel with multiple comparisons of all groups (n=3).

FAME	Tumor SCID-4w	Tumor SCID-5w	Tumor SCID-17w	*p*-value
SFA				
14:0	0.31 ± 0.02	0.33 ± 0.02	0.54 ± 0.05	***0.0103***
15:0	0.36 ± 0.05	0.46 ± 0.06	0.09 ± 0.07	***0.0142***
16:0	28.61 ± 0.07	29.23 ± 0.91	38.52 ± 1.90	***0.0053***
17:0	0.33 ± 0.01	0.45 ± 0.01	0.32 ± 0.04	***0.0357***

FAME	Tumor SCID-4w	Tumor SCID-5w	Tumor SCID-17w	*p*-value
18:0	12.56 ± 0.06	12.08 ± 0.23	18.39 ± 2.02	***0.0267***
MUFA				
16:1c6	0.26 ± 0.01	0.37 ± 0.08	0.22 ± 0.07	*0.2394*
16:1c9	1.47 ± 0.21	1.37 ± 0.05	1.15 ± 0.65	*0.8269*
18:1c9	16.05 ± 0.06	15.41 ± 0.53	12.10 ± 2.75	*0.2525*
18:1c11	1.94 ± 0.08	1.99 ± 0.12	1.81 ± 0.11	*0.4285*
20:1c11	0.37 ± 0.01	0.40 ± 0.01	0.24 ± 0.03	***0.0089***
PUFA ω6				
18:2	10.97 ± 0.12	11.61 ± 0.07	9.67 ± 2.05	*0.5189*
18:3	0.18 ± 0.01	0.09 ± 0.09	0.02 ± 0.03	*0.1602*
20:2	0.35 ± 0.03	0.33 ± 0.02	0.35 ± 0.15	*0.9857*
20:3	1.26 ± 0.10	1.26 ± 0.01	0.80 ± 0.08	***0.0088***
20:4	15.81 ± 0.04	14.20 ± 0.09	10.07 ± 2.01	***0.0463***
PUFA ω3				
18:3	0.19 ± 0.03	0.26 ± 0.07	0.17 ± 0.04	*0.3714*
20:5	0.52 ± 0.03	0.53 ± 0.04	0.32 ± 0.07	***0.0443***
22:5	0.76 ± 0.06	0.72 ± 0.05	0.87 ± 0.18	*0.5865*
22:6	7.07 ± 0.03	7.60 ± 0.01	4.04 ± 0.74	***0.0064***
trans				
18:1	0.20 ± 0.03	0.24 ± 0.07	0.03 ± 0.04	***0.0379***
18:2	0.28 ± 0.01	0.44 ± 0.09	0.14 ± 0.05	***0.0437***
20:4	0.07 ± 0.07	0.68 ± 0.15	0.15 ± 0.05	***0.0134***

4.2.3 Tumor-bearing SCID mice treated with iron nanoparticles and bleomycin

Previous research activity of CNR/Lipinutragen group has revealed the effects of bleomycin on the membrane lipidome of the neuroectodermal NTera2 tumor cell line and on biomimetic models (liposomes) [199, 200]. Our aim was to transfer the above studies to our *in vivo* model, which is a SCID mouse xenografted with the human glioblastoma U87MG cell line. In particular, 4-weeks old tumor-bearing SCID mice were randomly divided into four groups; Group 1 (control group) received normal saline, Group 2 received 3 mg/kg (0.6 mg/mL) Fe_3O_4 metallo-nanoparticles (Fe-NPs) suspended in saline, Group 3 received 15 mg/kg (3mg/mL) bleomycin and lastly, Group 4 received Fe-NPs plus bleomycin (co-treatment at the same concentrations as for groups 3 and 4). All administrations were performed intravenously. Animals were sacrificed 24 h after drug administration, red blood cells were isolated from whole blood and analyzed for assessing the membrane fatty acid composition, as depicted in Figure 4.4.

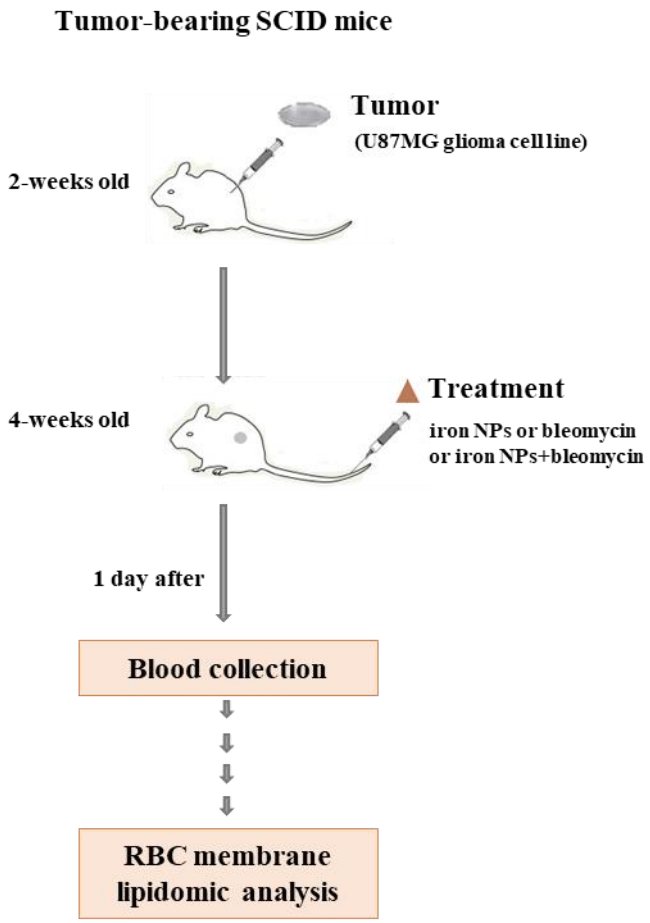

Figure 4.4: Protocol outline for the analysis and quantification of membrane fatty acid moieties in erythrocytes of tumor-bearing SCID mice after treatment with iron nanoparticles (NPs), bleomycin or combination of the them.

Tumor-bearing SCID mice that underwent any treatment (Fe-NPs, Bleomycin, Fe-NPs/Bleomycin) were characterized by an erythrocyte membrane lipidomic profile similar to untreated tumor-bearing SCID mice. The only significant difference observed was in the case of tumor-bearing SCID mice treated with the combination Fe-NPs/bleomycin, during which the ω-6/ω-3 ratio in RBC membrane was lower (p<0.05) compared to all other groups (Figure 4.5, Table 4.5). As far as the bleomycin is concerned, its administration (either alone or combined with Fe-NPs) did not provoke any alterations on erythrocytes membrane fatty acid composition.

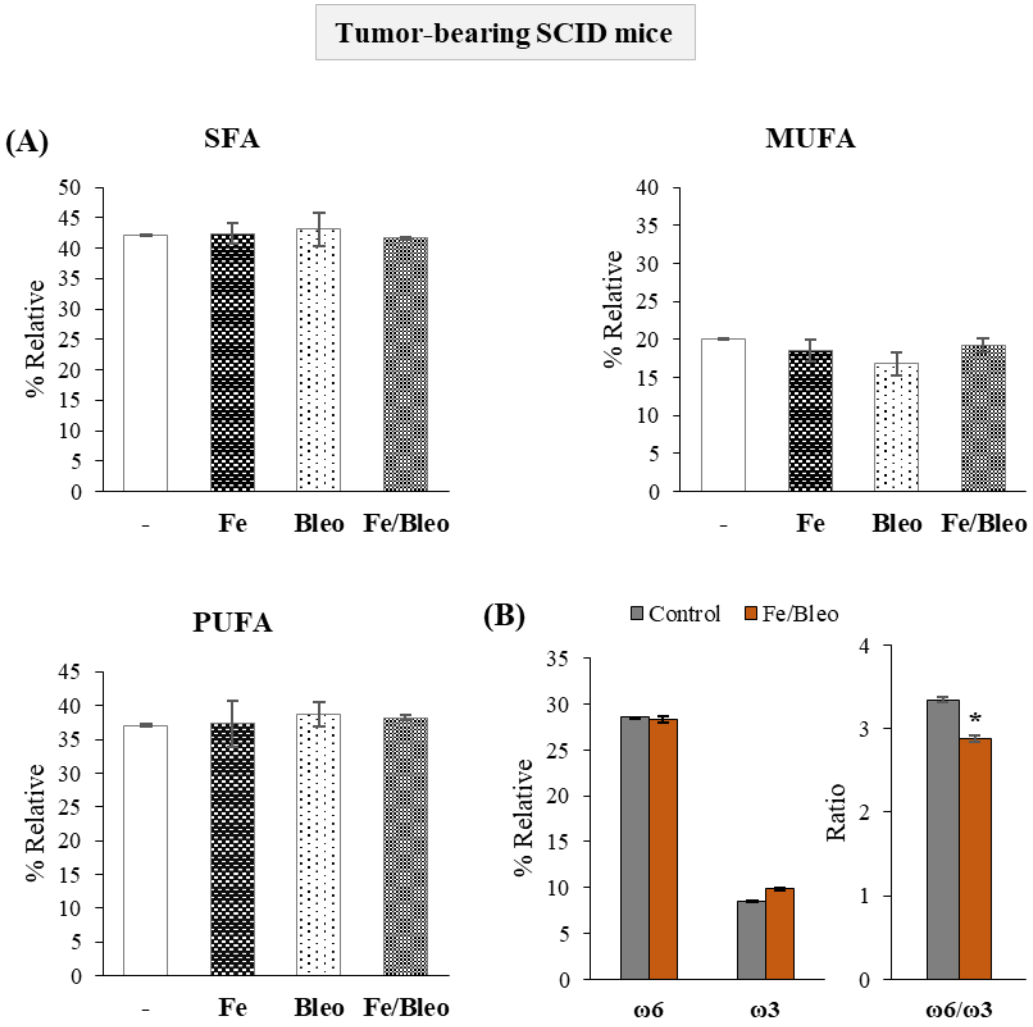

Figure 4.5: (A) Relative (%) distribution of fatty acid families in erythrocyte membranes of 4-weeks old tumor-bearing SCID mice treated with 3 mg/kg iron nanoparticles (Fe), 15 mg/kg bleomycin (Bleo) and the combination of them (Fe/Bleo) at the same concentrations. (B) Distribution of ω6 and ω3 polyunsaturated fatty acids and their ratio in erythrocyte membranes of 4-weeks old tumor-bearing SCID mice treated with Fe-NPs/Bleomycin. Fatty acid analysis was performed 1-day post-treatment. Values represent Mean ± SD (n=3). SFA, saturated fatty acids; MUFA, monounsaturated fatty acids; PUFA, polyunsaturated fatty acids. Statistical significance was tested with the unpaired *t*-test.

Table 4.5: Erythrocyte membrane fatty acid composition of tumor-bearing SCID mice (4 weeks old) treated with Fe nanoparticles [3 mg/kg], bleomycin [15 mg/kg] and the combination of them at the same concentrations. The variance of each fatty acid among the different groups was studied with the ANOVA test. Multiple comparison test was applied to compare the differences among the distinct groups (* control vs x-treated, * Fe-NPs vs bleomycin, * Fe-NPs vs Fe-NPs/bleomycin, * Bleomycin vs Fe-NPs/bleomycin).

FAME (% rel)	Control	Fe-NPs	Bleomycin	Fe-NPs/ Bleomycin	ANOVA (*p*-value)
SFA	42.16 ± 0.03	42.45 ± 1.78	43.10 ± 2.78	41.64 ± 0.21	*0.8689*
MUFA	20.08 ± 0.08	18.51 ± 1.43	16.79 ± 1.49	19.26 ± 0.91	*0.1572*
SFA/MUFA	2.10 ± 0.01	2.30 ± 0.18	2.60 ± 0.37	2.17 ± 0.11	*0.2487*
PUFA	37.09 ± 0.13	37.28 ± 3.34	38.70 ± 1.86	38.18 ± 0.40	*0.8649*
PUFA ω6	28.56 ± 0.04	28.62 ± 2.58	29.78 ± 1.53	28.33 ± 0.33	*0.8122*
PUFA ω3	8.54 ± 0.09	8.67 ± 0.79	8.92 ± 0.49	9.84 ± 0.13	*0.1379*
ω6/ω3	3.35 ± 0.03	3.30 ± 0.09	3.34 ± 0.16	2.88 ± 0.04*/*/*	***0.0080***
total trans	0.55 ± 0.11	1.75 ± 0.86	1.41 ± 0.39	0.93 ± 0.54	*0.3283*
UI	158.52 ± 0.43	156.32 ± 15.02	162.46 ± 8.60	166.56 ± 0.48	*0.7199*
PI	141.79 ± 0.53	140.90 ± 17.63	149.31 ± 8.40	153.93 ± 1.14	*0.6012*

4.2.4 Healthy Swiss mice treated with iron nanoparticles and bleomycin

In parallel, the above-mentioned treatments were performed under the same conditions in healthy Swiss mice. Again, 4-weeks old Swiss mice were randomly divided into four groups; Group 1 (control group) received normal saline, Group 2 received 3 mg/kg (0.6 mg/mL) Fe_3O_4 metallo-nanoparticles (Fe-NPs) suspended in saline, Group 3 received 15 mg/kg (3mg/mL) bleomycin and lastly, Group 4 received Fe-NPs plus bleomycin (co-treatment at the same concentrations as for groups 3 and 4). All administrations were performed intravenously. Animals were sacrificed 24 h after drug administration, red blood cells were isolated from whole blood and analyzed for assessing the membrane fatty acid composition, as depicted in Figure 4.6.

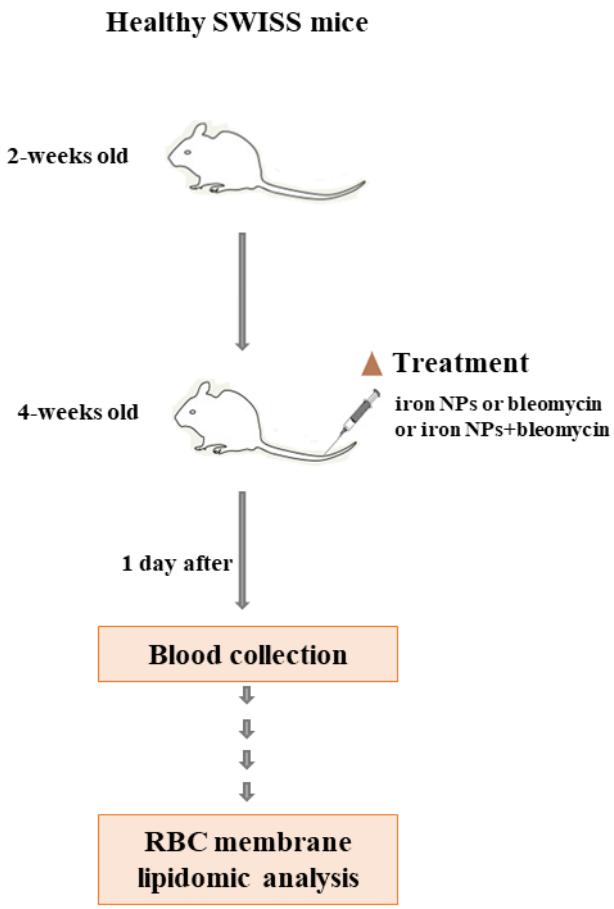

Figure 4.6: Protocol outline for the analysis and quantification of membrane fatty acid moieties in erythrocytes of healthy Swiss mice after treatment with iron nanoparticles (NPs), bleomycin or combination of the them.

Healthy Swiss mice treated with Fe nanoparticles were characterized by a significantly different membrane lipidomic profile, compared to untreated or any other treated group, as shown in Figure 4.7A-C. In comparison to control Swiss mice, the Fe-NPs treated group showed lower SFA ($p < 0.01$) and PUFA ($p < 0.001$) content, whereas the MUFA members were increased ($p < 0.001$) 24 h after iron nanoparticles administration. Regarding the PUFA, both ω-6 and ω-3 family members were significantly decreased ($p < 0.01$ and $p < 0.001$, respectively). However, Swiss mice that were treated with Fe-NPs showed higher ω-6/ω-3 ratio with respect to untreated ones ($p < 0.05$), thus indicating an extended consumption of PUFA-ω3 members compared to the ω6 (Figure 4.7D). Consequently, the observed membrane remodeling led to the diminution of both unsaturation (UI) and peroxidation (PI) indices ($p < 0.01$ and $p < 0.001$, respectively).

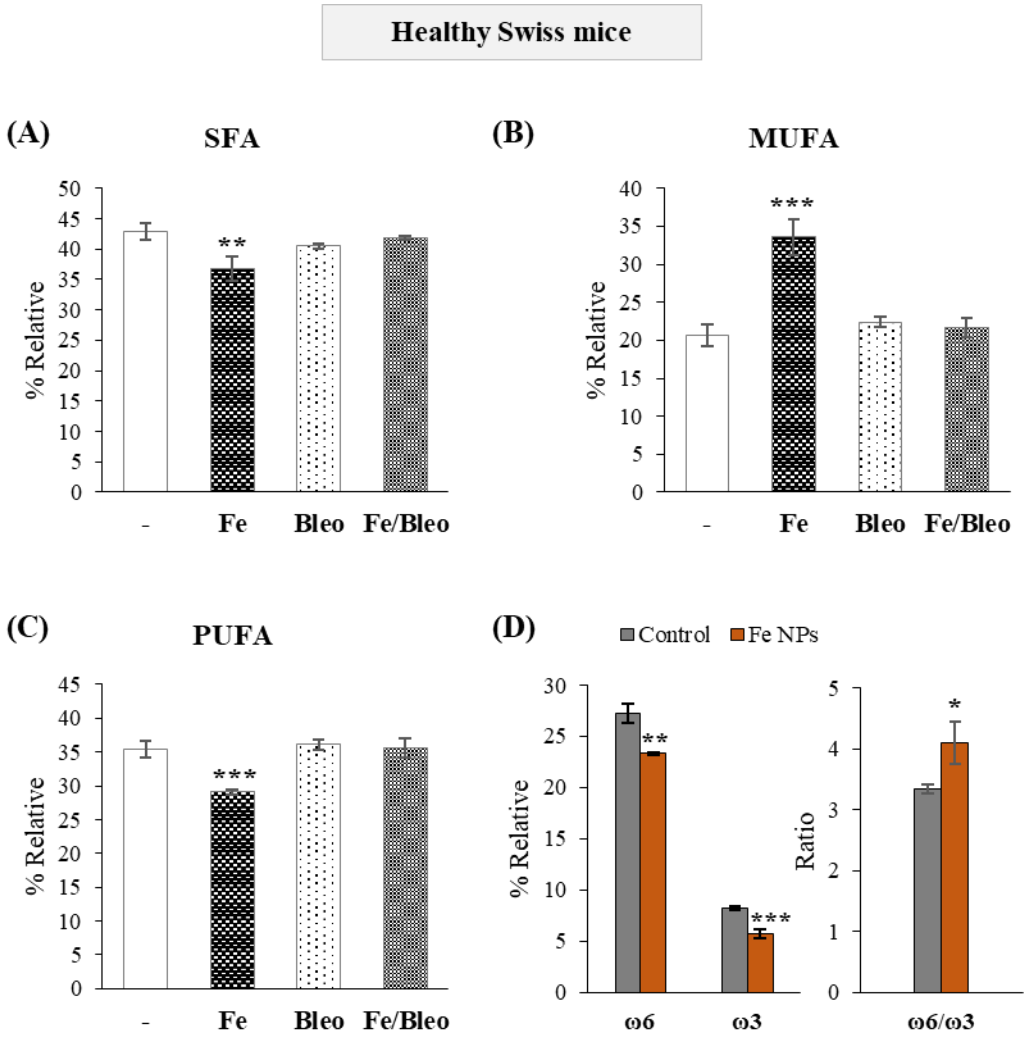

Figure 4.7: (A-C) Relative (%) distribution of fatty acid families (SFA, MUFA and PUFA) in erythrocyte membranes of 4-weeks old normal Swiss mice treated with 3 mg/kg iron nanoparticles (Fe), 15 mg/kg bleomycin (Bleo) and the combination of them (Fe/Bleo) at the same concentrations. (D) Distribution of ω6 and ω3 polyunsaturated fatty acids and their ratio in erythrocyte membranes of 4-weeks normal Swiss mice treated with Fe-NPs. Fatty acid analysis was performed 1-day post-treatment. Values represent Mean ± SD (n=3). SFA, saturated fatty acids; MUFA, monounsaturated fatty acids; PUFA, polyunsaturated fatty acids. Statistical significance was tested with the unpaired *t*-test. * ($p< 0.05$), ** ($p< 0.01$), *** ($p< 0.001$).

Iron mediates the formation of reactive oxygen species (ROS) through the catalytic decomposition of hydrogen peroxide (Fenton reaction), which in turn lead to the damage of biomolecules, including lipids, proteins and DNA [293]. Oxidative damages to cellular components play a key role in tumor initiation and propagation. Studies on experimental animals have indicated that excess of iron accumulation in the liver and kidney causes oxidative tissue damages and is associated with cancer development in the respective organ

[319-322]. Interestingly, when Fe-NPs were administered simultaneously with bleomycin there was no alteration of membrane fatty acid composition, as compared to untreated mice (Table 4.6). The quenching of Fe-NPs effect on membrane lipidome could be probably due to the coordination of iron with bleomycin, since the latter acts as an iron chelator [323, 324]. Consequently, this binding maybe blocks iron's ability to catalyze the formation of free radicals.

Although recent studies have shown that the bleomycin-iron complex can also interact with the membrane lipids due to its lipophilic characteristics [199, 200], we did not observe any similar effect on our *in vivo* models. More specifically, bleomycin has been found to induce *in vitro* a profound membrane remodeling at the level of the fatty acid constituents, which includes an increase of saturated fatty acid (SFA) content with a parallel decrease of monounsaturated and polyunsaturated fatty acids (MUFA and PUFA) [199]. Furthermore, studies on liposomes made of SFA, MUFA and PUFA-containing phospholipids have shown the occurrence of lipid isomerization, as well as the PUFA consumption, under biomimetic conditions of free radical and oxidative stress. In the present case, neither healthy Swiss mice, nor tumor-bearing SCID mice were characterized by such an eryhtrocyte membrane remodeling 24 h after bleomycin administration (Tables 4.5 and 4.6).

Table 4.6: Erythrocyte membrane fatty acid composition of healthy Swiss mice (4-weeks old) treated with Fe nanoparticles (3 mg/kg), bleomycin (15 mg/kg) and the combination of them at the same concentrations. The variance of each fatty acid among the different groups was studied with the ANOVA test. Multiple comparison test was applied to compare the differences among the distinct groups (* control vs x-treated, * Fe-NPs vs bleomycin, * Fe-NPs vs Fe-NPs/bleomycin, * Bleomycin vs Fe-NPs/bleomycin).

FAME (% rel)	Control	Fe-NPs	Bleomycin	Fe-NPs/ Bleomycin	ANOVA (*p*-value)
SFA	42.91 ± 1.41	36.74 ± 1.98**	40.50 ± 0.45	41.85 ± 0.25*	***0.0053***
MUFA	20.63 ± 1.49	33.56 ± 2.36***	22.41 ± 0.65***	21.63 ± 1.27***	***0.0001***
SFA/MUFA	2.10 ± 0.22	1.10 ± 0.13***	1.81 ± 0.07**	1.94 ± 0.11**	***0.0005***
PUFA	35.42 ± 1.15	29.08 ± 0.38***	36.09 ± 0.77***	35.60 ± 1.33***	***0.0003***
PUFA ω6	27.26 ± 0.97	23.34 ± 0.12**	28.08 ± 0.60**	27.52 ± 1.23**	***0.0018***
PUFA ω3	8.17 ± 0.21	5.74 ± 0.44***	8.02 ± 0.20***	8.08 ± 0.37***	***0.0002***
ω6/ω3	3.34 ± 0.07	4.09 ± 0.35*	3.50 ± 0.05	3.41 ± 0.21*	***0.0225***

FAME (% rel)	Control	Fe-NPs	Bleomycin	Fe-NPs/ Bleomycin	ANOVA (*p*-value)
Total *trans*	1.04 ± 0.74	0.62 ± 0.19	0.99 ± 0.40	0.93 ± 0.20	*0.7776*
UI	151.42 ± 5.36	128.14 ± 3.09**	153.24 ± 2.85**	152.38 ± 4.14**	***0.0006***
PI	133.03 ± 5.69	90.01 ± 7.64***	131.81 ± 3.85***	132.77 ± 5.31***	***0.0002***

Apart from the lipid peroxidation process, ROS production can induce the interconversion of the *cis* unsaturated fatty acids to their corresponding *trans* geometrical isomers. This process is catalyzed by thiyl radicals, which are generated endogenously under stress conditions [317, 325]. In this study, we did not observe significant changes on *trans* isomers. The total content of *trans* FA in healthy Swiss mice treated with Fe-NPs was decreased, not significantly though. These preliminary observations also suggest a different effect of iron nanoparticles on erythrocyte fatty acids composition between healthy and tumor-bearing mice. However, further investigation is needed to better evaluate the obtained results.

4.3 Conclusions

In the present research project, we monitored the fatty acid composition of erythrocyte membrane phospholipids during tumor development. The membrane lipidomic profiles were analyzed in tumor-bearing SCID mice, xenografted with the human glioblastoma U87MG cell line, at early and late stages of tumor progression. Regarding the membrane fatty acid remodeling, late stage, and early stage tumor-bearing mice showed significant differences. Specifically, they were characterized by statistically significant increase of SFA, accompanied by a decrease in PUFA (both ω-6 and ω-3 counterparts), unsaturation index (UI) and peroxidation index (PI) at late tumor progression. In parallel, we also studied the effect of iron nanoparticles and bleomycin administration at early stage of tumor occurrence in the same animal model, as well as in healthy Swiss mice. Bleomycin did no exert any significant effect on erythrocyte membrane lipidomic profile of either the tumor-bearing or the healthy mice. Co-treatment of tumor diseased mice with Fe-NPs and bleomycin led to lower ω-6/ω-3 ratio in erythrocyte membrane. Iron nanoparticles caused a notable membrane remodeling in healthy Swiss mice, characterized by lower SFA and

PUFA levels and higher MUFA content. Although both ω-6 and ω-3 PUFA families were decreased, their ratio (ω-6/ω-3) was found increased in Fe-NPs treated Swiss mice, compared to the untreated group. In this study, the erythrocytes were used as 'reporter cells' to evaluate the fatty acid composition of tumor-bearing mice, since they can be indicative of the membrane exposure to the redox status. The effect of high oxidative stress can be depicted through the PUFA consumption and the consequent membrane remodeling. As a result, fatty acid-based membrane lipidomics could be a valuable tool, which allows the follow-up of fatty acid alterations and contribute to the development of multi-targeted antitumoral approaches.

7. Abbreviations

ACC	Acetyl-CoA carboxylase
ACLY	Adenosine triphosphate (ATP) citrate lyase
ALA	α-linolenic acid
ARA	Arachidonic acid
CAT	Catalase
Co-A	Coenzyme A
Cu-TPMA-Phen	$[Cu(TPMA)(Phen)](ClO_4)_2$, TPMA = tris-(2-pyridylmethyl)amine, Phen = 1,10-phenanthroline
DAG	Diacylglycerol
DHA	Docosahexaenoic acid
DGLA	Dihomo-gamma-linolenic acid
DPA	Docosapentaenoic acid
EC_{50}	Half-maximal effective concentration
EDTA	Ethylenediaminetetraacetic acid
EGTA	Ethylene glycol tetraacetic acid
EPA	Eicosapentaenoic acid
ER	Endoplasmic reticulum
FA	Fatty acids
FAME	Fatty acid methyl esters
FADS	Fatty acid desaturase
FASN	Fatty acid synthase
Fe-NPs	Iron nanoparticles
GC	Gas chromatography
GLA	γ-linolenic acid
GPL	Glycerophospholipids
HDFM	Hyperspectral dark field microscopy
LA	Linoleic acid
MCF7	Michigan Cancer Foundation-7, breast cancer cell line
MTBE	Methyl tert-butyl ether
MUFA	Monounsaturated fatty acids
NAC	N-acetyl-cysteine
NADH	Nicotinamide adenine dinucleotide

NADPH	Nicotinamide adenine dinucleotide phosphate
NB100	Neuroblastoma-derived cell line
NCs	Nanocontainers
NEC-1	Necrostatin-1
PBS	Phosphate buffered saline
PC	Phosphatidylcholine
PE	Phosphatidylethanolamine
PI	Peroxidation index
PLA2	Phospholipase A2
PS	Phosphatidylserine
PUFA	Polyunsaturated fatty acids
RBC	Red blood cell
ROS	Reactive oxygen species
SCD	Stearoyl-CoA-desaturase
SCID	Severe combined immunodeficiency
SFA	Saturated fatty acids
SM	Sphingomyelin
SPL	Sphingophospholipids
SREBP	Sterol regulatory element-binding protein
TG	Triglycerides
TMSH	Trimethylsulfonium hydroxide solution
TFA	Trans fatty acids
U87MG	Uppsala 87 Malignant Glioma
UFA	Unsaturated fatty acids
UI	Unsaturation index
VLCFA	Very long chain fatty acids
Z-VAD	N-Benzyloxycarbonyl-Val-Ala-Asp(O-Me) fluoromethyl ketone

8. References

1. Alberts B, J.A., Lewis J, et al., *Molecular Biology of the Cell*. 2002, New York: Garland Science.

2. Escriba, P.V. and G.L. Nicolson, *Membrane structure and function: relevance of lipid and protein structures in cellular physiology, pathology and therapy.* Biochim Biophys Acta, 2014. **1838**(6): p. 1449-50.

3. Kamphorst, J.J., et al., *Hypoxic and Ras-transformed cells support growth by scavenging unsaturated fatty acids from lysophospholipids.* Proc Natl Acad Sci U S A, 2013. **110**(22): p. 8882-7.

4. Mercier, R., P. Domínguez-Cuevas, and J. Errington, *Crucial Role for Membrane Fluidity in Proliferation of Primitive Cells.* Cell Reports, 2012. **1**(5): p. 417-423.

5. Cooper GM, *The Cell: A Molecular Approach.* 2nd edition. ed. 2000: Sunderland (MA): Sinauer Associates;.

6. Singer, S.J., *A fluid lipid-globular protein mosaic model of membrane structure.* Ann N Y Acad Sci, 1972. **195**: p. 16-23.

7. Clarke, S., *The hydrophobic effect: Formation of micelles and biological membranes, 2nd edition (Tanford, Charles).* Journal of Chemical Education, 1981. **58**(8): p. A246.

8. Cooper, R.A., *Influence of increased membrane cholesterol on membrane fluidity and cell function in human red blood cells.* J Supramol Struct, 1978. **8**(4): p. 413-30.

9. Yeagle, P.L., *Chapter 10 - Membrane Proteins*, in *The Membranes of Cells (Third Edition)*, P.L. Yeagle, Editor. 2016, Academic Press: Boston. p. 219-268.

10. Evangelisti, E., et al., *Membrane lipid composition and its physicochemical properties define cell vulnerability to aberrant protein oligomers.* J Cell Sci, 2012. **125**(Pt 10): p. 2416-27.

11. Gupta, K., et al., *The role of interfacial lipids in stabilizing membrane protein oligomers.* Nature, 2017. **541**: p. 421.

12. Lodish H, B.A., Zipursky SL, et al., *Section 3.4, Membrane Proteins*, in *Molecular Cell Biology*. 2000, New York: W. H. Freeman.

13. Reitsma, S., et al., *The endothelial glycocalyx: composition, functions, and visualization.* Pflugers Archiv, 2007. **454**(3): p. 345-359.

14. R, M., *Membrane Glycolipids: Functional Heterogeneity: A Review.* Biochem Anal Biochem, 2012. **1**(108).

15. Marsh, D., *Lateral Pressure Profile, Spontaneous Curvature Frustration, and the Incorporation and Conformation of Proteins in Membranes.* Biophysical Journal, 2007. **93**(11): p. 3884-3899.

16. Bogdanov, M., P.N. Heacock, and W. Dowhan, *A polytopic membrane protein displays a reversible topology dependent on membrane lipid composition.* EMBO J, 2002. **21**(9): p. 2107-16.

17. White, S.H., et al., *How membranes shape protein structure.* J Biol Chem, 2001. **276**(35): p. 32395-8.

18. Dowhan, W., *Molecular basis for membrane phospholipid diversity: why are there so many lipids?* Annu Rev Biochem, 1997. **66**: p. 199-232.

19. Dowhan, W. and M. Bogdanov, *Chapter 1 Functional roles of lipids in membranes*, in *New Comprehensive Biochemistry*. 2002, Elsevier. p. 1-35.

20. Bolognesi, A., et al., *Membrane lipidome reorganization correlates with the fate of neuroblastoma cells supplemented with fatty acids.* PLoS One, 2013. **8**(2): p. e55537.

21. Ibarguren, M., D.J. Lopez, and P.V. Escriba, *The effect of natural and synthetic fatty acids on membrane structure, microdomain organization, cellular functions and human health.* Biochim Biophys Acta, 2014. **1838**(6): p. 1518-28.

22. Levental, K.R., et al., *Polyunsaturated Lipids Regulate Membrane Domain Stability by Tuning Membrane Order.* Biophys J, 2016. **110**(8): p. 1800-1810.

23. Maulucci, G., et al., *Fatty acid-related modulations of membrane fluidity in cells: detection and implications.* Free Radic Res, 2016. **50**(sup1): p. S40-S50.

24. Jicha, G.A. and W.R. Markesbery, *Omega-3 fatty acids: potential role in the management of early Alzheimer's disease.* Clin Interv Aging, 2010. **5**: p. 45-61.

25. Rezanka, T. and K. Sigler, *Odd-numbered very-long-chain fatty acids from the microbial, animal and plant kingdoms.* Prog Lipid Res, 2009. **48**(3-4): p. 206-38.

26. Fahy, E., et al., *A comprehensive classification system for lipids.* J Lipid Res, 2005. **46**(5): p. 839-61.

27. Köfeler, H.C., *Nomenclature of Fatty Acids*, in *Encyclopedia of Lipidomics*, M.R. Wenk, Editor. 2016, Springer Netherlands: Dordrecht. p. 1-3.

28. Cevc, G., *How membrane chain-melting phase-transition temperature is affected by the lipid chain asymmetry and degree of unsaturation: an effective chain-length model.* Biochemistry, 1991. **30**(29): p. 7186-93.

29. Uauy, R., et al., *Role of essential fatty acids in the function of the developing nervous system.* Lipids, 1996. **31 Suppl**: p. S167-76.

30. Niki, E., *Antioxidants in relation to lipid peroxidation.* Chem Phys Lipids, 1987. **44**(2-4): p. 227-53.

31. Tartaro Bujak, I., et al., *The influence of antioxidants in the thiyl radical induced lipid peroxidation and geometrical isomerization in micelles of linoleic acid.* Free Radical Research, 2016. **50**(sup1): p. S18-S23.

32. Fox, B.G., K.S. Lyle, and C.E. Rogge, *Reactions of the diiron enzyme stearoyl-acyl carrier protein desaturase.* Acc Chem Res, 2004. **37**(7): p. 421-9.

33. Ferreri, C., et al., *Comparison of phosphatidylcholine vesicle properties related to geometrical isomerism.* Photochem Photobiol, 2006. **82**(1): p. 274-80.

34. Ferreri, C., et al., *Probing the influence of cis-trans isomers on model lipid membrane fluidity using cis-parinaric acid and a stop-flow technique.* Chem Commun (Camb), 2006(5): p. 529-31.

35. Bezelgues, J.-B. and F. Destaillats, *Chapter 3 - Formation of trans fatty acids during deodorization of edible oils*, in *Trans Fatty Acids in Human Nutrition (Second Edition)*, F. Destaillats, et al., Editors. 2012, Woodhead Publishing. p. 65-75.

36. Bezelgues, J.-B. and A.J. Dijkstra, *Chapter 2 - Formation of trans fatty acids during catalytic hydrogenation of edible oils*, in *Trans Fatty Acids in Human Nutrition (Second Edition)*, F. Destaillats, et al., Editors. 2012, Woodhead Publishing. p. 43-63.

37. Dewanckele, L., et al., *Rumen Biohydrogenation and Microbial Community Changes Upon Early Life Supplementation of 22:6n-3 Enriched Microalgae to Goats.* Frontiers in Microbiology, 2018. **9**: p. 573.

38. Zhang, Y.M. and C.O. Rock, *Membrane lipid homeostasis in bacteria.* Nat Rev Microbiol, 2008. **6**(3): p. 222-33.

39. Chatgilialoglu, C. and C. Ferreri, *Trans lipids: the free radical path.* Acc Chem Res, 2005. **38**(6): p. 441-8.

40. Ferreri, C., et al., *Trans lipid formation induced by thiols in human monocytic leukemia cells.* Free Radic Biol Med, 2005. **38**(9): p. 1180-7.

41. Zambonin, L., et al., *Occurrence of trans fatty acids in rats fed a trans-free diet: a free radical-mediated formation?* Free Radic Biol Med, 2006. **40**(9): p. 1549-56.

42. Menendez, J.A. and R. Lupu, *Fatty acid synthase and the lipogenic phenotype in cancer pathogenesis.* Nat Rev Cancer, 2007. **7**(10): p. 763-77.

43. Colli, W., P.C. Hinkle, and M.E. Pullman, *Characterization of the fatty acid elongation system in soluble extracts and membrane preparations of rat liver mitochondria.* J Biol Chem, 1969. **244**(23): p. 6432-43.

44. Wakil, S.J., *Fatty acid synthase, a proficient multifunctional enzyme.* Biochemistry, 1989. **28**(11): p. 4523-30.

45. Wakil, S.J., J.K. Stoops, and V.C. Joshi, *Fatty acid synthesis and its regulation.* Annu Rev Biochem, 1983. **52**: p. 537-79.

46. Cinti, D.L., et al., *The fatty acid chain elongation system of mammalian endoplasmic reticulum.* Prog Lipid Res, 1992. **31**(1): p. 1-51.

47. Nugteren, D.H., *The enzymic chain elongation of fatty acids by rat-liver microsomes.* Biochim Biophys Acta, 1965. **106**(2): p. 280-90.

48. Osei, P., et al., *Topography of rat hepatic microsomal enzymatic components of the fatty acid chain elongation system.* J Biol Chem, 1989. **264**(12): p. 6844-9.

49. Jump, D.B., *Mammalian fatty acid elongases.* Methods Mol Biol, 2009. **579**: p. 375-89.

50. Jakobsson, A., R. Westerberg, and A. Jacobsson, *Fatty acid elongases in mammals: Their regulation and roles in metabolism.* Progress in Lipid Research, 2006. **45**(3): p. 237-249.

51. Tvrzicka, E., et al., *Fatty acids as biocompounds: their role in human metabolism, health and disease--a review. Part 1: classification, dietary sources and biological functions.* Biomed Pap Med Fac Univ Palacky Olomouc Czech Repub, 2011. **155**(2): p. 117-30.

52. Enoch, H.G., A. Catala, and P. Strittmatter, *Mechanism of rat liver microsomal stearyl-CoA desaturase. Studies of the substrate specificity, enzyme-substrate interactions, and the function of lipid.* J Biol Chem, 1976. **251**(16): p. 5095-103.

53. Heinemann, F.S. and J. Ozols, *Stearoyl-CoA desaturase, a short-lived protein of endoplasmic reticulum with multiple control mechanisms.* Prostaglandins Leukot Essent Fatty Acids, 2003. **68**(2): p. 123-33.

54. Strittmatter, P. and H.G. Enoch, *Purification of stearyl-CoA desaturase from liver.* Methods Enzymol, 1978. **52**: p. 188-93.

55. Paton, C.M. and J.M. Ntambi, *Biochemical and physiological function of stearoyl-CoA desaturase.* Am J Physiol Endocrinol Metab, 2009. **297**(1): p. E28-37.

56. Nakamura, M.T. and T.Y. Nara, *Structure, function, and dietary regulation of delta6, delta5, and delta9 desaturases.* Annu Rev Nutr, 2004. **24**: p. 345-76.

57. Zhang, L., et al., *Human stearoyl-CoA desaturase: alternative transcripts generated from a single gene by usage of tandem polyadenylation sites.* Biochem J, 1999. **340 (Pt 1)**: p. 255-64.

58. Ge, L., et al., *Identification of the Δ-6 Desaturase of Human Sebaceous Glands: Expression and Enzyme Activity.* Journal of Investigative Dermatology, 2003. **120**(5): p. 707-714.

59. Berg JM, T.J., Stryer L., *Section 22.6, Elongation and Unsaturation of Fatty Acids Are Accomplished by Accessory Enzyme Systems.* , in *Biochemistry*. 2002, W H Freeman: New York.

60. Hansen, H.S., *The essential nature of linoleic acid in mammals.* Trends in Biochemical Sciences, 1986. **11**(6): p. 263-265.

61. Neuringer, M., G.J. Anderson, and W.E. Connor, *The essentiality of n-3 fatty acids for the development and function of the retina and brain.* Annu Rev Nutr, 1988. **8**: p. 517-41.

62. Harizi, H., J.-B. Corcuff, and N. Gualde, *Arachidonic-acid-derived eicosanoids: roles in biology and immunopathology.* Trends in Molecular Medicine, 2008. **14**(10): p. 461-469.

63. Bazan, H.E., et al., *Chain elongation and desaturation of eicosapentaenoate to docosahexaenoate and phospholipid labeling in the rat retina in vivo.* Biochim Biophys Acta, 1982. **712**(1): p. 123-8.

64. Guillou, H., et al., *The key roles of elongases and desaturases in mammalian fatty acid metabolism: Insights from transgenic mice.* Progress in Lipid Research, 2010. **49**(2): p. 186-199.

65. Sprecher, H., *Biochemistry of essential fatty acids.* Prog Lipid Res, 1981. **20**: p. 13-22.

66. Ferdinandusse, S., et al., *Identification of the peroxisomal beta-oxidation enzymes involved in the biosynthesis of docosahexaenoic acid.* J Lipid Res, 2001. **42**(12): p. 1987-95.

67. Sprecher, H., et al., *Reevaluation of the pathways for the biosynthesis of polyunsaturated fatty acids.* J Lipid Res, 1995. **36**(12): p. 2471-7.

68. Qiu, X., H. Hong, and S.L. MacKenzie, *Identification of a Delta 4 fatty acid desaturase from Thraustochytrium sp. involved in the biosynthesis of docosahexanoic acid by heterologous expression in Saccharomyces cerevisiae and Brassica juncea.* J Biol Chem, 2001. **276**(34): p. 31561-6.

69. Bretillon, L., et al., *Desaturation and chain elongation of [1-14C]mono-trans isomers of linoleic and alpha-linolenic acids in perfused rat liver.* J Lipid Res, 1998. **39**(11): p. 2228-36.

70. Cook, H.W. and E.A. Emken, *Geometric and positional fatty acid isomers interact differently with desaturation and elongation of linoleic and linolenic acids in cultured glioma cells.* Biochem Cell Biol, 1990. **68**(3): p. 653-60.

71. Lauritzen, L., et al., *The essentiality of long chain n-3 fatty acids in relation to development and function of the brain and retina.* Progress in Lipid Research, 2001. **40**(1): p. 1-94.

72. Rohrig, F. and A. Schulze, *The multifaceted roles of fatty acid synthesis in cancer.* Nat Rev Cancer, 2016. **16**(11): p. 732-749.

73. Park, J.B., et al., *Phospholipase signalling networks in cancer.* Nat Rev Cancer, 2012. **12**(11): p. 782-92.

74. Griner, E.M. and M.G. Kazanietz, *Protein kinase C and other diacylglycerol effectors in cancer.* Nat Rev Cancer, 2007. **7**(4): p. 281-94.

75. Pyne, N.J. and S. Pyne, *Sphingosine 1-phosphate and cancer.* Nat Rev Cancer, 2010. **10**(7): p. 489-503.

76. Meyer zu Heringdorf, D. and K.H. Jakobs, *Lysophospholipid receptors: signalling, pharmacology and regulation by lysophospholipid metabolism.* Biochim Biophys Acta, 2007. **1768**(4): p. 923-40.

77. Fernandis, A.Z. and M.R. Wenk, *Membrane lipids as signaling molecules.* Curr Opin Lipidol, 2007. **18**(2): p. 121-8.

78. Choi, J.W., et al., *LPA receptors: subtypes and biological actions.* Annu Rev Pharmacol Toxicol, 2010. **50**: p. 157-86.

79. Lands, W.E., *Metabolism of glycerolipides; a comparison of lecithin and triglyceride synthesis.* J Biol Chem, 1958. **231**(2): p. 883-8.

80. Bandoh, K., et al., *Lysophosphatidic acid (LPA) receptors of the EDG family are differentially activated by LPA species. Structure-activity relationship of cloned LPA receptors.* FEBS Lett, 2000. **478**(1-2): p. 159-65.

81. Chan, L.C., et al., *LPA3 receptor mediates chemotaxis of immature murine dendritic cells to unsaturated lysophosphatidic acid (LPA).* J Leukoc Biol, 2007. **82**(5): p. 1193-200.

82. Resh, M.D., *Fatty Acylation of Proteins: The Long and the Short of it.* Progress in lipid research, 2016. **63**: p. 120-131.

83. Schepers, A. and H. Clevers, *Wnt signaling, stem cells, and cancer of the gastrointestinal tract.* Cold Spring Harb Perspect Biol, 2012. **4**(4): p. a007989.

84. Nile, A.H. and R.N. Hannoush, *Fatty acylation of Wnt proteins.* Nat Chem Biol, 2016. **12**(2): p. 60-9.

85. Kim, H., et al., *Unsaturated Fatty Acids Stimulate Tumor Growth through Stabilization of beta-Catenin.* Cell Rep, 2015. **13**(3): p. 495-503.

86. Jump, D.B., *The biochemistry of n-3 polyunsaturated fatty acids.* J Biol Chem, 2002. **277**(11): p. 8755-8.

87. Spector, A.A., *Essentiality of fatty acids.* Lipids, 1999. **34 Suppl**: p. S1-3.

88. Simopoulos, A.P., *Omega-3 fatty acids in inflammation and autoimmune diseases.* J Am Coll Nutr, 2002. **21**(6): p. 495-505.

89. Harizi, H. and N. Gualde, *The impact of eicosanoids on the crosstalk between innate and adaptive immunity: the key roles of dendritic cells.* Tissue Antigens, 2005. **65**(6): p. 507-14.

90. Wang, D. and R.N. Dubois, *Eicosanoids and cancer.* Nat Rev Cancer, 2010. **10**(3): p. 181-93.

91. Marini, M., et al., *Aerobic training affects fatty acid composition of erythrocyte membranes.* Lipids Health Dis, 2011. **10**: p. 188.

92. Robichaud, P.P. and M.E. Surette, *Polyunsaturated fatty acid-phospholipid remodeling and inflammation.* Curr Opin Endocrinol Diabetes Obes, 2015. **22**(2): p. 112-8.

93. Schug, Z.T. and E. Gottlieb, *Cardiolipin acts as a mitochondrial signalling platform to launch apoptosis.* Biochim Biophys Acta, 2009. **1788**(10): p. 2022-31.

94. Chicco, A.J. and G.C. Sparagna, *Role of cardiolipin alterations in mitochondrial dysfunction and disease.* Am J Physiol Cell Physiol, 2007. **292**(1): p. C33-44.

95. Cantor, J.R. and D.M. Sabatini, *Cancer cell metabolism: one hallmark, many faces.* Cancer Discov, 2012. **2**(10): p. 881-98.

96. Hanahan, D. and R.A. Weinberg, *Hallmarks of cancer: the next generation.* Cell, 2011. **144**(5): p. 646-74.

97. DeBerardinis, R.J., et al., *The biology of cancer: metabolic reprogramming fuels cell growth and proliferation.* Cell Metab, 2008. **7**(1): p. 11-20.

98. Phan, L.M., S.C. Yeung, and M.H. Lee, *Cancer metabolic reprogramming: importance, main features, and potentials for precise targeted anti-cancer therapies.* Cancer Biol Med, 2014. **11**(1): p. 1-19.

99. Warburg, O., *On respiratory impairment in cancer cells.* Science, 1956. **124**(3215): p. 269-70.

100. Warburg, O., *On the origin of cancer cells.* Science, 1956. **123**(3191): p. 309-14.

101. Swinnen, J.V., K. Brusselmans, and G. Verhoeven, *Increased lipogenesis in cancer cells: new players, novel targets.* Curr Opin Clin Nutr Metab Care, 2006. **9**(4): p. 358-65.

102. Medes, G., A. Thomas, and S. Weinhouse, *Metabolism of neoplastic tissue. IV. A study of lipid synthesis in neoplastic tissue slices in vitro.* Cancer Res, 1953. **13**(1): p. 27-9.

103. Santos, C.R. and A. Schulze, *Lipid metabolism in cancer.* FEBS J, 2012. **279**(15): p. 2610-23.

104. Ferreri, C., et al., *Fatty Acids in Membranes as Homeostatic, Metabolic and Nutritional Biomarkers: Recent Advancements in Analytics and Diagnostics.* Diagnostics (Basel), 2016. **7**(1).

105. Currie, E., et al., *Cellular fatty acid metabolism and cancer.* Cell Metab, 2013. **18**(2): p. 153-61.

106. Tosi, F., et al., *Delta-5 and delta-6 desaturases: crucial enzymes in polyunsaturated fatty acid-related pathways with pleiotropic influences in health and disease.* Adv Exp Med Biol, 2014. **824**: p. 61-81.

107. Li, J.N., et al., *Sterol regulatory element-binding protein-1 participates in the regulation of fatty acid synthase expression in colorectal neoplasia.* Exp Cell Res, 2000. **261**(1): p. 159-65.

108. Swinnen, J.V., et al., *Selective activation of the fatty acid synthesis pathway in human prostate cancer.* Int J Cancer, 2000. **88**(2): p. 176-9.

109. Alo, P.L., et al., *Immunohistochemical expression and prognostic significance of fatty acid synthase in pancreatic carcinoma.* Anticancer Res, 2007. **27**(4B): p. 2523-7.

110. Cai, Y., et al., *Expressions of fatty acid synthase and HER2 are correlated with poor prognosis of ovarian cancer.* Med Oncol, 2015. **32**(1): p. 391.

111. Di Vizio, D., et al., *Caveolin-1 interacts with a lipid raft-associated population of fatty acid synthase.* Cell Cycle, 2008. **7**(14): p. 2257-67.

112. Long, Q.Q., et al., *Fatty acid synthase (FASN) levels in serum of colorectal cancer patients: correlation with clinical outcomes.* Tumour Biol, 2014. **35**(4): p. 3855-9.

113. Walter, K., et al., *Serum fatty acid synthase as a marker of pancreatic neoplasia.* Cancer Epidemiol Biomarkers Prev, 2009. **18**(9): p. 2380-5.

114. Witkiewicz, A.K., et al., *Co-expression of fatty acid synthase and caveolin-1 in pancreatic ductal adenocarcinoma: implications for tumor progression and clinical outcome.* Cell Cycle, 2008. **7**(19): p. 3021-5.

115. Cai, Y., et al., *Expressions of fatty acid synthase and HER2 are correlated with poor prognosis of ovarian cancer.* Medical Oncology (Northwood, London, England), 2015. **32**: p. 391.

116. Duan, J., et al., *Overexpression of fatty acid synthase predicts a poor prognosis for human gastric cancer.* Molecular Medicine Reports, 2016. **13**(4): p. 3027-3035.

117. Horiguchi, A., et al., *Fatty Acid Synthase Over Expression is an Indicator of Tumor Aggressiveness and Poor Prognosis in Renal Cell Carcinoma.* The Journal of Urology, 2008. **180**(3): p. 1137-1140.

118. Takahiro, T., K. Shinichi, and S. Toshimitsu, *Expression of fatty acid synthase as a prognostic indicator in soft tissue sarcomas.* Clin Cancer Res, 2003. **9**(6): p. 2204-12.

119. Vazquez-Martin, A., et al., *Overexpression of fatty acid synthase gene activates HER1/HER2 tyrosine kinase receptors in human breast epithelial cells.* Cell Prolif, 2008. **41**(1): p. 59-85.

120. Kusakabe, T., et al., *Fatty acid synthase is expressed mainly in adult hormone-sensitive cells or cells with high lipid metabolism and in proliferating fetal cells.* J Histochem Cytochem, 2000. **48**(5): p. 613-22.

121. Long, X.H., et al., *Interaction between fatty acid synthase and human epidermal growth receptor 2 (HER2) in osteosarcoma cells.* Int J Clin Exp Pathol, 2014. **7**(12): p. 8777-83.

122. Menendez, J.A., et al., *Inhibition of fatty acid synthase (FAS) suppresses HER2/neu (erbB-2) oncogene overexpression in cancer cells.* Proc Natl Acad Sci U S A, 2004. **101**(29): p. 10715-20.

123. Pizer, E.S., et al., *Malonyl-coenzyme-A is a potential mediator of cytotoxicity induced by fatty-acid synthase inhibition in human breast cancer cells and xenografts.* Cancer Res, 2000. **60**(2): p. 213-8.

124. Jones, S.F. and J.R. Infante, *Molecular Pathways: Fatty Acid Synthase.* Clin Cancer Res, 2015. **21**(24): p. 5434-8.

125. Resh, M.D., *Membrane targeting of lipid modified signal transduction proteins.* Subcell Biochem, 2004. **37**: p. 217-32.

126. Chen, L., et al., *Stearoyl-CoA desaturase-1 mediated cell apoptosis in colorectal cancer by promoting ceramide synthesis.* Sci Rep, 2016. **6**: p. 19665.

127. Noto, A., et al., *Stearoyl-CoA-desaturase 1 regulates lung cancer stemness via stabilization and nuclear localization of YAP/TAZ.* Oncogene, 2017. **36**(32): p. 4573-4584.

128. Noto, A., et al., *Stearoyl-CoA desaturase-1 is a key factor for lung cancer-initiating cells.* Cell Death Dis, 2013. **4**: p. e947.

129. Zhang, J., et al., *EGFR modulates monounsaturated fatty acid synthesis through phosphorylation of SCD1 in lung cancer.* Mol Cancer, 2017. **16**(1): p. 127.

130. Igal, R.A., *Stearoyl-CoA desaturase-1: a novel key player in the mechanisms of cell proliferation, programmed cell death and transformation to cancer.* Carcinogenesis, 2010. **31**(9): p. 1509-15.

131. Igal, R.A., *Roles of StearoylCoA Desaturase-1 in the Regulation of Cancer Cell Growth, Survival and Tumorigenesis.* Cancers (Basel), 2011. **3**(2): p. 2462-77.

132. Fritz, V., et al., *Abrogation of de novo lipogenesis by stearoyl-CoA desaturase 1 inhibition interferes with oncogenic signaling and blocks prostate cancer progression in mice.* Mol Cancer Ther, 2010. **9**(6): p. 1740-54.

133. Ide, Y., et al., *Human breast cancer tissues contain abundant phosphatidylcholine(36ratio1) with high stearoyl-CoA desaturase-1 expression.* PLoS One, 2013. **8**(4): p. e61204.

134. Morgan-Lappe, S.E., et al., *Identification of Ras-related nuclear protein, targeting protein for xenopus kinesin-like protein 2, and stearoyl-CoA desaturase 1 as*

promising cancer targets from an RNAi-based screen. Cancer Res, 2007. **67**(9): p. 4390-8.

135. Roongta, U.V., et al., *Cancer cell dependence on unsaturated fatty acids implicates stearoyl-CoA desaturase as a target for cancer therapy.* Mol Cancer Res, 2011. **9**(11): p. 1551-61.

136. Scaglia, N., J.M. Caviglia, and R.A. Igal, *High stearoyl-CoA desaturase protein and activity levels in simian virus 40 transformed-human lung fibroblasts.* Biochim Biophys Acta, 2005. **1687**(1-3): p. 141-51.

137. Hess, D., J.W. Chisholm, and R.A. Igal, *Inhibition of stearoylCoA desaturase activity blocks cell cycle progression and induces programmed cell death in lung cancer cells.* PLoS One, 2010. **5**(6): p. e11394.

138. Scaglia, N., J.W. Chisholm, and R.A. Igal, *Inhibition of stearoylCoA desaturase-1 inactivates acetyl-CoA carboxylase and impairs proliferation in cancer cells: role of AMPK.* PLoS One, 2009. **4**(8): p. e6812.

139. Li, J., et al., *Lipid Desaturation Is a Metabolic Marker and Therapeutic Target of Ovarian Cancer Stem Cells.* Cell Stem Cell, 2017. **20**(3): p. 303-314 e5.

140. Holder, A.M., et al., *High stearoyl-CoA desaturase 1 expression is associated with shorter survival in breast cancer patients.* Breast Cancer Res Treat, 2013. **137**(1): p. 319-27.

141. Huang, G.M., et al., *SCD1 negatively regulates autophagy-induced cell death in human hepatocellular carcinoma through inactivation of the AMPK signaling pathway.* Cancer Lett, 2015. **358**(2): p. 180-190.

142. Igal, R.A., *Stearoyl CoA desaturase-1: New insights into a central regulator of cancer metabolism.* Biochim Biophys Acta, 2016. **1861**(12 Pt A): p. 1865-1880.

143. Hardie, D.G., *Molecular Pathways: Is AMPK a Friend or a Foe in Cancer?* Clin Cancer Res, 2015. **21**(17): p. 3836-40.

144. Polakis, P., *The many ways of Wnt in cancer.* Curr Opin Genet Dev, 2007. **17**(1): p. 45-51.

145. Vivanco, I. and C.L. Sawyers, *The phosphatidylinositol 3-Kinase AKT pathway in human cancer.* Nat Rev Cancer, 2002. **2**(7): p. 489-501.

146. Zoncu, R., A. Efeyan, and D.M. Sabatini, *mTOR: from growth signal integration to cancer, diabetes and ageing.* Nat Rev Mol Cell Biol, 2011. **12**(1): p. 21-35.

147. Nolan, C.J. and C.Z. Larter, *Lipotoxicity: why do saturated fatty acids cause and monounsaturates protect against it?* J Gastroenterol Hepatol, 2009. **24**(5): p. 703-6.

148. Williams, K.J., et al., *An essential requirement for the SCAP/SREBP signaling axis to protect cancer cells from lipotoxicity.* Cancer Res, 2013. **73**(9): p. 2850-62.

149. Bauer, D.E., et al., *ATP citrate lyase is an important component of cell growth and transformation.* Oncogene, 2005. **24**(41): p. 6314-22.

150. Hatzivassiliou, G., et al., *ATP citrate lyase inhibition can suppress tumor cell growth.* Cancer Cell, 2005. **8**(4): p. 311-21.

151. Beckers, A., et al., *Chemical inhibition of acetyl-CoA carboxylase induces growth arrest and cytotoxicity selectively in cancer cells.* Cancer Res, 2007. **67**(17): p. 8180-7.

152. Guo, D., et al., *An LXR agonist promotes glioblastoma cell death through inhibition of an EGFR/AKT/SREBP-1/LDLR-dependent pathway.* Cancer Discov, 2011. **1**(5): p. 442-56.

153. Hardie, D.G., *AMP-activated/SNF1 protein kinases: conserved guardians of cellular energy.* Nat Rev Mol Cell Biol, 2007. **8**(10): p. 774-85.

154. Accioly, M.T., et al., *Lipid bodies are reservoirs of cyclooxygenase-2 and sites of prostaglandin-E2 synthesis in colon cancer cells.* Cancer Res, 2008. **68**(6): p. 1732-40.

155. Chavarro, J.E., et al., *Blood levels of saturated and monounsaturated fatty acids as markers of de novo lipogenesis and risk of prostate cancer.* Am J Epidemiol, 2013. **178**(8): p. 1246-55.

156. Yang, B., et al., *Biospecimen long-chain N-3 PUFA and risk of colorectal cancer: a meta-analysis of data from 60,627 individuals.* PLoS One, 2014. **9**(11): p. e110574.

157. Pala, V., et al., *Erythrocyte membrane fatty acids and subsequent breast cancer: a prospective Italian study.* J Natl Cancer Inst, 2001. **93**(14): p. 1088-95.

158. Shannon, J., et al., *Erythrocyte fatty acids and breast cancer risk: a case-control study in Shanghai, China.* Am J Clin Nutr, 2007. **85**(4): p. 1090-7.

159. Kuriki, K., et al., *Breast cancer risk and erythrocyte compositions of n-3 highly unsaturated fatty acids in Japanese.* Int J Cancer, 2007. **121**(2): p. 377-85.

160. Zaridze, D.G., et al., *Fatty acid composition of phospholipids in erythrocyte membranes and risk of breast cancer.* Int J Cancer, 1990. **45**(5): p. 807-10.

161. Cottet, V., et al., *Erythrocyte membrane phospholipid fatty acid concentrations and risk of colorectal adenomas: a case-control nested in the French E3N-EPIC cohort study.* Cancer Epidemiol Biomarkers Prev, 2013. **22**(8): p. 1417-27.

162. Rifkin, S.B., et al., *PUFA levels in erythrocyte membrane phospholipids are differentially associated with colorectal adenoma risk.* Br J Nutr, 2017. **117**(11): p. 1615-1622.

163. Coviello, G., et al., *Erythrocyte membrane fatty acids profile in colorectal cancer patients: a preliminary study.* Anticancer Res, 2014. **34**(9): p. 4775-9.

164. Kuriki, K., et al., *Risk of colorectal cancer is linked to erythrocyte compositions of fatty acids as biomarkers for dietary intakes of fish, fat, and fatty acids.* Cancer Epidemiol Biomarkers Prev, 2006. **15**(10): p. 1791-8.

165. Okuno, M., et al., *Abnormalities in fatty acids in plasma, erythrocytes and adipose tissue in Japanese patients with colorectal cancer.* In Vivo, 2013. **27**(2): p. 203-10.

166. Kuriki, K., et al., *Gastric cancer risk and erythrocyte composition of docosahexaenoic acid with anti-inflammatory effects.* Cancer Epidemiol Biomarkers Prev, 2007. **16**(11): p. 2406-15.

167. Lin, S., et al., *Abnormal octadeca-carbon fatty acids distribution in erythrocyte membrane phospholipids of patients with gastrointestinal tumor.* Medicine (Baltimore), 2017. **96**(24): p. e7189.

168. Jurczyszyn, A., et al., *Erythrocyte membrane fatty acids in multiple myeloma patients.* Leuk Res, 2014. **38**(10): p. 1260-5.

169. Aclimandos, W.A., et al., *Erythrocyte stearic to oleic acid ratio in patients with ocular melanoma.* Eye (Lond), 1992. **6 (Pt 4)**: p. 416-9.

170. Harris, R.B., et al., *Fatty acid composition of red blood cell membranes and risk of squamous cell carcinoma of the skin.* Cancer Epidemiol Biomarkers Prev, 2005. **14**(4): p. 906-12.

171. Mikirova, N., et al., *Erythrocyte membrane fatty acid composition in cancer patients.* P R Health Sci J, 2004. **23**(2): p. 107-13.

172. Wood, C.B., et al., *Increase of oleic acid in erythrocytes associated with malignancies.* Br Med J (Clin Res Ed), 1985. **291**(6489): p. 163-5.

173. Roy, S., et al., *Associations of erythrocyte omega-3 fatty acids with biomarkers of omega-3 fatty acids and inflammation in breast tissue.* Int J Cancer, 2015. **137**(12): p. 2934-46.

174. Bagga, D., et al., *Long-Chain n-3-to-n-6 Polyunsaturated Fatty Acid Ratios in Breast Adipose Tissue From Women With and Without Breast Cancer.* Nutrition and Cancer, 2002. **42**(2): p. 180-185.

175. Notarnicola, M., et al., *Differential Tissue Fatty Acids Profiling between Colorectal Cancer Patients with and without Synchronous Metastasis.* International Journal of Molecular Sciences, 2018. **19**(4): p. 962.

176. Apostolov, K., et al., *Reduction in the stearic to oleic acid ratio in leukaemic cells--a possible chemical marker of malignancy.* Blut, 1985. **50**(6): p. 349-54.

177. Wood, C.B., et al., *Reduction in the stearic to oleic acid ratio in human malignant liver neoplasms.* Eur J Surg Oncol, 1985. **11**(4): p. 347-8.

178. Dimanche-Boitrel, M.-T., et al., *Role of early plasma membrane events in chemotherapy-induced cell death.* Drug Resistance Updates, 2005. **8**(1): p. 5-14.

179. Tekpli, X., et al., *Importance of plasma membrane dynamics in chemical-induced carcinogenesis.* Recent Pat Anticancer Drug Discov, 2011. **6**(3): p. 347-53.

180. Tekpli, X., et al., *Role for membrane remodeling in cell death: Implication for health and disease.* Toxicology, 2013. **304**: p. 141-157.

181. Zhang, Y., et al., *Plasma membrane changes during programmed cell deaths.* Cell Research, 2018. **28**(1): p. 9-21.

182. Alves, A.C., et al., *Biophysics in cancer: The relevance of drug-membrane interaction studies.* Biochim Biophys Acta, 2016. **1858**(9): p. 2231-2244.

183. Hopperton, K.E., et al., *Fatty acid synthase plays a role in cancer metabolism beyond providing fatty acids for phospholipid synthesis or sustaining elevations in glycolytic activity.* Exp Cell Res, 2014. **320**(2): p. 302-10.

184. van Meer, G., D.R. Voelker, and G.W. Feigenson, *Membrane lipids: where they are and how they behave.* Nat Rev Mol Cell Biol, 2008. **9**(2): p. 112-24.

185. Zalba, S. and T.L. Ten Hagen, *Cell membrane modulation as adjuvant in cancer therapy.* Cancer Treat Rev, 2017. **52**: p. 48-57.

186. Lacour, S., et al., *Cisplatin-induced CD95 redistribution into membrane lipid rafts of HT29 human colon cancer cells.* Cancer Res, 2004. **64**(10): p. 3593-8.

187. Rebillard, A., et al., *Cisplatin-induced apoptosis involves membrane fluidification via inhibition of NHE1 in human colon cancer cells.* Cancer Res, 2007. **67**(16): p. 7865-74.

188. Maheswari, K.U., T. Ramachandran, and D. Rajaji, *Interaction of cisplatin with planar model membranes – dose dependent change in electrical characteristics.* Biochimica et Biophysica Acta (BBA) - Biomembranes, 2000. **1463**(2): p. 230-240.

189. Modrak, D.E., et al., *Synergistic interaction between sphingomyelin and gemcitabine potentiates ceramide-mediated apoptosis in pancreatic cancer.* Cancer Res, 2004. **64**(22): p. 8405-10.

190. Liang, X. and Y. Huang, *Physical state changes of membrane lipids in human lung adenocarcinoma A(549) cells and their resistance to cisplatin.* Int J Biochem Cell Biol, 2002. **34**(10): p. 1248-55.

191. Becker, S., et al., *Increased Lipiodol uptake in hepatocellular carcinoma possibly due to increased membrane fluidity by dexamethasone and tamoxifen.* Nucl Med Biol, 2010. **37**(7): p. 777-84.

192. Chang, H., et al., *3,6-Dihydroxyflavone induces apoptosis in leukemia HL-60 cell via reactive oxygen species-mediated p38 MAPK/JNK pathway.* Eur J Pharmacol, 2010. **648**(1-3): p. 31-8.

193. de Medina, P., et al., *Ligands of the antiestrogen-binding site induce active cell death and autophagy in human breast cancer cells through the modulation of cholesterol metabolism.* Cell Death Differ, 2009. **16**(10): p. 1372-84.

194. de Medina, P., S. Silvente-Poirot, and M. Poirot, *Tamoxifen and AEBS ligands induced apoptosis and autophagy in breast cancer cells through the stimulation of sterol accumulation.* Autophagy, 2009. **5**(7): p. 1066-7.

195. Eom, Y.W., et al., *Two distinct modes of cell death induced by doxorubicin: apoptosis and cell death through mitotic catastrophe accompanied by senescence-like phenotype.* Oncogene, 2005. **24**(30): p. 4765-77.

196. Jedrzejczak, M., et al., *Changes in plasma membrane fluidity of immortal rodent cells induced by anticancer drugs doxorubicin, aclarubicin and mitoxantrone.* Cell Biol Int, 1999. **23**(7): p. 497-506.

197. Kobayashi, S., et al., *Transcription factor GATA4 inhibits doxorubicin-induced autophagy and cardiomyocyte death.* J Biol Chem, 2010. **285**(1): p. 793-804.

198. Oth, D., et al., *Induction, by adriamycin and mitomycin C, of modifications in lipid composition, size distribution, membrane fluidity and permeability of cultured RDM4 lymphoma cells.* Biochim Biophys Acta, 1987. **900**(2): p. 198-208.

199. Cort, A., et al., *Effects of bleomycin and antioxidants on the fatty acid profile of testicular cancer cell membranes.* Biochim Biophys Acta, 2016. **1858**(2): p. 434-41.

200. Cort, A., et al., *Bleomycin-induced trans lipid formation in cell membranes and in liposome models.* Org Biomol Chem, 2015. **13**(4): p. 1100-5.

201. Pron, G., et al., *Internalisation of the bleomycin molecules responsible for bleomycin toxicity: a receptor-mediated endocytosis mechanism.* Biochem Pharmacol, 1999. **57**(1): p. 45-56.

202. Chen, J. and J. Stubbe, *Bleomycins: towards better therapeutics.* Nat Rev Cancer, 2005. **5**(2): p. 102-12.

203. Ming, L.J., *Structure and function of "metalloantibiotics".* Med Res Rev, 2003. **23**(6): p. 697-762.

204. Ekimoto, H., et al., *Lipid peroxidation by bleomycin-iron complexes in vitro.* J Antibiot (Tokyo), 1985. **38**(8): p. 1077-82.

205. Hiraiwa, K., T. Oka, and K. Yagi, *Effect of Bleomycin on Lipid Peroxides, Glutatbione Peroxidase and Collagenase in Cultured Lung Fibroblasts.* The Journal of Biochemistry, 1983. **93**(4): p. 1203-1210.

206. Mehdizadeh, A., et al., *Common chemotherapeutic agents modulate fatty acid distribution in human hepatocellular carcinoma and colorectal cancer cells.* Bioimpacts, 2017. **7**(1): p. 31-39.

207. Llado, V., et al., *Minerval induces apoptosis in Jurkat and other cancer cells.* J Cell Mol Med, 2010. **14**(3): p. 659-70.

208. Martinez, J., et al., *Membrane structure modulation, protein kinase C alpha activation, and anticancer activity of minerval.* Mol Pharmacol, 2005. **67**(2): p. 531-40.

209. Abel, S., S. Riedel, and W.C. Gelderblom, *Dietary PUFA and cancer.* Proc Nutr Soc, 2014. **73**(3): p. 361-7.

210. D'Archivio, M., et al., *Recent Evidence on the Role of Dietary PUFAs in Cancer Development and Prevention.* Curr Med Chem, 2018. **25**(16): p. 1818-1836.

211. Liu, J. and D.W. Ma, *The role of n-3 polyunsaturated fatty acids in the prevention and treatment of breast cancer.* Nutrients, 2014. **6**(11): p. 5184-223.

212. Mayne, S.T., M.C. Playdon, and C.L. Rock, *Diet, nutrition, and cancer: past, present and future.* Nat Rev Clin Oncol, 2016. **13**(8): p. 504-15.

213. Roynette, C.E., et al., *n-3 Polyunsaturated fatty acids and colon cancer prevention.* Clinical Nutrition, 2004. **23**(2): p. 139-151.

214. Caygill, C.P. and M.J. Hill, *Fish, n-3 fatty acids and human colorectal and breast cancer mortality.* Eur J Cancer Prev, 1995. **4**(4): p. 329-32.

215. Qiu, W., et al., *Dietary fat intake and ovarian cancer risk: a meta-analysis of epidemiological studies.* Oncotarget, 2016. **7**(24): p. 37390-37406.

216. Park, M. and H. Kim, *Anti-cancer Mechanism of Docosahexaenoic Acid in Pancreatic Carcinogenesis: A Mini-review.* J Cancer Prev, 2017. **22**(1): p. 1-5.

217. Roynette, C.E., et al., *n-3 polyunsaturated fatty acids and colon cancer prevention.* Clin Nutr, 2004. **23**(2): p. 139-51.

218. Larsson, S.C., et al., *Dietary long-chain n−3 fatty acids for the prevention of cancer: a review of potential mechanisms.* The American Journal of Clinical Nutrition, 2004. **79**(6): p. 935-945.

219. Turk, H.F. and R.S. Chapkin, *Membrane lipid raft organization is uniquely modified by n-3 polyunsaturated fatty acids.* Prostaglandins Leukot Essent Fatty Acids, 2013. **88**(1): p. 43-7.

220. Arshad, A., et al., *Reduction in circulating pro-angiogenic and pro-inflammatory factors is related to improved outcomes in patients with advanced pancreatic cancer treated with gemcitabine and intravenous omega-3 fish oil.* HPB (Oxford), 2013. **15**(6): p. 428-32.

221. Merendino, N., et al., *Docosahexaenoic acid induces apoptosis in the human PaCa-44 pancreatic cancer cell line by active reduced glutathione extrusion and lipid peroxidation.* Nutr Cancer, 2005. **52**(2): p. 225-33.

222. Song, K.S., et al., *Omega-3-polyunsaturated fatty acids suppress pancreatic cancer cell growth in vitro and in vivo via downregulation of Wnt/Beta-catenin signaling.* Pancreatology, 2011. **11**(6): p. 574-84.

223. Hawkins, R.A., K. Sangster, and M.J. Arends, *Apoptotic death of pancreatic cancer cells induced by polyunsaturated fatty acids varies with double bond number and involves an oxidative mechanism.* J Pathol, 1998. **185**(1): p. 61-70.

224. Rao, C.V., et al., *Modulating effect of amount and types of dietary fat on colonic mucosal phospholipase A2, phosphatidylinositol-specific phospholipase C activities, and cyclooxygenase metabolite formation during different stages of colon tumor promotion in male F344 rats.* Cancer Res, 1996. **56**(3): p. 532-7.

225. Reddy, B.S. and E.L. Wynder, *Large-bowel carcinogenesis: fecal constituents of populations with diverse incidence rates of colon cancer.* J Natl Cancer Inst, 1973. **50**(6): p. 1437-42.

226. Rao, C.V., et al., *Modulation of experimental colon tumorigenesis by types and amounts of dietary fatty acids.* Cancer Res, 2001. **61**(5): p. 1927-33.

227. Singh, J., R. Hamid, and B.S. Reddy, *Dietary fat and colon cancer: modulation of cyclooxygenase-2 by types and amount of dietary fat during the postinitiation stage of colon carcinogenesis.* Cancer Res, 1997. **57**(16): p. 3465-70.

228. Berquin, I.M., I.J. Edwards, and Y.Q. Chen, *Multi-targeted therapy of cancer by omega-3 fatty acids.* Cancer Letters, 2008. **269**(2): p. 363-377.

229. Nicolson, G.L., *Lipid replacement/antioxidant therapy as an adjunct supplement to reduce the adverse effects of cancer therapy and restore mitochondrial function.* Pathol Oncol Res, 2005. **11**(3): p. 139-44.

230. Simopoulos, A.P., *Essential fatty acids in health and chronic disease.* Am J Clin Nutr, 1999. **70**(3 Suppl): p. 560S-569S.

231. Arends, J., et al., *ESPEN guidelines on nutrition in cancer patients.* Clin Nutr, 2017. **36**(1): p. 11-48.

232. Bozzetti, F., *Nutritional support of the oncology patient.* Critical Reviews in Oncology/Hematology, 2013. **87**(2): p. 172-200.

233. Nakamura, K., et al., *Influence of preoperative administration of omega-3 fatty acid-enriched supplement on inflammatory and immune responses in patients undergoing major surgery for cancer.* Nutrition, 2005. **21**(6): p. 639-49.

234. Bougnoux, P., et al. *Docosahexaenoic acid (DHA) intake during first line chemotherapy improves survival in metastatic breast cancer*. in *Proc. Am. Assoc. Cancer Res.* 2006.

235. Nicolson, G.L., *Lipid replacement therapy: a nutraceutical approach for reducing cancer-associated fatigue and the adverse effects of cancer therapy while restoring mitochondrial function.* Cancer Metastasis Rev, 2010. **29**(3): p. 543-52.

236. Subczynski, W.K. and A. Wisniewska, *Physical properties of lipid bilayer membranes: relevance to membrane biological functions.* Acta Biochim Pol, 2000. **47**(3): p. 613-25.

237. Agadjanyan, M., et al., *Nutritional Supplement (NT Factor™) Restores Mitochondrial Function and Reduces Moderately Severe Fatigue in Aged Subjects.* Journal of Chronic Fatigue Syndrome, 2003. **11**(3): p. 23-36.

238. Colodny, L., et al., *Results of a study to evaluate the use of Propax to reduce adverse effects of chemotherapy.* J Am Nutraceut Assoc, 2000. **2**(1): p. 17-25.

239. Zuin Fantoni, N., et al., *Polypyridyl-based Copper Phenanthrene Complexes: A New Type of Stabilized Artificial Chemical Nuclease.* Chemistry, 2018.

240. Polito, L., et al., *Apoptosis and necroptosis induced by stenodactylin in neuroblastoma cells can be completely prevented through caspase inhibition plus catalase or necrostatin-1.* Phytomedicine, 2016. **23**(1): p. 32-41.

241. Paton, C.M. and J.M. Ntambi, *Biochemical and physiological function of stearoyl-CoA desaturase.* American Journal of Physiology - Endocrinology and Metabolism, 2009. **297**(1): p. E28-E37.

242. Sjogren, P., et al., *Fatty acid desaturases in human adipose tissue: relationships between gene expression, desaturation indexes and insulin resistance.* Diabetologia, 2008. **51**(2): p. 328-35.

243. Klein, E. and N. Weber, *Simultaneous derivatization of acyl and S-alkyl moieties of acyl thioesters by using trimethylsulfonium hydroxide for gas chromatographic analysis.* Lipids, 2000. **35**(5): p. 575-7.

244. Sansone, A., et al., *Hexadecenoic fatty acid isomers: a chemical biology approach for human plasma biomarker development.* Chem Res Toxicol, 2013. **26**(11): p. 1703-9.

245. Lepage, G. and C.C. Roy, *Direct transesterification of all classes of lipids in a one-step reaction.* J Lipid Res, 1986. **27**(1): p. 114-20.

246. Puca, A.A., et al., *Fatty acid profile of erythrocyte membranes as possible biomarker of longevity.* Rejuvenation Res, 2008. **11**(1): p. 63-72.

247. Efthimiadou, E.K., et al., *Versatile quarto stimuli nanostructure based on Trojan Horse approach for cancer therapy: Synthesis, characterization, in vitro and in vivo studies.* Mater Sci Eng C Mater Biol Appl, 2017. **79**: p. 605-612.

248. Marzano, C., et al., *Copper complexes as anticancer agents.* Anticancer Agents Med Chem, 2009. **9**(2): p. 185-211.

249. Santini, C., et al., *Advances in copper complexes as anticancer agents.* Chem Rev, 2014. **114**(1): p. 815-62.

250. Molphy, Z., et al., *Copper phenanthrene oxidative chemical nucleases.* Inorg Chem, 2014. **53**(10): p. 5392-404.

251. Molphy, Z., et al., *DNA oxidation profiles of copper phenanthrene chemical nucleases.* Front Chem, 2015. **3**: p. 28.

252. Kellett, A., et al., *Radical-induced DNA damage by cytotoxic square-planar copper(II) complexes incorporating o-phthalate and 1,10-phenanthroline or 2,2'-dipyridyl.* Free Radic Biol Med, 2012. **53**(3): p. 564-76.

253. Slator, C., et al., *[Cu(o-phthalate)(phenanthroline)] Exhibits Unique Superoxide-Mediated NCI-60 Chemotherapeutic Action through Genomic DNA Damage and Mitochondrial Dysfunction.* ACS Chem Biol, 2016. **11**(1): p. 159-71.

254. Slator, C., et al., *Di-copper metallodrugs promote NCI-60 chemotherapy via singlet oxygen and superoxide production with tandem TA/TA and AT/AT oligonucleotide discrimination.* Nucleic Acids Res, 2018. **46**(6): p. 2733-2750.

255. Brewer, G.J., *Risks of copper and iron toxicity during aging in humans.* Chem Res Toxicol, 2010. **23**(2): p. 319-26.

256. Hecht, S.M., *Bleomycin: new perspectives on the mechanism of action.* J Nat Prod, 2000. **63**(1): p. 158-68.

257. Wang, D. and S.J. Lippard, *Cellular processing of platinum anticancer drugs.* Nat Rev Drug Discov, 2005. **4**(4): p. 307-20.

258. Pitie, M. and G. Pratviel, *Activation of DNA carbon-hydrogen bonds by metal complexes.* Chem Rev, 2010. **110**(2): p. 1018-59.

259. Rebillard, A., et al., *Cisplatin-Induced Apoptosis Involves Membrane Fluidification via Inhibition of NHE1 in Human Colon Cancer Cells.* Cancer Research, 2007. **67**(16): p. 7865.

260. Beloribi-Djefaflia, S., S. Vasseur, and F. Guillaumond, *Lipid metabolic reprogramming in cancer cells.* Oncogenesis, 2016. **5**: p. e189.

261. Humphreys, K.J., K.D. Karlin, and S.E. Rokita, *Efficient and specific strand scission of DNA by a dinuclear copper complex: comparative reactivity of complexes with linked tris(2-pyridylmethyl)amine moieties.* J Am Chem Soc, 2002. **124**(21): p. 6009-19.

262. Li, L., K.D. Karlin, and S.E. Rokita, *Changing selectivity of DNA oxidation from deoxyribose to Guanine by ligand design and a new binuclear copper complex.* J Am Chem Soc, 2005. **127**(2): p. 520-1.

263. Thyagarajan, S., et al., *Selective DNA strand scission with binuclear copper complexes: implications for an active Cu2-O2 species.* J Am Chem Soc, 2006. **128**(21): p. 7003-8.

264. Larragy, R., et al., *Protein engineering with artificial chemical nucleases.* Chem Commun (Camb), 2015. **51**(65): p. 12908-11.

265. Prisecaru, A., et al., *Potent oxidative DNA cleavage by the di-copper cytotoxin: [Cu2(mu-terephthalate)(1,10-phen)4]2+*. Chem Commun (Camb), 2012. **48**(55): p. 6906-8.

266. Pratviel, G., J. Bernadou, and B. Meunier, *Carbon—Hydrogen Bonds of DNA Sugar Units as Targets for Chemical Nucleases and Drugs.* Angewandte Chemie International Edition in English, 1995. **34**(7): p. 746-769.

267. Serment-Guerrero, J., et al., *Genotoxicity of the copper antineoplastic coordination complexes casiopeinas.* Toxicol In Vitro, 2011. **25**(7): p. 1376-84.

268. Rock, K.L. and H. Kono, *The inflammatory response to cell death.* Annual review of pathology, 2008. **3**: p. 99-126.

269. Degterev, A., M. Boyce, and J. Yuan, *A decade of caspases.* Oncogene, 2003. **22**(53): p. 8543-67.

270. McIlwain, D.R., T. Berger, and T.W. Mak, *Caspase functions in cell death and disease.* Cold Spring Harb Perspect Biol, 2015. **7**(4).

271. Bouchier-Hayes, L. and D.R. Green, *Caspase-2: the orphan caspase.* Cell Death And Differentiation, 2011. **19**: p. 51.

272. Fava, L.L., et al., *Caspase-2 at a glance.* Journal of Cell Science, 2012. **125**(24): p. 5911.

273. Miao, E.A., J.V. Rajan, and A. Aderem, *Caspase-1-induced pyroptotic cell death.* Immunol Rev, 2011. **243**(1): p. 206-14.

274. Harijith, A., D.L. Ebenezer, and V. Natarajan, *Reactive oxygen species at the crossroads of inflammasome and inflammation.* Frontiers in Physiology, 2014. **5**: p. 352.

275. Vandenabeele, P., et al., *Molecular mechanisms of necroptosis: an ordered cellular explosion.* Nat Rev Mol Cell Biol, 2010. **11**(10): p. 700-14.

276. Shindo, R., et al., *Critical contribution of oxidative stress to TNFalpha-induced necroptosis downstream of RIPK1 activation.* Biochem Biophys Res Commun, 2013. **436**(2): p. 212-6.

277. Zong, W.X., et al., *Alkylating DNA damage stimulates a regulated form of necrotic cell death.* Genes Dev, 2004. **18**(11): p. 1272-82.

278. Wang, X., et al., *Pyruvate Protects Mitochondria from Oxidative Stress in Human Neuroblastoma SK-N-SH Cells.* Brain research, 2007. **1132**(1): p. 1-9.

279. Olivieri, G., et al., *N-acetyl-L-cysteine protects SHSY5Y neuroblastoma cells from oxidative stress and cell cytotoxicity: effects on beta-amyloid secretion and tau phosphorylation.* J Neurochem, 2001. **76**(1): p. 224-33.

280. Slator, C., et al., *Triggering autophagic cell death with a di-manganese(II) developmental therapeutic.* Redox Biol, 2017. **12**: p. 150-161.

281. Sugihara, K., et al., *Stimulatory effect of cisplatin on production of lipid peroxidation in renal tissues.* Jpn J Pharmacol, 1987. **43**(3): p. 247-52.

282. Rysman, E., et al., *De novo lipogenesis protects cancer cells from free radicals and chemotherapeutics by promoting membrane lipid saturation.* Cancer Res, 2010. **70**(20): p. 8117-26.

283. Lv, Y., et al., *Novel multifunctional pH-sensitive nanoparticles loaded into microbubbles as drug delivery vehicles for enhanced tumor targeting.* Sci Rep, 2016. **6**: p. 29321.

284. Comba, A., et al., *Basic aspects of tumor cell fatty acid-regulated signaling and transcription factors.* Cancer Metastasis Rev, 2011. **30**(3-4): p. 325-42.

285. Fuentes, N.R., et al., *Omega-3 fatty acids, membrane remodeling and cancer prevention.* Molecular Aspects of Medicine, 2018.

286. Dorr, R.T., *Bleomycin pharmacology: mechanism of action and resistance, and clinical pharmacokinetics.* Semin Oncol, 1992. **19**(2 Suppl 5): p. 3-8.

287. Pratviel, G., J. Bernadou, and B. Meunier, *Evidence for high-valent iron-oxo species active in the DNA breaks mediated by iron-bleomycin.* Biochem Pharmacol, 1989. **38**(1): p. 133-40.

288. Cotin, G., et al., *Chapter 2 - Iron Oxide Nanoparticles for Biomedical Applications: Synthesis, Functionalization, and Application*, in *Iron Oxide Nanoparticles for Biomedical Applications*, M. Mahmoudi and S. Laurent, Editors. 2018, Elsevier. p. 43-88.

289. Ali, A., et al., *Synthesis, characterization, applications, and challenges of iron oxide nanoparticles.* Nanotechnology, Science and Applications, 2016. **9**: p. 49-67.

290. Edge, D., et al., *Pharmacokinetics and bio-distribution of novel super paramagnetic iron oxide nanoparticles (SPIONs) in the anaesthetized pig.* Clin Exp Pharmacol Physiol, 2016. **43**(3): p. 319-26.

291. Richter, G.W., *The cellular transformation of injected colloidal iron complexes into ferritin and hemosiderin in experimental animals; a study with the aid of electron microscopy.* J Exp Med, 1959. **109**(2): p. 197-216.

292. Ruiz, A., et al., *Biodistribution and pharmacokinetics of uniform magnetite nanoparticles chemically modified with polyethylene glycol.* Nanoscale, 2013. **5**(23): p. 11400-8.

293. Braughler, J.M., L.A. Duncan, and R.L. Chase, *The involvement of iron in lipid peroxidation. Importance of ferric to ferrous ratios in initiation.* J Biol Chem, 1986. **261**(22): p. 10282-9.

294. Dranoff, G., *Experimental mouse tumour models: what can be learnt about human cancer immunology?* Nat Rev Immunol, 2011. **12**(1): p. 61-6.

295. Morton, C.L. and P.J. Houghton, *Establishment of human tumor xenografts in immunodeficient mice.* Nat Protoc, 2007. **2**(2): p. 247-50.

296. Viviani Anselmi, C., et al., *Fatty acid percentage in erythrocyte membranes of atrial flutter/fibrillation patients and controls.* J Interv Card Electrophysiol, 2010. **27**(2): p. 95-9.

297. Folch, J., M. Lees, and G.H. Sloane Stanley, *A simple method for the isolation and purification of total lipides from animal tissues.* J Biol Chem, 1957. **226**(1): p. 497-509.

298. Buttari, B., E. Profumo, and R. Rigano, *Crosstalk between red blood cells and the immune system and its impact on atherosclerosis.* Biomed Res Int, 2015. **2015**: p. 616834.

299. Kuhn, V., et al., *Red Blood Cell Function and Dysfunction: Redox Regulation, Nitric Oxide Metabolism, Anemia.* Antioxid Redox Signal, 2017. **26**(13): p. 718-742.

300. Diederich, L., et al., *On the Effects of Reactive Oxygen Species and Nitric Oxide on Red Blood Cell Deformability.* Frontiers in Physiology, 2018. **9**(332).

301. Sinha, A., et al., *Single-cell evaluation of red blood cell bio-mechanical and nano-structural alterations upon chemically induced oxidative stress.* Scientific Reports, 2015. **5**: p. 9768.

302. Lucantoni, G., et al., *The red blood cell as a biosensor for monitoring oxidative imbalance in chronic obstructive pulmonary disease: an ex vivo and in vitro study.* Antioxid Redox Signal, 2006. **8**(7-8): p. 1171-82.

303. Minetti, M. and W. Malorni, *Redox control of red blood cell biology: the red blood cell as a target and source of prooxidant species.* Antioxid Redox Signal, 2006. **8**(7-8): p. 1165-9.

304. Rogowski, O., et al., *The erythrosense as a real-time biomarker to reveal the presence of enhanced red blood cell aggregability in atherothrombosis.* Am J Ther, 2005. **12**(4): p. 286-92.

305. Lauritzen, L., et al., *The essentiality of long chain n-3 fatty acids in relation to development and function of the brain and retina.* Prog Lipid Res, 2001. **40**(1-2): p. 1-94.

306. Ferreri, C. and C. Chatgilialoglu, *Membrane Lipidomics for Personalized Health*. 2015: Wiley.

307. Prasinou, P., et al., *Fatty acid-based lipidomics and membrane remodeling induced by apoE3 and apoE4 in human neuroblastoma cells.* Biochim Biophys Acta, 2017. **1859**(10): p. 1967-1973.

308. Buckley, D., et al., *Fatty acid synthase – Modern tumor cell biology insights into a classical oncology target.* Pharmacology & Therapeutics, 2017. **177**: p. 23-31.

309. Huang, M., et al., *Diet-induced alteration of fatty acid synthase in prostate cancer progression.* Oncogenesis, 2016. **5**(2): p. e195.

310. Pflug, B.R., et al., *Increased fatty acid synthase expression and activity during progression of prostate cancer in the TRAMP model.* The Prostate, 2003. **57**(3): p. 245-254.

311. Zaytseva, Y.Y., et al., *Inhibition of Fatty Acid Synthase Attenuates CD44-Associated Signaling and Reduces Metastasis in Colorectal Cancer.* Cancer Research, 2012.

312. Azrad, M., C. Turgeon, and W. Demark-Wahnefried, *Current evidence linking polyunsaturated Fatty acids with cancer risk and progression.* Front Oncol, 2013. **3**: p. 224.

313. Zheng, H., et al., *Inhibition of endometrial cancer by n-3 polyunsaturated fatty acids in preclinical models.* Cancer Prev Res (Phila), 2014. **7**(8): p. 824-34.

314. Ferreri, C. and C. Chatgilialoglu, *Role of fatty acid-based functional lipidomics in the development of molecular diagnostic tools.* Expert Rev Mol Diagn, 2012. **12**(7): p. 767-80.

315. Fiaschi, T. and P. Chiarugi, *Oxidative Stress, Tumor Microenvironment, and Metabolic Reprogramming: A Diabolic Liaison.* International Journal of Cell Biology, 2012. **2012**: p. 762825.

316. Bell, E., et al., *Cell survival signalling through PPARdelta and arachidonic acid metabolites in neuroblastoma.* PLoS One, 2013. **8**(7): p. e68859.

317. Chatgilialoglu, C., et al., *Lipid geometrical isomerism: from chemistry to biology and diagnostics.* Chem Rev, 2014. **114**(1): p. 255-84.

318. Fujii, K., et al., *Pro-metastatic intracellular signaling of the elaidic trans fatty acid.* Int J Oncol, 2017. **50**(1): p. 85-92.

319. Ali, M.A., et al., *Reliability of serum iron, ferritin, nitrite, and association with risk of renal cancer in women.* Cancer detection and prevention, 2003. **27**(2): p. 116-121.

320. Kew, M.C., *Hepatic Iron Overload and Hepatocellular Carcinoma.* Liver Cancer, 2014. **3**(1): p. 31-40.

321. Nahon, P., et al., *Hepatic iron overload and risk of hepatocellular carcinoma in cirrhosis.* Gastroenterol Clin Biol, 2010. **34**(1): p. 1-7.

322. Toyokuni, S., *Mysterious link between iron overload and CDKN2A/2B.* Journal of Clinical Biochemistry and Nutrition, 2011. **48**(1): p. 46-49.

323. Lin, P.S., et al., *Effects of iron, copper, cobalt, and their chelators on the cytotoxicity of bleomycin.* Cancer Res, 1983. **43**(3): p. 1049-53.

324. Oppenheimer, N.J., L.O. Rodriguez, and S.M. Hecht, *Structural studies of of "active complex" of bleomycin: assignment of ligands to the ferrous ion in a ferrous-bleomycin-carbon monoxide complex.* Proceedings of the National Academy of Sciences of the United States of America, 1979. **76**(11): p. 5616-5620.

325. Ferreri, C. and C. Chatgilialoglu, *Geometrical trans lipid isomers: a new target for lipidomics.* Chembiochem, 2005. **6**(10): p. 1722-34.